

**STRUCTURAL ANALYSIS OF SUGAR BINDING TO
RICE β -GLUCOSIDASE BGLU1 E176Q AND ITS
TRANSGLYCOSYLATION PRODUCTS**

Por-ngam Prasert



**A Thesis Submitted in Partial Fulfillment of the Requirements for the
Degree of Master of Science in Biochemistry
Suranaree University of Technology
Academic Year 2012**

การวิเคราะห์โครงสร้างของเอนไซม์ BGLU1 E176Q ที่จับน้ำตาลและ
การวิเคราะห์โครงสร้างผลิตภัณฑ์ที่เกิดจากทรานซ์โกลโคซิเลชันของเอนไซม์



วิทยานิพนธ์นี้เป็นส่วนหนึ่งของการศึกษาตามหลักสูตรปริญญาวิทยาศาสตรมหาบัณฑิต
สาขาวิชาชีวเคมี
มหาวิทยาลัยเทคโนโลยีสุรนารี
ปีการศึกษา 2555

**STRUCTURAL ANALYSIS OF SUGAR BINDING TO RICE
β-GLUCOSIDASE BGLU1 E176Q AND ITS
TRANSGLYCOSYLATION**

Suranaree University of Technology has approved this thesis submitted in partial fulfillment of the requirements for a Master's Degree.

Thesis Examining Committee

(Assoc. Prof. Dr. Jatuporn Wittayakun)

Chairperson

(Prof. Dr. James R. Ketudat-Cairns)

Member (Thesis Advisor)

(Asst. Prof. Dr. Jaruwan Siritapetawee)

Member

(Asst. Prof. Dr. Panida Khunkaewla)

Member

(Prof. Dr. Sukit Limpijumnong)

Vice Rector for Academic Affairs

(Assoc. Prof. Dr. Prapun Manyum)

Dean of Institute of Science

พองาม ประเสริฐ : การวิเคราะห์โครงสร้างของเอนไซม์ BGLu1 E176Q ที่จับน้ำตาลและการวิเคราะห์โครงสร้างผลิตภัณฑ์ที่เกิดจากทรานส์ไกลโคซิเลชันของเอนไซม์

(STRUCTURAL ANALYSIS OF SUGAR BINDING TO RICE β -GLUCOSIDASE

BGLu1 E176Q AND ITS TRANSGLYCOSYLATION PRODUCTS) อาจารย์ที่ปรึกษา :

ศาสตราจารย์ ดร.เจมส์ เกตุทัต-คาร์นส์, 115 หน้า.

เอนไซม์ BGLu1 (Os3BGLu7) เป็นเอนไซม์ของข้าว (*Oryza sativa*) ซึ่งจัดอยู่ในตระกูล glycoside hydrolase family 1 (GH1) และมีการแสดงออกสูงในดอกและลำต้นของข้าว เอนไซม์ BGLu1 E176Q ถูกผลิตใน *Escherichia coli* สายพันธุ์ Origami(DE3) ในรูปของโปรตีนที่มีปลายอะมิโนต่อกับโปรตีนไทโอรีดอกซินและบริเวณที่มีกรดอะมิโนฮิสติดีนเรียงต่อกัน 6 ตัวต่ออยู่ที่ส่วนปลายของโปรตีน เอนไซม์ BGLu1 E176Q สามารถทำให้บริสุทธิ์โดยใช้เทคนิคโครมาโตกราฟีแบบจำเพาะที่มีลิแกนด์ต่อกับเรซิน (IMAC) สองขั้นตอน เอนไซม์ที่ได้จากการทำให้บริสุทธิ์ในคอลัมน์ IMAC ครั้งที่หนึ่งมีน้ำหนักโมเลกุล 66 กิโลดาลตัน โปรตีนไทโอรีดอกซินและบริเวณที่มีกรดอะมิโนฮิสติดีนเรียงต่อกัน 6 ตัวต่ออยู่ที่ส่วนปลายของโปรตีนถูกตัดออกจากเอนไซม์ BGLu1 E176Q ด้วยเอนไซม์เอนเทอโรไคเนสและแยกส่วนนี้ออกด้วยวิธี IMAC และใช้เทคนิค gel-filtration ด้วยคอลัมน์ Superdex S-200 เอนไซม์ BGLu1 E176Q ที่ได้มีน้ำหนักโมเลกุล 55 กิโลดาลตัน การตกผลึกของเอนไซม์ BGLu1 E176Q ประสบความสำเร็จมาแล้วด้วยวิธี hanging drop vapor diffusion ร่วมกับเทคนิค microseeding ผลึกของเอนไซม์ BGLu1 E176Q กับ 2,4-dinitrophenyl-2-deoxy-2-fluoro-mannoside (DNP2FM) และเอนไซม์กับน้ำตาลแมนโนส (MAN) สามารถตกผลึกได้ใน 23% (w/v) PEG MME 5000, 0.2 M $(\text{NH}_4)_2\text{SO}_4$, 0.1 M MES, pH 6.7 และ 10 mM DNP2FM และ 21% (w/v) PEG MME 5000, 0.2 M $(\text{NH}_4)_2\text{SO}_4$, 0.1 M MES, pH 6.7 และ pNPMAN ตามลำดับ ข้อมูลจากการเลี้ยวเบนรังสีเอกซ์ของผลึกเอนไซม์ BGLu1 E176Q กับ DNP2FM หรือ เอนไซม์กับ MAN เก็บได้ที่ 1.95 อังสตรอมและ 1.69 อังสตรอม ตามลำดับ โครงสร้างของเอนไซม์ BGLu1 E176Q กับ DNP2FM และเอนไซม์กับ MAN วิเคราะห์ได้ด้วยวิธี molecular replacement โดยอาศัยโครงสร้างเชิงซ้อนของเอนไซม์ BGLu1 E176Q กับ 2-deoxy-2-fluoroglucoside (3AHT) กับโปรตีน 2 โมเลกุลต่อหน่วยของสมมาตร พบว่าในโครงสร้างเชิงซ้อนของเอนไซม์ มีปริมาณน้ำในผลึกประมาณร้อยละ 47.63 และค่าสัมประสิทธิ์ของ Matthews คือ $2.35 \text{ \AA}^3 \text{ Da}^{-1}$ สำหรับโครงสร้างเชิงซ้อนของเอนไซม์กับ DNP2FM และปริมาณน้ำในผลึกประมาณร้อยละ 47.63 และค่าสัมประสิทธิ์ของ Matthews คือ $2.35 \text{ \AA}^3 \text{ Da}^{-1}$ สำหรับโครงสร้างเชิงซ้อนของเอนไซม์กับ MAN หมู่ น้ำตาลไพแรโนสในโครงสร้างของ BGLu1 E176Q กับ DNP2FM บริเวณเร่งมีโครงสร้างแบบ

รีแลกซ์แซร์ 4C_1 คล้ายกับโครงสร้างของ BGlul E176Q กับ 2-deoxy-2-fluoro- β -D-glucoside (DNP2FG) และพบ MAN ในบริเวณเร่งของ BGlul E176Q ที่ตกผลึกกับ *p*NPMan

การทดสอบการทำงานของเอนไซม์ BGlul E176Q ด้วยปฏิกิริยาแทนซ์ไกลโคซิเลชัน ในการย้ายน้ำตาลจาก *p*NPGlc หรือ *p*NPMan ซึ่งเป็นหมู่ให้ ไปให้ *p*-nitrobenzenethiol (NBT) ซึ่งเป็นหมู่รับในการผลิต *p*-nitrophenyl-thioglycoside ผลึกภัณฑ์ที่ได้จากปฏิกิริยาแทนซ์ไกลโคซิเลชัน พบในตำแหน่งเดียวกับ *p*-nitrophenyl-thioglycoside ในโครมาโทกราฟีแผ่นบาง (TLC) และเครื่องโครมาโทกราฟีของเหลวสมรรถนะสูง (HPLC) การเพิ่มความเข้มข้นของ NBT ถึง 10 มิลลิโมลาร์ ในปฏิกิริยาที่ใช้ *p*NPGlc มีการเพิ่มขึ้นที่เห็นได้ของอัตราร้อยละของ *p*NPGlc เปลี่ยนเป็น *p*-nitrophenyl thioglucoside ในลักษณะเดียวกันร้อยละที่เห็นได้ของการเกิดผลิตภัณฑ์จากการเกิดแทนซ์ไกลโคซิเลชัน ของผลิตภัณฑ์ *p*-nitrophenyl thiomannoside โดยเพิ่มความเข้มข้นของ *p*NPMan

5 และ 10 มิลลิโมลาร์ และเพิ่มความเข้มข้นของ NBT ถึง 10 มิลลิโมลาร์ แต่ที่ความเข้มข้นของ NBT ที่ 10 มิลลิโมลาร์ และ 2 มิลลิโมลาร์ของสารตั้งต้น *p*NPMan ซึ่งเป็นหมู่ให้ยับยั้งการเกิดผลิตภัณฑ์ ผลการศึกษานี้แสดงให้เห็นว่า เอนไซม์กลายพันธุ์ BGlul E176Q กรด/เบส (acid/base) สามารถใช้ในการผลิต *p*-nitrophenyl-thiomannoside ซึ่งสามารถผลิตได้ยาก โดยการสังเคราะห์แยกอินทรีย์



POR-NGAM PRASERT : STRUCTURAL ANALYSIS OF SUGAR
BINDING TO RICE β -GLUCOSIDASE BGLU1 E176Q AND ITS
TRANSGLYCOSYLATION PRODUCTS. THESIS ADVISOR :
PROF. JAMES R. KETUDAT-CAIRNS, Ph.D. 115 PP.

BGLU1 E176Q/ β -GLUCOSIDASE/TRANSGLYCOSYLATION/ GLYCOSIDE
HYDROLASE FAMILY 1

Rice BGlu1 (systematically named Os3BGlu7) is a rice (*Oryza sativa*) β -glucosidase that is classified in glycoside hydrolase family 1 (GH1) and is highly expressed in flowers and germinating shoots. The BGlu1 catalytic acid/base mutant E176Q was expressed as an N-terminal thioredoxin/His6 fusion protein in *Escherichia coli* strain Origami(DE3). BGlu1 E176Q was purified by two steps of immobilized metal affinity chromatography (IMAC) with a proteolytic digestion in between. The fusion protein purified by the first IMAC had an apparent molecular weight of 66 kDa. The thioredoxin/His6 tag was cleaved from the protein with enterokinase, and the tag-free BGlu1 E176Q protein of 55 kDa was purified by IMAC and gel-filtration on a Superdex 200 column. The crystallization of BGlu1 E176Q was accomplished by optimization of the previously utilized conditions in hanging drop vapor diffusion with microseeding. Crystals of BGlu1 E176Q in covalent complexes with 2-deoxy-2-fluoro- β -D-mannoside (DNP2FM) and D-mannose (MAN) were obtained by crystallization of the protein in 23% (w/v) PEG MME 5000, 0.2 M $(\text{NH}_4)_2\text{SO}_4$, 0.1 M MES, pH 6.7, and 10 mM DNP2FM and 21% (w/v) PEG MME 5000, 0.2 M $(\text{NH}_4)_2\text{SO}_4$, 0.1 M MES, pH 6.7, and *p*NPMan, respectively. The data sets from diffraction of X-rays with crystals of BGlu1 E176Q with DNP2FM or MAN were collected to 1.95 Å and 1.69 Å resolution,

respectively. The structure of BGlu1 E176Q with DNP2FM and MAN were solved by molecular replacement with the BGlu1 E176Q structure with 2-deoxy-2-fluoroglucoside (3AHT) with two protein molecules per asymmetric unit. These solutions gave a solvent content of 47.63% and Matthews coefficient (VM) of $2.35 \text{ \AA}^3 \text{ Da}^{-1}$ for the BGlu1 E176Q with DNP2FM complex data set, and a solvent content of 47.63% and VM of $2.35 \text{ \AA}^3 \text{ Da}^{-1}$ for the MAN complex data set. The sugar pyranose ring in the BGlu1 E176Q complex with DNP2FM in the active site had a 4C_1 relaxed chair conformation similar to that in the BGlu1 E176Q complex with 2-deoxy-2-fluoro- β -D-glucoside (DNP2FG). Free MAN was found in the active site of BGlu1 E176Q with *p*NPMan.

Rice BGlu1 E176Q transglycosylation activity in moving sugars from *p*NPGlc or *p*NPMan donors to *p*-nitrobenzenethiol (NBT) acceptor to produce *p*-nitrophenyl-thioglycosides was characterized. The products of these transglycosylation reactions were found at the same positions as the respective *p*-nitrophenyl-thioglycosides in thin layer chromatography (TLC) and high performance liquid chromatography (HPLC). Increasing the concentration of NBT up to 10 mM in the reactions with *p*NPGlc resulted in an increased apparent percentage of the *p*NPGlc converted to *p*-nitrophenyl-thioglycoside. Similarly the apparent percent conversion to the transglycosylation product *p*-nitrophenyl-thiomannoside with 5 and 10 mM *p*NPMan increased as the concentration of NBT increased to 10 mM, but 10 mM NBT appeared to inhibit conversion at the 2 mM *p*NPMan donor substrate concentration. These results suggest that the BGlu1 E176Q acid/base mutant may be used to produce *p*-nitrophenyl-thiomannoside, which is difficult to produce by organic synthesis.

School of Biochemistry

Student's Signature _____

Academic Year 2012

Advisor's Signature _____

ACKNOWLEDGEMENTS

I would like to express the deepest gratitude to my thesis advisor, Prof. Dr. James R. Ketudat-Cairns for his kind advice, guidance and encouragement along this project. I am very grateful to Prof. Dr. Chun-Jung Chen, Dr. Phimonphan Chuankhayan and the staff at the National Synchrotron Radiation Research Center (NSRRC), Taiwan for their kind help in solving problems during X-ray diffraction data collection.

I would like to thank Dr. Watchalee Chuenchor for cloning and construction of pET32a/*BGlu1 E176Q*, and I also thank Dr. Salila Pengthaisong for her guidance on the crystallization techniques.

I would like to thank Assoc. Prof. Dr. Jatuporn Wittayakun, Asst. Prof. Dr. Jaruwan Siritapetawee and Dr. Panida Khunkaewla for patiently reading this dissertation and providing helpful comments.

This work was supported by the Thailand Research Fund and Suranaree University of Technology. Data collection was carried out at the National Synchrotron Radiation Research Center (NSRRC), a national user facility supported by the National Science Council of Taiwan, ROC. The Synchrotron Radiation Protein Crystallography Facility is supported by the National Research Program for Genomic Medicine.

Special thanks are extended to all my friends in the School of Biochemistry, Suranaree University of Technology for their help.

Finally, I would like to express my deepest gratitude to my parents and members of my family for their love, understanding and encouragement.

Por-ngam Prasert



CONTENTS

	Page
ABSTRACT IN THAI	I
ABSTRACT IN ENGLISH	III
ACKNOWLEDGEMENTS	V
CONTENTS	VII
LIST OF TABLES	XII
LIST OF FIGURES	XIII
LIST OF ABBREVIATIONS AND SYMBOLS	XVII
CHAPTER	
I INTRODUCTION	1
1.1 β -Glucosidase	1
1.2 Glycosidase mechanism	2
1.3 Acid/base and nucleophile mutants with rescued activity	5
1.4 Transglycosylation	7
1.5 Transition state itineries of β -D-glucosidases and β -D-mannosidase	10
1.6 Rice β -glucosidase	13
1.7 Research objectives	16
II METERIALS AND METHODS	17
2.1 Materials	17
2.1.1 Recombinant plasmid and bacterial strains	17

CONTENTS (Continued)

	Page
2.1.2 Chemicals and reagents	17
2.2 Methods	19
2.2.1 Transformation of expression host with recombinant expression plasmid	19
2.2.2 Protein expression of BGlu1 E176Q	19
2.2.3 Protein purification of BGlu1 E176Q	20
2.2.3.1 Thioredoxin fusion protein	20
2.2.3.2 Removal of the fusion tag and purification of tag-free protein	21
2.3 Protein analysis	22
2.3.1 SDS-PAGE electrophoresis	22
2.3.2 β -Glucosidase activity	22
2.3.3 Bio-Rad protein assay	23
2.4 Protein crystallization	23
2.4.1 Crystallization by hanging drop	23
2.4.2 Microseeding method	24
2.4.3 Co-crystallization with complex	25
2.4.4 Soaking of crystal	25
2.4.5 Data collection and processing	26
2.4.5.1 Freezing in cryoprotectant	26
2.4.5.2 Synchrotron X-ray diffraction	26

CONTENTS (Continued)

	Page
2.4.5.3 Structure solution by molecular replacement	27
2.4.5.4 Model building, structure refinement and validation of the final model	27
2.5 Rescue of <i>p</i> NPMan and <i>p</i> NPGlc hydrolysis by small nucleophiles	28
2.5.1 Reaction of <i>p</i> NPMan and <i>p</i> NPGlc	28
2.6 Transglycosylation of <i>p</i> -nitrobenzenethiol.....	29
2.6.1 TLC analysis.....	29
2.6.2 HPLC analysis.....	30
III RESULTS	31
3.1 Recombinant expression and purification of BGlu1 E176Q.....	31
3.2 Crystallization of BGlu1 E176Q.....	35
3.2.1 Crystallization by hanging drop.....	35
3.2.2 Datasets collected for crystals produced for mannoside complexes	37
3.2.3 Preliminary structures of BGlu1 E176Q in complexes with DNP2FM and <i>p</i> NPMan by X-ray diffraction.....	39
3.2.4 Overall structure and quality of models	40
3.3 Rescue of <i>p</i> NPMan and <i>p</i> NPGlc hydrolysis by small nucleophiles	47
3.4 Transglycosylation of <i>p</i> -nitrobenzenethiol.....	55
3.5 Analysis of transglycosylation products by HPLC	65

CONTENTS (Continued)

	Page
IV DISCUSSION	89
4.1 Protein expression and purification.....	89
4.2 Protein crystallization.....	90
4.3 Structure of BGlu1 E176Q.....	90
4.4 Rescue of <i>p</i> NPMan and <i>p</i> NPGlc hydrolysis by small nucleophiles	92
4.5 Transglycosylation of <i>p</i> -nitrobenzenethiol.....	93
V CONCLUSION	95
REFERENCES.....	98
APPENDICES	107
APPENDIX A STANDARD CURVE OF HPLC.....	108
1.1 Standard curve of <i>p</i> NP from 254 nm absorbance peak area per concentration of <i>p</i> NP.....	108
1.2 Standard curve for <i>p</i> NPGlc from 254 nm absorbance peak area per concentration of <i>p</i> NPGlc	109
1.3 Standard curve of <i>p</i> NP β-D-thioglucoside from 254 nm absorbance peak area per concentration of <i>p</i> NP β-D-thioglucoside.....	110
1.4 Standard cuve for <i>p</i> NPMan from absorbance at 254 nm peak area per concentration of <i>p</i> NPMan	111
1.5 Standard curve for <i>p</i> NP β-D-thiomannoside from 254 nm absorbance peak area per concentration of <i>p</i> NP β-D-thiomannoside.....	112

CONTENTS (Continued)

APPENDIX B LIST OF PROCEEDINGS AND ABSTRACTS.....	113
CURRICULUM VITAE	115



LIST OF TABLES

Table	Page
2.1	The gradient for HPLC separation of the products of transglycosylation 30
3.1	Data collection statistics for crystals not used for final structure solution 38
3.2	Data collection statistics for the datasets used to solve the structures of BGlul E176Q in covalent complexes with α -D-2-fluoromannoside and D-mannose 42
3.3	Refinement statistics for the structural models of BGlul E176Q with α -D-fluoromannopyranoside and α -D-mannopyranoside 43
3.4	The apparent concentrations of products in transglycosylation reactions with 10 mM <i>p</i> NPGlc and NBT determined by reverse phase HPLC 71
3.5	The concentrations of products of reactions with 2 mM <i>p</i> NPMan and different concentrations of NBT determined by reverse phase HPLC 78
3.6	The concentrations of products of reactions with 5 mM <i>p</i> NPMan with and without NBT quantified by reverse phase HPLC 83
3.7	The concentrations of products of reactions of 10 mM <i>p</i> NPMan with and without NBT quantified by reverse phase HPLC 88

LIST OF FIGURES

Figure	Page
1.1 β -Glucosidase structures from different GH families	2
1.2 General mechanisms of inverting and retaining glycosidase	4
1.3 Mechanisms of azide rescue of the activity of a nucleophile mutant and an acid/base mutant	6
1.4 A natural version of chemical rescue with <i>Sinapis alba</i> myrosinase utilizes ascorbate as a general base catalyst	7
1.5 Mechanisms of hydrolysis and transglycosylation by retaining glycosidases	9
1.6 Mechanism of glycosylation and deglycosylation with wild-type and acid/base mutant retaining β -glycosidases	10
1.7 The conformations of sugars near the transition state during hydrolysis by glycosidases	12
1.8 Partial map of pyranoside ring interconversion	12
1.9 Binding of 2-fluroglucoside (G2F) in the active site of rice BGlu1	15
2.1 Map of the protein sequence encoded by the recombinant pET32a(+) with the <i>bglu1/E176Q</i> cDNA inserted after the enterokinase cleavage site	17
3.1 SDS-PAGE of recombinant thioredoxin and His ₆ tagged BGlu1 E176Q protein IMAC purification fractions	32

LIST OF FIGURES (Continued)

Figure	Page
3.2	SDS-PAGE of fractions from purification of BGlu1 E176Q by cleavage with enterokinase and adsorption of tag protein with a second IMAC step ... 33
3.3	Elution profile of the BGlu1 E176Q protein without fusion tag obtained from Superdex S-200 gel filtration chromatography and SDS-PAGE of the protein peak fractions 34
3.4	Crystals of BGlu1 E176Q 36
3.5	The electron density in the active site of BGlu1 E176Q..... 39
3.6	Ribbon diagram representation of the dimeric structure of BGlu1 E176Q complex with DNP2FM (M2F) and <i>p</i> NPMan (MAN) complex..... 44
3.7	The electron densities of M2F and MAN in the -1 subsite of BGlu1E176 45
3.8	Comparison of the active sites of BGlu1 E176Q complex with M2F, MAN and G2F 46
3.9	TLC of reactions of BGLu1 E176Q with <i>p</i> NPMan and <i>p</i> NPGlc rescued with azide at 18 h 48
3.10	TLC of reactions of BGLu1 E176Q with <i>p</i> NPMan and <i>p</i> NPGlc rescued with azide at 24 h 49
3.11	TLC of reactions of BGlu1 E176Q with <i>p</i> NPMan and <i>p</i> NPGlc rescued with azide at 36 h 50
3.12	TLC of reactions of BGLu1 E176Q with <i>p</i> NPMan and <i>p</i> NPGlc rescued with azide at 48 h 51

LIST OF FIGURES (Continued)

Figure	Page
3.13	Products of reactions of BGlu1 E176Q with <i>p</i> NPMan with and without azide at different enzyme concentrations 52
3.14	TLC analysis of products of reactions of <i>p</i> NPMan with nucleophiles/ catalyzed by BGlu1 E176Q..... 54
3.15	TLC analysis of the transglycosylation products of <i>p</i> -nitrobenzenethiol with <i>p</i> NPGLc in various buffers..... 57
3.16	TLC analysis of transglycosylation product of <i>p</i> -nitrobenzenethiol with <i>p</i> NPMan in various buffers 60
3.17	TLC analysis of transglycosylation reactions of <i>p</i> -nitrobenzenethiol (NBT) with <i>p</i> NPMan with various concentrations of BGlu1 E176Q for various times 63
3.18	Reverse phase HPLC analysis of 10 mM <i>p</i> NP, 10 mM <i>p</i> NPGLc, 10 mM <i>p</i> NP β -D-thioglucoside, and 100 mM NBT standard..... 66
3.19	Reverse phase HPLC analysis of transglycosylation products of BGlu1 E176Q with <i>p</i> NPGLc and NBT as substrates 68
3.20	Reverse phase HPLC of <i>p</i> NPMan, <i>p</i> NP β -D-thiomannoside, <i>p</i> NP α -D-thiomannoside 73
3.21	Reverse phase HPLC analysis of transglycosylation products of BGlu1 E176Q with 2 mM <i>p</i> NPMan and NBT as substrates 75

LIST OF FIGURES (Continued)

Figure	Page
3.22 Reverse phase HPLC analysis of the products of the transglycosylation reaction of BGlu1 E176Q with 5 mM <i>p</i> NPMan and NBT as substrates	80
3.23 Reverse phase HPLC analysis of transglycosylation products of BGlu1 E176Q with 10 mM <i>p</i> NPMan and NBT as substrates	85



LIST OF ABBREVIATIONS AND SYMBOLS

DNP2FG	2,4-Dinitrophenyl 2-deoxy-2-fluoro- β -D-glucopyranoside
DNP2FM	2,4-Dinitrophenyl 2-deoxy-2-fluoro- β -D-mannopyranoside
(m, μ)l	(milli, micro) Liter
(m, μ)g	(milli, micro) Gram
(m, μ)M	(milli, micro) Molar
(μ)mol	(micro) Mole
bp	Base pairs
BSA	Bovine serum albumin
CV	Column volume
DMSO	Dimethyl sulfoxide
DNA	Deoxyribonucleic acid
DNase	Deoxyribonuclease
DTT	Dithiothreitol
GH	Glycoside hydrolase
GH1	Glycoside hydrolase family 1
HPLC	High performance liquid chromatography
h	Hour
IMAC	Immobilized metal affinity chromatography

LIST OF ABBREVIATIONS AND SYMBOLS (Continued)

IPTG	Isopropyl thio- β -D-galactoside
kDa	Kilo Dalton
l	Liter
M	Molar
MES	2-Morpholinoethanesulfonic acid
min	Minute
MWCO	Molecular weight cut off
NaCl	Sodium chloride
NBT	<i>p</i> -Nitrobenzenethiol
(NH ₄) ₂ SO ₄	Ammonium sulphate
nm	Nanometer
OD	Optical density
PAGE	Polyacrylamide gel electrophoresis
PEG MME	Polyethylene glycol monomethyl ether
PMSF	Phenyl methylsulfonyl fluoride
<i>p</i> NP	<i>para</i> -Nitrophenyl
<i>p</i> NPGlc	<i>p</i> -Nitrophenyl- β -D-glucopyranoside
<i>p</i> NPMan	<i>p</i> -Nitrophenyl- β -D-mannopyranoside
rpm	Revolutions per minute
SDS	Sodium dodecyl sulfate
TEMED	Tetramethylenediamine
TLC	Thin layer chromatography

LIST OF ABBREVIATIONS AND SYMBOLS (Continued)

Tris	Tris-(hydroxymethyl)-aminoethane
v/v	Volume per volume
w/v	Weight per volume



CHAPTER I

INTRODUCTION

1.1 β -Glucosidase

β -Glucosidases (E.C.3.2.1.21) are enzymes that catalyse the hydrolysis of the β -glycosidic bond between the reducing side of a D-glucosyl residue and an aryl- or alkyl- moiety or an oligosaccharide releasing β -D-glucose and an aglycone or saccharide (Ketudat Cairns and Esen, 2010; Reese, 1977). These enzymes play important roles in many biological mechanisms, such as chemical defense (Morant *et al.*, 2008), lignification (Escamilla-Trevino *et al.*, 2006), cell wall modification (Hrmova and Fincher, 2001) and phytohormone activation (Schroeder and Nambara, 2006). Plant beta-glucosidases that have been characterized so far can be classified in the glycoside hydrolase (GH) families 1, 3 and 5 (Henrissat, 1991; Opassiri *et al.*, 2006). Glycoside hydrolase family 1 (GH1) also contains myrosinases (thio- β -glucosidases), which hydrolyse the *S*-glycosidic bonds of plant 1-thio- β -D-glucosides (glucosinolates) (Burmeister *et al.*, 1997), β -mannosidases, β -galactosidases, β -glucuronidases, β -fucosidases, 6-phospho- β -galactosidases, diglycosidases, including primeverosidase (Mizutani *et al.*, 2002), furcatin hydrolase (Ahn *et al.*, 2004) and isoflavone 7-*O*- β -apiosyl- β -1,6-glucosidase (Chuankhayan *et al.*, 2005), and hydroxyisourate hydrolase, which hydrolyses a bond in the purine ring of hydroxyisourate rather than a glycosidic bond (Raychaudhuri and Tipton, 2002). The structures of β -glucosidases are known for five GH families. Families GH1, GH 5,

and GH 30 belong to Clan GH-A, and have similar $(\beta/\alpha)_8$ barrel domains that contain their active sites. In contrast, GH3 enzymes have two domains, one $(\beta/\alpha)_8$ barrel and one $(\beta/\alpha)_6$ sandwich domain, with their active sites between these domains, while GH 9 enzymes have $(\alpha/\alpha)_6$ barrel structures and the structure of GH116 β -glucosidases is yet unknown (Ketudat Cairns and Esen, 2010) (Figure 1.1).

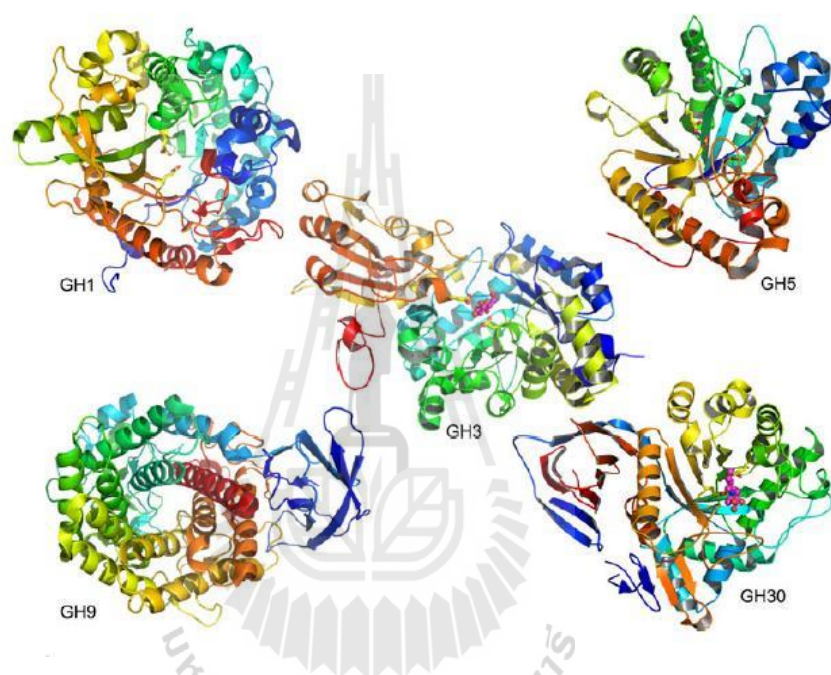


Figure 1.1 β -Glucosidase structures from different GH families (Ketudat Cairns and Esen, 2010).

1.2 Glycosidase mechanism

Glycoside hydrolase enzymes use general acid catalysis, which involves two acidic catalytic residues in the active site that act as a general acid or proton donor and a general base or nucleophile (Koshland, 1953; Sinnott, 1990). The hydrolysis of glycosidic bonds by glycoside hydrolases enzymes have two elementary mechanisms,

which are the inverting and retaining mechanisms (Sinnott, 1990; McCarter and Withers, 1994; Ly and Withers, 1999).

Inverting glycosidases (Figure 1.2 A) catalyze hydrolysis via a single oxocarbenium ion-like transition state and lack a covalent enzyme intermediate formed during of catalysis. The two carboxyl groups in inverting glycosidases are usually two carboxylic acid residues (Asp or Glu), which are located about 10.5 Å apart on opposite sides of the active site (Zechel and Withers, 2000; Rempel and Withers, 2008) one of the carboxylic acids is deprotonated allowing it to remove a proton from the incoming nucleophile (water in the hydrolysis mechanism) and this carboxylic acid acts as a general base. The other carboxylic acid acts as a general acid residue to protonate the leaving group oxygen atom and thereby assist in cleavage of the glycosidic bond to release the aglycone.

The reaction of the classic retaining glycosidases (Figure 1.2 B) differs from that of inverting glycosidases by the formation of a covalently bound glycosyl-enzyme intermediate and the use two steps, each with its own oxocarbenium ion-like transition state. The retaining mechanism has a pair of essential carboxylic residues (Asp or Glu) located on opposite sides of the active site, but they are normally closer together, about 5.5 Å apart (Zechel and Withers, 2000; Rempel and Withers, 2008). In the first step, the glycosidic oxygen is protonated by one of the carboxylic acid residues, which acts as the general acid, while the other carboxylate group acts as a nucleophile and attacks the anomeric carbon, resulting in the formation of a covalently linked glycosyl-enzyme intermediate. In the second step, the carboxylate residue that first acted as an acid catalyst acts as a base to receive a proton from the incoming

nucleophile, the water molecule, which attacks at the anomeric center to cleave the covalent intermediate and release the sugar.

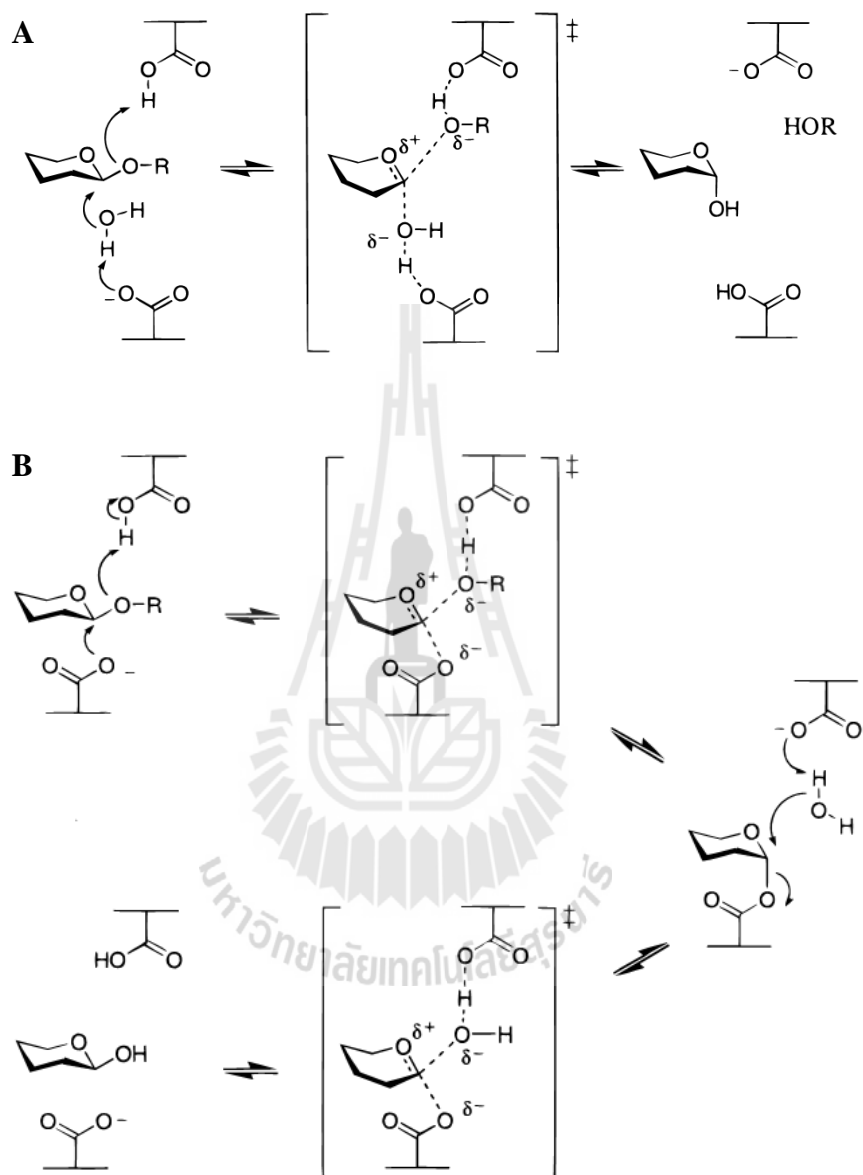


Figure 1.2 General mechanisms of inverting and retaining glycosidase. The mechanisms of inverting glycosidases (A) and classic retaining glycosidases (B) are shown (Zechel and Withers, 2000).

1.3 Acid/base and nucleophile mutants with rescued activity

Rescue of the activity of mutant enzymes by azide may be used to identify the acid/base and nucleophile residues. The Ala mutant of the catalytic nucleophile of *Agrobacterium* β -glucosidase (Abg) enzyme, shown in (Figure 1.3 A), which completely lacks activity, can be reactivated for hydrolysis of dinitrophenyl glucoside by azide, formate, or acetate, which results in the formation of glucosides with inverted anomeric configuration, i.e. α -glucosyl azide (Wang *et al.*, 1994). The opposite result, a glycoside with the same anomeric configuration as the substrate, such as β -glucosyl azide is obtained from azide rescue of the activity of the Abg acid/base mutant (Figure 1.3 B) (Wang *et al.*, 1995). In this case, the good leaving group has a low pK_a so that it does not require protonation, which eliminates the need for acid catalysis in glycosylation step.



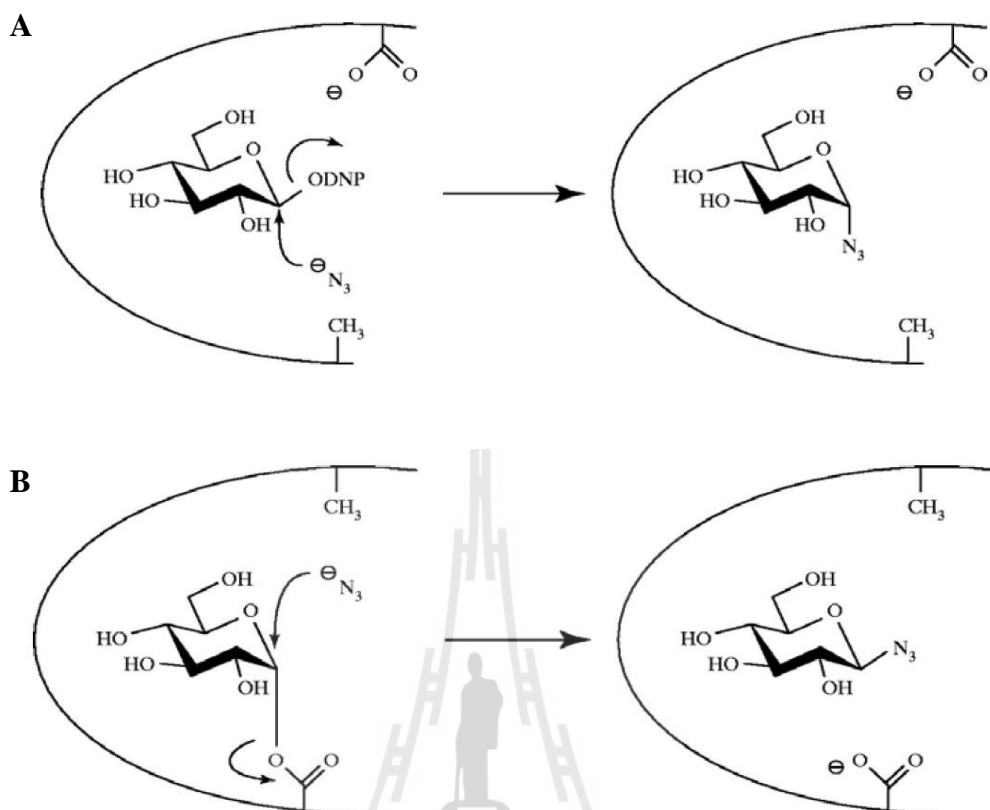


Figure 1.3 Mechanisms of azide rescue of the activity of a nucleophile mutant (**A**) and an acid/base mutant (**B**) (Ly and Withers, 1999).

In one catalytic residue variation found in nature, the acid/base glutamate residue, which is highly conserved in *O*-glycosidases, is changed to glutamine in GH1 enzyme *Sinapis alba* myrosinase, which is an *S*-glycosidase (thioglucosidase) (Burmeister *et al.*, 2000). Although it lacks a glutamic acid residue carboxyl group as an acid/base catalyst, myrosinase can hydrolyze its highly reactive substrates, such as sinigrin and other glucosinolates, to perform the glycosylation step without protonic assistance. Ascorbate acts as a base catalyst in the deglycosylation step after departure of the aglycone (Figure 1.4).

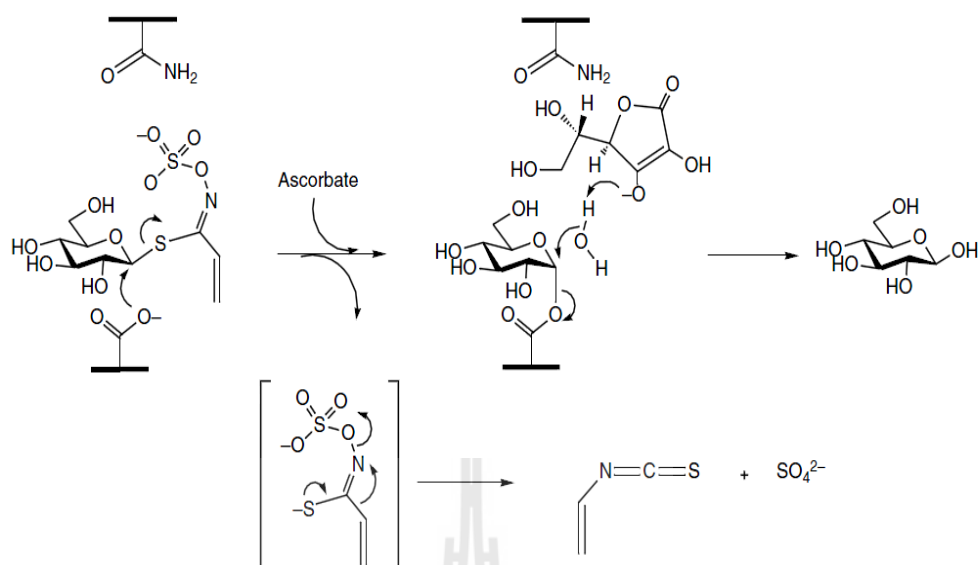


Figure 1.4 A natural version of chemical rescue with *Sinapis alba* myrosinase utilizes ascorbate as a general base catalyst (Burmeister *et al.*, 2000; Zechel and Withers, 2001).

1.4 Transglycosylation

The chemical synthesis of carbohydrate by using of enzymes has two different approaches. One involves the use of glycosyltransferases, whereas the other exploits the transglycosylation ability of glycoside-degrading enzymes (Koeller and Wong, 2000). Glycosyl transferases catalyze the transfer of a sugar from activated nucleotide phospho-sugar donor to a suitable acceptor (Thiem, 1995). However, the limited availability of glycosyl transferases, their membrane association and the high cost of their substrates limits their use (Perugino *et al.*, 2004; Shaikh and Withers, 2008). Glycoside hydrolases are able to catalyze transglycosylation reactions to make new glycosidic bonds between donor and acceptor moieties, leading to synthesis of oligosaccharides and alkyl glucosides (Makropoulou *et al.*, 1998; Svasti *et al.*, 2003; Opassiri *et al.*, 2003; 2004; Hommalai *et al.*, 2005). Glycosidases catalyze reverse

hydrolysis and transglucosylation to form glycosidic linkages by transferring the glycone of the glycosyl enzyme to an acceptor sugar or other alcohol rather than to water (Figure 1.5). Therefore, retaining glycosidases can be used to synthesize glycosides. However, glycosidases produce poor yields from synthetic reactions, because of the hydrolysis of the products (Perugino *et al.*, 2004; Shaikh and Withers, 2008).

Helpful variations have been added to the application of glycoside hydrolyases to transglycosylation reactions by the use of mutant enzymes, namely glycosynthases (Mackenzie *et al.*, 1998), thioglycoligases (Jahn *et al.*, 2003) and thioglycosynthases (Jahn *et al.*, 2004). Thioglycoligases are made from glycosidases by mutation of the acid/base catalyst, allowing them to transglycosylate from an activated glycosyl donor to a thio- sugar acceptor (Jahn *et al.*, 2003; Müllegger *et al.*, 2005). As noted above, retaining exoglucosidases hydrolyze β -glucosidic bonds via a two step mechanism. In the first step, glycosylation, the acid/base catalyst protonates the glycosidic oxygen and the same acid/base catalyst deprotonates and thereby activates the incoming acceptor molecule forming of the covalent glycosyl-enzyme intermediate (Figure 1.6 A). If a glycosyl donor with a highly active leaving group (meaning one with a low pK_a for the free aglycone, such as dinitrophenylate) is used, the first step can proceed without the acid/base catalyst. In the second step, the deglycosylation of the glycosidase acid/base mutant glycosyl-enzyme intermediate can be achieved with nucleophiles that do not require basic assistance, such as thiols or azide (Figure 1.6 B) (Jahn *et al.*, 2003; Müllegger *et al.*, 2005). Because the hydrolysis reaction is very inefficient without basic assistance to the water acceptor, this type of enzyme allows

efficient formation of thioglycosides and thio-linked oligosaccharides without hydrolysis.

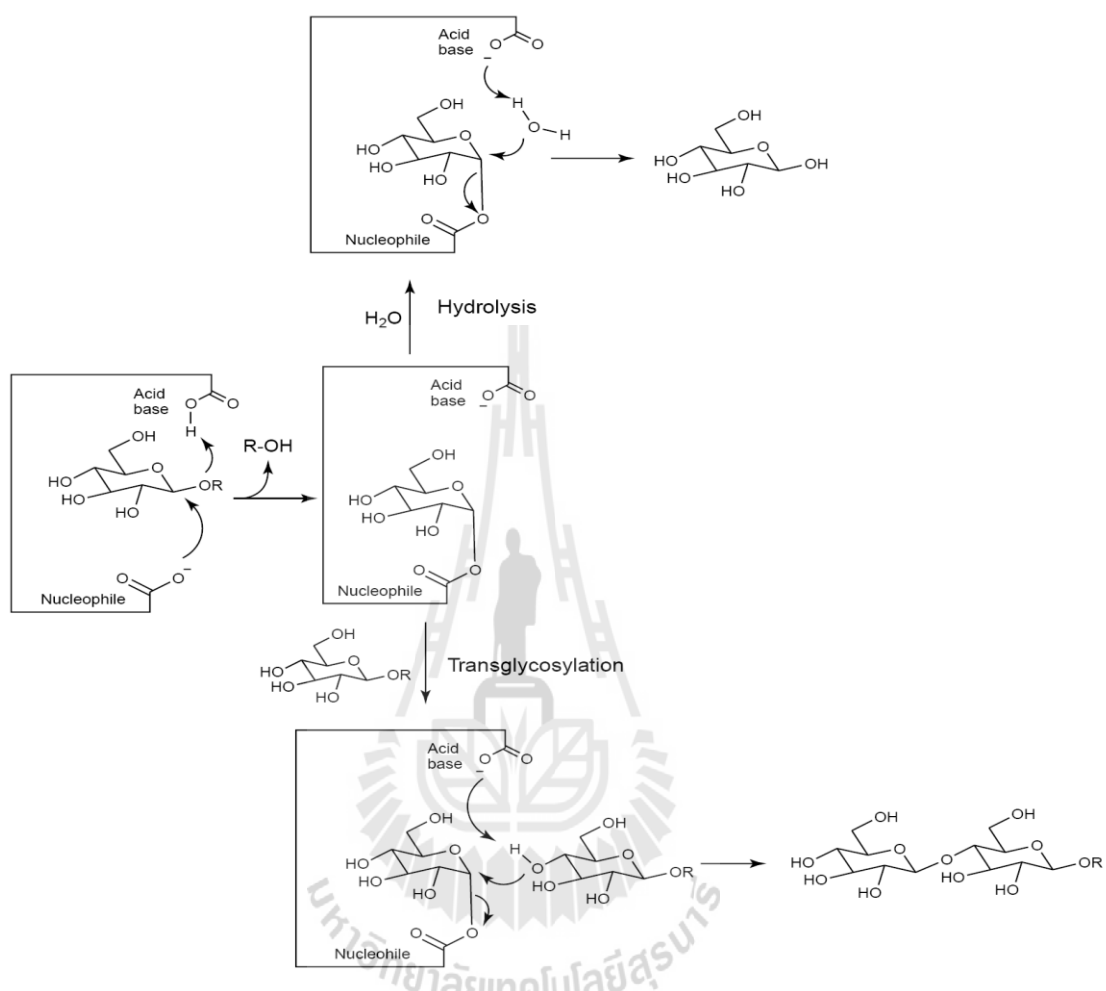


Figure 1.5 Mechanisms of hydrolysis and transglycosylation by retaining glycosidases (Perugino *et al.*, 2004).

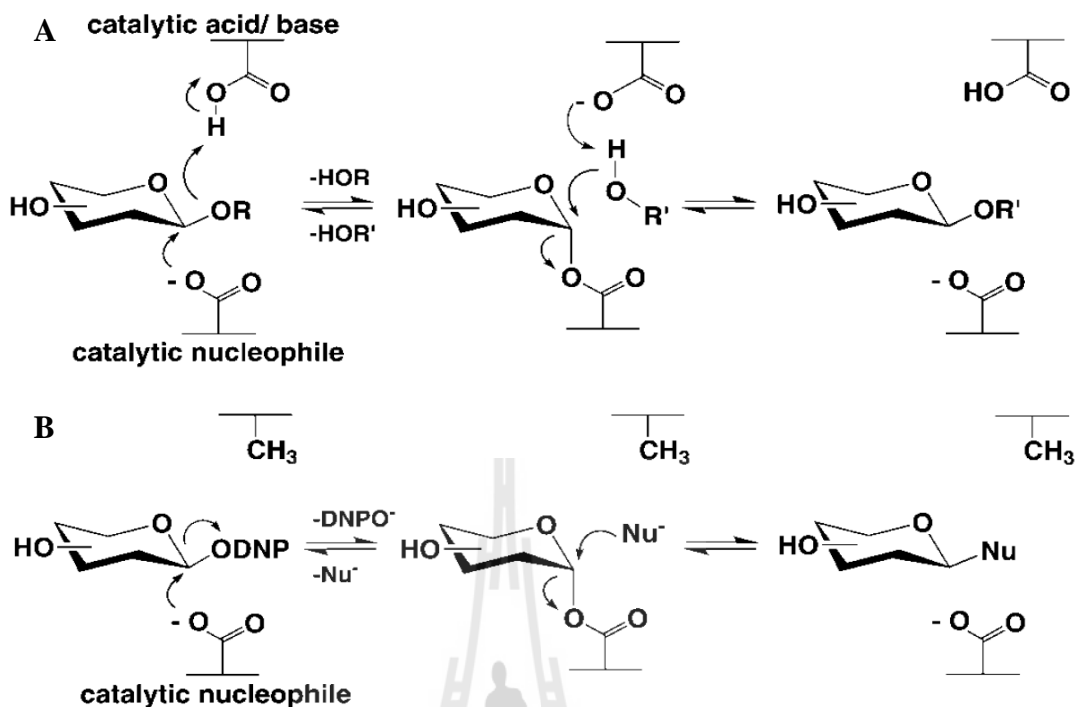


Figure 1.6 Mechanism of glycosylation and deglycosylation with wild-type (A) and acid/base mutant (B) retaining β -glycosidases. DNP = dinitrophenyl, Nu = nucleophile (Jahn *et al.*, 2003).

1.5 Transition state itineraries of β -D-glucosidases and β -D-mannosidase

Transition states occur at the anomeric center of the glycosidic bond when it is cut by either inverting or retaining mechanisms of hydrolysis or transglycosylation. Inverting glycosidases use a general acid/base mechanism to catalyze direct displacement at the anomeric center via an oxocarbenium ion-like transition state. Retaining glycosidases use a double-displacement mechanism in the formation and hydrolysis of a covalent glycosyl enzyme intermediate via a general acid/base catalyzed process, in which both half reactions are thought to pass through oxocarbenium ion-like transition state (Notenboom *et al.*, 1998). The basis for the

oxocarbenium cation-like transition state is the assumption that the glycosidic bond will begin to break before the nucleophile forms a new bond. The development of positive charge on the anomeric carbon draws a free electron pair on the neighboring oxygen into a partial double bond, which requires this electron pair to be in a p-orbital to form a π -bond. This causes the remaining orbitals on the ring oxygen and anomeric carbon to rehybridize to sp^2 , giving them a planar trigonal geometry, in which all other atoms attached to O₅ and C₁ fall in the same plane, including C₅, O₅, C₁, and C₂ (as well as H₁).

This stereoelectronic requirement suggests that the pyranose ring should be deformed at or near the transition state, to the conformation of either a boat ($B_{2,5}$ or $^{2,5}B$) (Figure 1.7 A) or a half-chair (4H_3 or 3H_4) (Figure 1.7 B) or closely related envelope conformations (4E or E_4 , which look similar to the half-chairs). β -mannoside substrates can be hydrolyzed by β -mannosidases and β -mannanases by a retaining mechanism and the crystallographic description of a GH26 β -mannanase reaction coordinate suggested that a unique $B_{2,5}$ mannoside ring conformation may in fact be the transition state conformation (Ducros *et al.*, 2002). This conformation allows a close approach of the mannose 2-hydroxyl to the nucleophile and a strong hydrogen bond forms between the 2-hydroxyl and nonreacting oxygen of the nucleophilic carboxylate in the oxocarbenium ion transition state, as shown in Figure 1.7 (Zechel *et al.*, 2003). The interaction between the 2-hydroxyl and nucleophile would be encouraged in a transition state as the pyranose ring is flattened to a half-chair (4H_3) or boat ($B_{2,5}$) conformation and the nucleophile begins to attack the anomeric carbon. The positive charge at anomeric carbon can be expected to temporarily acidify the

2-hydroxyl to make it a better hydrogen bond donor to the nucleophile (Zechel *et al.*, 2003; Tailford *et al.*, 2008).

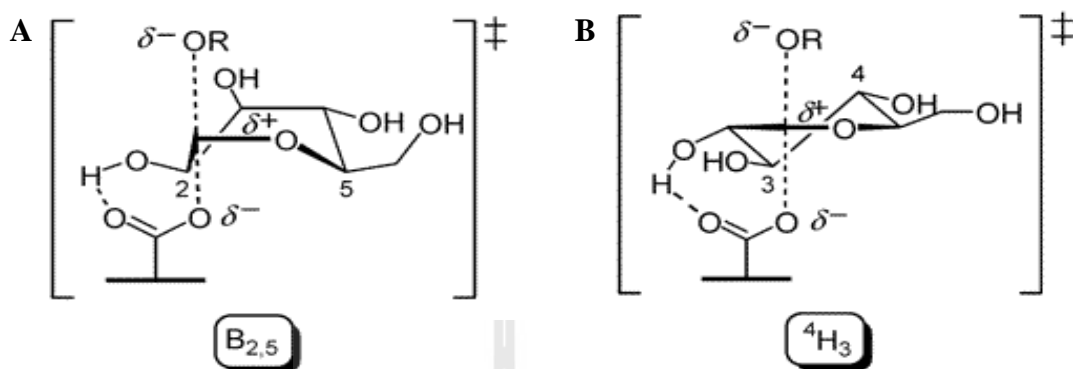


Figure 1.7 The conformations of sugars near the transition state during hydrolysis by glycosidases; (A) transition state of the $B_{2,5}$ boat and (B) transition state of the 4H_3 half-chair (Zechel *et al.*, 2003).

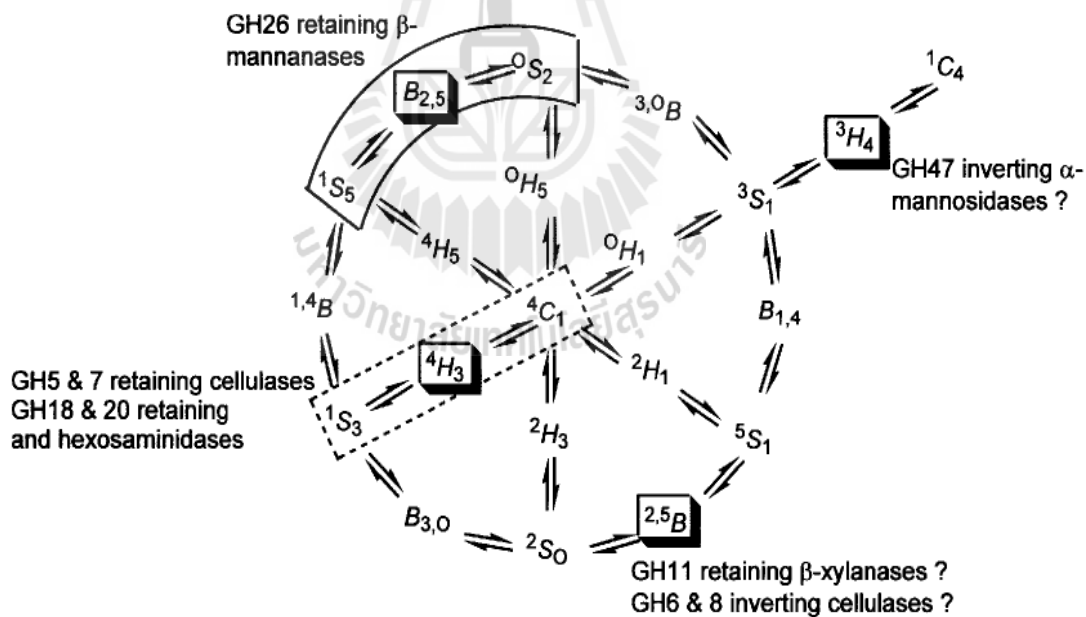
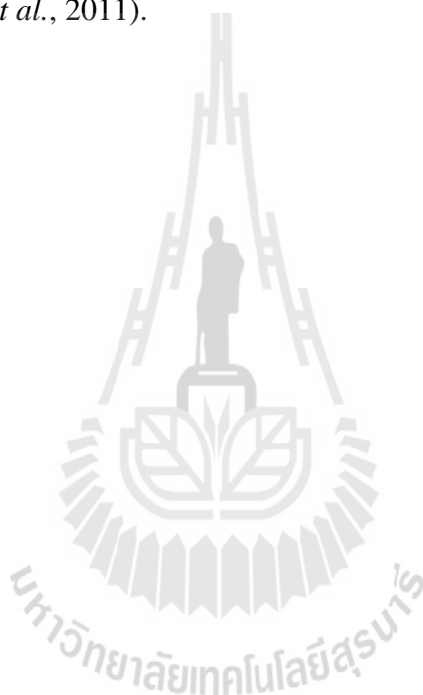


Figure 1.8 Partial map of pyranoside ring interconversion (Davies *et al.*, 2003).

1.6 Rice β -glucosidase

The rice β -glucosidases, which the characterization has been reported to date, can be found in GH1 and the GH1 β -glucosidase BGlu1 (systematically named Os3BGlu7), and is highly expressed in rice (*Oryza sativa*) flower and germinating shoots which is likely the best characterized (Opassiri *et al.*, 2003; 2006). BGlu1 has been expressed in *Escherichia coli*, purified, and characterized (Opassiri *et al.*, 2003; 2004; Chuenchor *et al.*, 2006; 2008), BGlu1 can hydrolyze β -1,3- and β -1,4- linked oligosaccharides and pyridoxine 5'-O- β -D-glucoside, and also has high transglucosylation activity with pyridoxine acceptor (vitamin B₆) to synthesize pyridoxine 5'-O- β -D-glucoside (Opassiri *et al.*, 2004). Glycosynthase E386G, E386A, and E386S mutants of BGlu1 (residue E414 in precursor protein) have been described, and they were able to synthesize long β -1,4-linked gluco-oligosaccharides of at least 11 glucosyl residues (Hommalai *et al.*, 2007). The BGlu1 and a closely related β -mannosidase/ β -glucosidase from barley (rHvBII) both hydrolyze celooligosaccharides with increasing efficiency as their degrees of polymerization (DP) increase from 3 to 6 glucosyl residues. The BGlu1 can hydrolyze *p*-nitrophenyl- β -D-glucopyranoside (*p*NPGlc) faster than *p*-nitrophenyl β -D-mannopyranoside (*p*NPMan), but barley rHvBII is more efficient as a β -mannosidase. Among these and the closely related rice enzymes Os4BGlu8 and Os7BGlu26, only rHvBII can hydrolyze cellobiose with a higher k_{cat}/K_m value than celotriose (Hrmova *et al.*, 1998; Kuntothom *et al.*, 2009). The acid /base mutant of BGlu1 E176Q can be effectively rescued by small nucleophiles, including acetate, azide, and ascorbate in MES and universal buffer at the optimum pH of BGlu1 E176Q of pH 5.0 and this mutant is unusually active with high capacity to transglycosylate anionic nucleophiles

(Chuenchor *et al.*, 2011). In the structure of BGlu1 with 2-deoxy-2-fluoro-glucoside (G2F, PDB code 2RGM), the catalytic nucleophile, E386, and G2F form a covalent bond between the E386 O ϵ 1 atom and G2F anomeric carbon, and also shows five hydrogen bonds between G2F and amino acids at the -1 subsite (Figure 1.9 A) (Chuenchor *et al.*, 2008). The covalent intermediate of BGlu1 E176Q with G2F (3AHV) exhibited similar glucosyl binding as that described for the wild type BGlu1 (2RGM) (Chuenchor *et al.*, 2011).



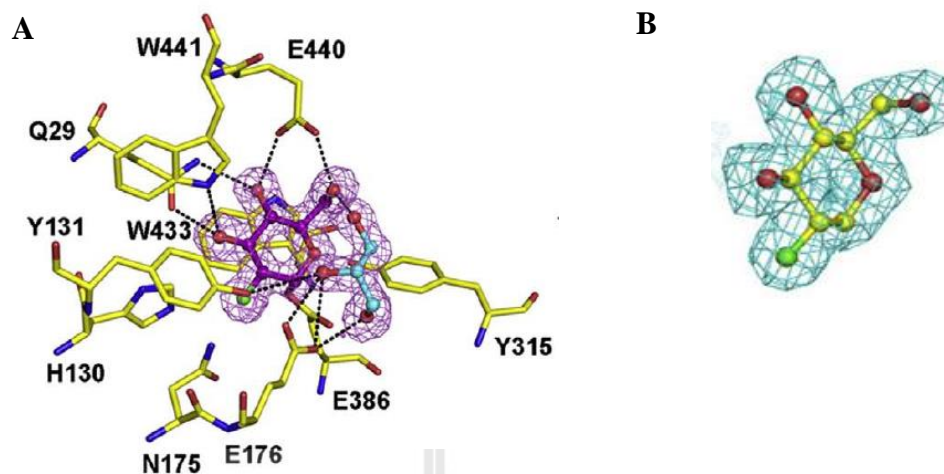


Figure 1.9 Binding of 2-fluoroglucoside (G2F) in the active site of rice BGLu1. (A) The active site of the BGLu1-G2F complex. The amino acid residues surrounding the G2F moiety are shown in stick representation, with carbon in yellow, nitrogen in blue, oxygen in red, and fluoride in green. G2F and glycerol are drawn in ball and stick representation in the same colors, except that the carbon atoms are purple and cyan, respectively. Hydrogen bonds between the protein and the glycone at subsite -1 and glycerol at subsite +1 are drawn as dashed black lines (Chuenchor *et al.*, 2008). (B) The electron density in the active site of BGLu1 E176Q-G2F complex. The amino acid residues surrounding the G2F moiety are presented in stick representation, with carbon in yellow, oxygen in red and fluoride in green (Chuenchor *et al.*, 2011).

1.7 Research objectives

1) To crystallize and determine the structure of BGlu1 E176Q with saturating *p*NPMan, and/or 2,4-dinitrophenyl-2-deoxy-2-fluoro-mannoside.

2) To test whether hydrolysis of *p*NPMan by BGlu1 E176Q can be rescued by small nucleophiles and BGlu1 E176Q can be used to produce transglycosylation products.

3) To optimize the transglycosylation reactions of BGlu1 E176Q with *p*NPGlc and *p*NPMan and *p*-nitrobenzenethiol.



CHAPTER II

MATERIALS AND METHODS

2.1 Materials

2.1.1 Recombinant plasmid and bacterial strains

Production of the recombinant plasmid pET32a(+)*bglu1/E176Q* encoding the E176Q mutant of rice BGlu1 β -glucosidase was previously described (Chuenchor *et al.*, 2006). This plasmid was used to produce the fusion protein of BGlu1 E176Q that contains N-terminal thioredoxin His₆ and S tags and an enterokinase cleavage site. The recombinant plasmid pET32a(+)*bglu1/E176Q* was used for expression in the bacterial host cells *E. coli* strain Origami(DE3), and *E. coli* strain XL1 blue was used for plasmid production.

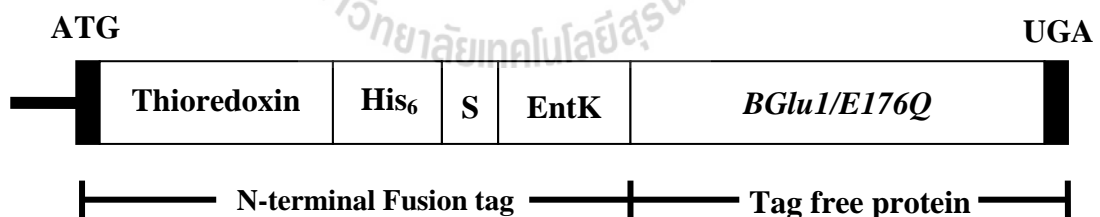


Figure 2.1 Map of the protein sequence encoded by the recombinant pET32a(+) with the *bglu1/E176Q* cDNA inserted after the enterokinase cleavage site.

2.1.2 Chemicals and reagents

Chelating sepharose fast flow resin, lysozyme, *N,N'*-methylene-bisacrylamide, *N,N',N'',N'''*-tetramethylethylenediamine (TEMED) and Triton X-100

were purchased from GE Healthcare (Uppsala, Sweden). Bromophenol blue, Coomassie Brilliant Blue R-250, sodium acetate, sodium carbonate, sodium chloride, sodium dodecyl sulfate (SDS), sodium hydroxide, disodium ethylenediamine tetraacetate (Na₂-EDTA), sulfuric acid, Tris base, methanol, ethanol, glacial acetic acid, glycine and ethyl acetate were purchased from Carlo ERBA (Milano, Italy). Acrylamide, imidazole, bovine serum albumin (BSA), dichlorodimethylsilane, polyethylene glycol monomethyl ether (PEG MME) 5000, 2-(N-morpholino)-ethanesulfonic acid (MES) were purchased from Fluka (Steinheim, Switzerland). Ammonium sulfate, calcium chloride and thin layer chromatography silica gel 60 aluminum F₂₅₄ plates for oligosaccharide detection were purchased from Merck (Darmstadt, Germany). Isopropyl thio-β-D-galactoside (IPTG) was purchased from United States Biological (Swampscott, MA, USA). Ammonium persulfate, ampicillin, tetracycline, DNase I, Bis-Tris, 2-mercaptoethanol, *p*-nitrophenyl-β-D-glucopyranoside (*p*NPGlc), *p*-nitrophenyl-β-D-mannopyranoside (*p*NPMan) and phenylmethylsulfonylfluoride (PMSF) were purchased from Sigma (St. Louis, MO, USA). Peptone, yeast extract and bacto-agar were purchased from Hi-Media (Mumbai, India). Ultrafiltration membranes (Centricon, 30 kDa MW and 10 kDa MW cut off) and Ultrafree MC 0.22 μm filters were purchased from Millipore Corporation (Bedford, MA, USA). High vacuum grease was purchased from Dow Corning (Midland, MI, USA). HPLC-grade distilled water and acetonitrile were purchased from RCI Labscan (Bangkok, Thailand). Liquid nitrogen was obtained from the Center for Scientific and Technological Equipment of Suranaree University of Technology and the National Synchrotron Radiation Research Center, Hsinchu, Taiwan.

2.2 Methods

2.2.1 Transformation of expression host with recombinant expression plasmid

Each expression experiment was started with a fresh transformation of recombinant pET32a(+)*bglu1/E176Q* to the expression host, *E. coli* strain Origami (DE3) competent cells. Ten to one hundred nanograms of plasmid DNA was added to 50 μ l of thawed competent Origami(DE3) cells, which were then mixed gently by swirling the tube and incubated on ice for 30 min. The mixed cells were transformed by heat shocking at 42°C for 45 s and immediately chilled on ice for 3 min. Then, 450 μ l of Lennox broth (LB, 10 g/l tryptone, 5 g/l yeast extract, and 5 g/l sodium chloride) was added, and the cells were incubated at 37°C for 45 min. Then, 100 μ l of cells were spread on an LB agar plate containing 15 μ g/ml kanamycin, 12.5 μ g/ml tetracycline and 50 μ g/ml ampicillin, and incubated at 37°C, overnight.

2.2.2 Protein expression of BGLu1 E176Q

For expression, a single colony was inoculated into 5 ml of LB broth containing 15 μ g/ml, kanamycin, 12.5 μ g/ml tetracycline and 100 μ g/ml ampicillin and the culture was incubated at 37°C in an incubator shaker for 16 h. This starter culture was inoculated at 1% volume in LB broth containing 15 μ g/ml kanamycin, 12.5 μ g/ml tetracycline and 50 μ g/ml ampicillin, and incubated for 4-5 h at 37°C, 200 rpm, until the OD₆₀₀ reached 0.4-0.6. Then, IPTG was added to a final concentration of 0.4 mM to induce expression of the protein target, and the culture was grown for a further 18 h at 20°C. The induced cells were collected by

centrifugation at 4,500 rpm for 15 min., and then were kept at -80°C. The frozen cells were extracted with extraction buffer (50 mM sodium phosphate buffer, pH 7.0, 150 mM sodium chloride, 200 µg/ml lysozyme, 1% Triton-X 100, 1 mM PMSF, 4 µg/ml DNase I). The pellet suspension was incubated at room temperature 30 min and soluble protein was separated from insoluble debris by centrifugation at 12,000 rpm for 15 min. at 4°C.

2.2.3 Protein purification of BGlu1 E176Q

2.2.3.1 Thioredoxin fusion protein

The fusion protein was purified by immobilized metal-affinity chromatography (IMAC) on cobalt resin. Ten milliliters of soluble protein was added to cobalt resin (1 ml), and the slurry was gently shaken (60 rpm) for 30 min and centrifuged at 1,000 rpm. The resin was then put into a column, washed with 5 column volumes (CV) of equilibration buffer (50 mM phosphate buffer, pH 7.0 and 150 mM NaCl), 5 CV of 5 mM imidazole in equilibration buffer, and 5 CV of 10 mM imidazole in equilibration buffer. The protein was eluted with elution buffer (150 mM imidazole in equilibration buffer) with collection of 1 ml fractions. The purification fractions were assayed for β-glucosidase activity with 1 mM *p*-nitrophenol β-D-glucopyranoside (*p*NPGlc) as described by Opassiri *et al.* (2003). Then, the fractions of protein containing activity were pooled and imidazole was removed and the buffer changed to 20 mM Tris-HCl, pH 8.0, in a 30 kDa molecular weight cut-off (MWCO) Centricon centrifugal filter (Millipore, Beverly, MA, USA).

2.2.3.2 Removal of the fusion tag and purification of tag-free protein

Since the thioredoxin fusion tag might interfere with crystallization, only the non-fusion protein was used for crystallization. To remove the N-terminal fusion tag, the BGlu1 E176Q fusion protein was cleaved with 0.1 μ g enterokinase (New England Biolabs, Ipswich, MA, USA) per milligram of protein in 20 mM Tris-HCl, pH 8.0, at 23°C for 16 h. The tag-free protein was separated from the fusion tag and uncleaved fusion protein by loading the protein onto a cobalt-bound IMAC column, and collecting the fractions of unbound protein. The resin was washed with 5 and 10 mM imidazole in equilibration buffer (50 mM phosphate buffer, pH 7.0 and 150 mM NaCl) to elute remaining tag-free protein and the fusion tag was eluted from the resin with 150 mM imidazole in equilibration buffer. The fractions were evaluated by β -glucosidase assays and SDS-PAGE to determine the fractions containing tag-free β -glucosidase. The unbound and wash fractions containing tag-free BGlu1 E176Q were combined, and the protein was concentrated in a 10 kDa MWCO centricon centrifugal filter until the volume was 50 μ l. The protein was finally further purified by gel-filtration on a Superdex S-200 column (HR10/300, GE Healthcare, England) eluted with 20 mM Tris-HCl, and 150 mM NaCl at 1 ml/min, as previously described (Chuenchor *et al.*, 2006; 2008; 2011). The peak fractions containing the purified protein were pooled and concentrated with a 10 kDa MWCO centricon centrifugal filter to obtain approximately 10 mg/ml pure protein for crystallization in complexes with 2-deoxy-2-fluoro- β -D-mannoside (DNP2FM) and *p*NPMan.

2.3 Protein analysis

2.3.1 SDS-PAGE electrophoresis

SDS-polyacrylamide gel electrophoresis (SDS-PAGE) was done by the method of Laemmli (Laemmli, 1970). The 12% SDS-PAGE separating gel consisted of 12% (w/v) acrylamide, 0.375 M Tris-HCl, pH 8.8, 0.1% SDS, 0.1% ammonium persulfate and 0.05% TEMED and the 4% stacking gel consisted of 5% (w/v) acrylamide, 0.126 M Tris-HCl, pH 6.8, 0.1% SDS, 0.1% ammonium persulfate, and 0.05% TEMED. Protein samples were mixed with 4:1 with 5X loading buffer (0.05 M Tris-HCl, pH 6.8, 10% SDS, 0.2 mg/ml bromophenol blue, 50% glycerol, and 20% 2-mercaptoethanol) and boiled for 5 min to denature the proteins. Aliquots of 10 μ l were loaded into sample wells and electrophoresed at 120 V in 1X Tris-glycine electrode buffer (0.05 M Tris base, 0.125 M glycine and 0.1% SDS, pH 8.3) until the bromophenol blue dye front reached the bottom of the gel plate. The gels were stained in staining solution containing 0.1% (w/v) Coomassie Brilliant Blue R250, 40% (v/v) methanol, 10% (v/v) acetic acid for 1 h and destained with destaining solution [40% (v/v) methanol and 10% (v/v) acetic acid] for 1-2 h. The protein molecular weights were estimated by comparison to standard of low molecular weight protein markers (GE Healthcare, Uppsala, Sweden), which consist of phosphorylase b (97.4 kDa), bovine serum albumin (66 kDa), ovalbumin (45 kDa), bovine carbonic anhydrase (31 kDa), trypsin inhibitor (21.5 kDa) and bovine α -lactalbumin (14.0 kDa).

2.3.2 β -Glucosidase activity

The β -D-glucosidase activity of BGlu1 E176Q was determined by mixing with 1 mM *p*NPGlc in 50 mM sodium acetate, pH 5.0, in 140 μ l reactions.

The reactions were incubated at 37°C for 10 min. and stopped with 70 µl 2 M sodium carbonate. The *p*-nitrophenol (*p*NP) released was quantified by measuring the absorbance of *p*-nitrophenolate at 405 nm in an iEMS reader MF microplate photometer (Labsystem iMES MF, Finland) and subtracting the absorbance of a control of reaction without enzyme. The *p*NP released was determined by comparing the absorbance with that of a *p*NP standard curve in the same buffers.

2.3.3 Bio-Rad protein assay

The concentration of protein in the purification fractions was determined by Bradford assay (Bradford *et al.*, 1976) with a Bio-Rad kit (Hercules, CA, USA) with bovine serum albumin (BSA) as a standard (0-10 µg). The assay solution contained suitably diluted enzyme in distilled water in a total volume of 800 µl and 200 µl of Bio-Rad reagent. The solution was mixed and incubated at room temperature for 10 min, and the absorbance at 595 nm was measured with a Genesys 10 UV-visible spectrophotometer (Spectronic Instruments, Rochester, NY, USA).

2.4 Protein crystallization

2.4.1 Crystallization by hanging drop

Purified protein was concentrated by Centricon centrifugal filter to 10-20 mg/ml in 20 mM Tris-HCl, pH 8.0, 150 mM NaCl. Before crystallization, the protein solution was filtered through an Ultrafree-M 0.22 µm filter (Millipore) at 4,000 g for 5 min. BGlu1 E176Q was crystallized as free crystals of BGlu1 E176Q and co-crystallized with varied concentrations of 2-deoxy-2-fluoro-β-D-mannoside (DNP2FM) and *p*-nitrophenol β-D-mannopyranoside (*p*NPMan) by the hanging drop

vapor diffusion method with microseeding (Weber, 1997) in a 24 well TC-plate (Hampton Research or Greiner Bio-One, Germany). Glass cover slips (Menzel-Glaser, Braunschweig, Germany) were siliconized to prevent spreading of the protein drop on the surface of the cover slips. For siliconization, the glass cover slips were washed with the ratio of 1: 3 (v/v) of 0.1 M HCl and absolute methanol for 30 min, then washed with deionized water three time. Finally, 400 μ l of dimethyldichlorosilane was added and the cover slips were incubated at 60°C overnight. Then, high vacuum grease (Dow Corning, Michigan, USA) was spread around the top edge of each well, and each well was filled with 0.5 ml of the appropriate precipitant. The protein and precipitant solutions were pipetted together on the cover slip and the cover slip with the protein drop was inverted to hang the drop over the well.

Conditions for the crystallization were optimized from the conditions used for crystallization of BGlu1 (Chuenchor *et al.*, 2006; 2008) by varying the precipitant concentration around 20% to 23% polyethylene glycol 5000 monomethyl ether (PEG 5000 MME) and 0.17 M to 0.22 M $(\text{NH}_4)_2\text{SO}_4$, in 0.1 M MES, pH 6.7, and varying the BGlu1 E176Q protein concentration from 2 mg/ml to 5 mg/ml. A drop of 2 μ l of pure protein was mixed with 1 μ l of precipitant solution on a siliconized cover slip and the drops were equilibrated against a reservoir containing 0.5 ml of precipitant solution. The crystallization plate was incubated at 15°C and the development of the crystals was checked under a microscope.

2.4.2 Microseeding method

The microseeds were prepared from crystal clusters or small crystals. These were removed from their initial drop, and then transferred to 10 μ l of reservoir

solution to wash the crystal three times. They were then crushed with a cat whisker on the cover slip, the fragments were suspended in the reservoir solution, and the suspension was added to 1.5 ml microcentrifuge tube containing 100 μ l of reservoir solution and kept for a stock. Before use, the stock was diluted with mother liquor to 1/100 and was stored at 4°C. Pre-equilibration time before seeding was 2 h. A cat whisker was dipped in a seeding solution and streaked into the drop containing protein and the plate was incubated at 15°C (Chuenchor *et al.*, 2006; 2008).

2.4.3 Co-crystallization with complex

BGlu1 E176Q mixtures with DNP2FM and *p*NPMan were used for hanging drop vapor diffusion crystallization at 15°C. A concentration of 1 mM DNP2FM or *p*NPMan was mixed with the protein solution in the concentration range from 2 to 5 mg/ml at 4°C. The hanging drops consisted of 2 μ l of protein mixture solution and 1 μ l of precipitant solution and the drops were equilibrated with 0.5 ml of precipitant solution, then after 2 h equilibration the BGlu1 E176Q seeds were added, as described above, and the crystallization plates were kept at 15°C.

2.4.4 Soaking of crystal

A free crystal of BGlu1 E176Q was removed from the drop with a nylon loop and cleaned in a series of fresh precipitant solution drops on a cover slip. Then, the crystal was transferred to a new drop of precipitant solution containing 100 mM *p*NPMan for 10 min, 20 min, 30 min or 1 h.

2.4.5 Data collection and processing

2.4.5.1 Freezing in cryoprotectant

The crystals of BGlu1 E176Q were soaked in cryoprotectant solution containing 18% (v/v) glycerol and the precipitant components at concentrations that were increased 15% compared to the original precipitant components to protect the crystals from dissolving and from ice crystal formation. The crystals were frozen on liquid nitrogen. The crystals were soaked in 5 μ l of cryoprotectant for 30 min, 1 or 2 h at 15°C. The crystals were mounted in a nylon loop (Hampton Research, Laguna, CA, USA, 0.1-0.2 mm) and transferred into 5 μ l of cryoprotectant solution for 30 s, then flash vitrified in liquid nitrogen at -180°C for X-ray diffraction.

2.4.5.2 Synchrotron X-ray diffraction

The BGlu1 E176Q complex crystals were diffracted with synchrotron radiation as the X-ray source at the BL13B1 beamline of the National Synchrotron Radiation Research Center (NSRRC), Hsinchu, Taiwan. The reflections were collected with the ADSC Quantum 315 CCD detector at BL13B1. The crystal within its cryo-loop was placed onto the goniometer head between the X-ray beam and the detector. During X-ray diffraction, the distance between the crystal and detector was 300.0 mm for the BGlu1 E176Q complexes. The X-ray wavelength was set at 1.00 Å and crystals were kept at 100 K with a nitrogen stream from an Oxford Cryosystems Cryo-stream during diffraction. A crystal was collected for 180° rotation or until the data were complete with 0.50° oscillations, and the exposure time per

frame of 5-30 s. All the diffraction images were indexed, integrated and scaled with the HKL-2000 program (Otwinowski and Minor, 1997).

2.4.5.3 Structure solution by molecular replacement

The crystal structure of BGlu1 E176Q was solved by the molecular replacement method, using the *MOLREP* program (Vagin and Teplyakov, 1997). The data sets of the BGlu1 E176Q complex crystals were solved with the native structure of rice BGlu1 E176Q (3AHT, Chuenchor *et al.*, 2011) as a search model for rigid body refinement, including the two molecules per asymmetric unit.

2.4.5.4 Model building, structure refinement and validation of the final model

The analysis of the $F_{\text{obs}} - F_{\text{cal}}$ and $2F_{\text{obs}} - F_{\text{cal}}$ electron density maps, and model building were done in the Coot program (Emsley and Cowtan, 2004). The refinement was done with REFMAC5 in the CCP4 suit, by varying of the non-crystallographic symmetry (NCS) restraints for structure refinement. The water molecule positions were checked in the refinement stages by inspecting the $2F_{\text{obs}} - F_{\text{cal}}$ electron density map for peaks at a height of at least 1.3σ and seeing if they were within hydrogen-bonding distance of other hydrogen bonding groups. The stereochemistry of the final models was checked with PROCHECK (Laskowski *et al.*, 1993).

2.5 Rescue of *p*NPMan and *p*NPGlc hydrolysis by small nucleophiles

2.5.1 Reaction of *p*NPMan and *p*NPGlc

Reactions of 1 mM *p*NPMan or *p*NPGlc with 50 mM azide in 50 mM sodium acetate buffer, pH 5.0, and 50 mM MES buffer, pH 5.0, were set-up with 1 mg/ml of BGlu1 E176Q for varied incubation times of 18, 24, 36, and 48 h.

The activity of BGlu1 E176Q was tested with small nucleophiles, including azide, acetate, formate, fluoride (KF), ascorbate, dithiothreitol (DTT), pyridine, imidazole, β -mercaptoethanol, sulphite, cyanide, thiocyanate and benzoic acid in 50 mM MES buffer, pH 5.0, and 50 mM sodium acetate buffer, pH 5.0. For the transglycosylation reactions, the concentration of *p*NPMan was varied at 1 mM and 10 mM in 50 mM MES buffer, pH 5.0, or 50 mM sodium acetate buffer, pH 5.0, and the concentration of protein was varied from 1 mg/ml to 4 mg/ml. The time of reaction was varied from 1 day to 4 days at 30°C, the reactions were stopped by boiling for 5 min, and the products were checked by thin layer chromatography (TLC) on analytical F₂₅₄ silica gel plates. The TLC used a mobile phase of 2:1:1 (v/v) ethylacetate: acetic acid: water. The products containing sugar were detected by staining with 10% (v/v) sulfuric acid in ethyl alcohol and heating at 120°C for 10 min. The reaction of small nucleophiles in MES buffer, pH 5.0, and sodium acetate buffer, pH 5.0, contained 10 mM *p*NPMan, 50 mM nucleophile and 4 mg/ml of BGlu1 E176Q, which was incubated at 30°C for 1 day. The reactions were stopped by boiling them for 5 min, and then the products were checked on TLC.

2.6 Transglycosylation of *p*-nitrobenzenethiol

The transglycosylation of BGlu1 E176Q with *p*-nitrophenyl- β -D-glucopyranoside (*p*NPGlc) was previously studied by Cheunchor *et al.* (2011) by comparing the release of *p*NP in various anion nucleophiles to that without nucleophiles, and the analyzing the unknown compounds produced by TLC. In this study, the transglycosylation of *p*NPGlc with *p*-nitrobenzenethiol (NBT) in water, 10, 50 mM MES buffer, pH 5.0 and 10, 50 mM sodium acetate, pH 5.0, in a reaction consisting of 10 mM *p*NPGlc and 2 mM, 5 mM and 10 mM concentrations of NBT in water, 10 or 50 mM MES buffer, pH 5.0, or 10 or 50 mM sodium acetate, pH 5.0. The time was varied from 1 to 4 days at 30°C, and the concentration of protein varied from 1 mg/ml to 4 mg/ml. The reactions were stopped by boiling 5 min. The products of the reactions were checked on TLC and HPLC.

Transglycosylation reactions of *p*-nitrophenyl- β -D-glucopyranoside (*p*NPMan) with *p*-nitrobenzenethiol (NBT) were optimized by varying the concentrations of *p*NPMan and NBT at 2, 5, and 10 mM, the concentration of protein from 1 mg/ml to 5 mg/ml and the reaction times at 18 h, and 2, 3, and 4 days in 30°C, and varying the buffer by setting the reactions in water, 10 and 50 mM sodium acetate buffer, pH 5.0, and 10 and 50 mM MES buffer, pH 5.0. The reactions were stopped by boiling 5 min. Products of the reactions were checked on TLC and HPLC.

2.6.1 TLC analysis

The products of the transglycosylation of NBT reactions in section 2.6 were spotted onto analytical F₂₅₄ TLC plates and compared with the standards of *p*NP, *p*NPGlc, glucose, β -thioglucoside, and NBT for the reactions with *p*NPGlc donor and

with the standards of *p*NP, *p*NPMan, mannose, β -thiomannoside, α -thiomanoside, and NBT for the reactions with *p*NPMan. The mobile phase was 15:2:2:1 (v/v/v/v) butanol: acetic acid: water: methanol. The product sugar was detected by staining with 10% (v/v) sulfuric acid in ethyl alcohol and heating at 120°C for 10 min.

2.6.2 HPLC analysis

The product of the transglycosylation reaction in section 2.6 was also detected by HPLC to quantify it in comparison to the *p*NP, *p*NPGlc, β -thioglucoside, *p*NPMan, β -thiomannoside, α -thiomanoside, and NBT standards. The column used was a ZORBAX Eclipse XDB-C18 analytical 4.6×150 mm 5 micron (Agilent Technologies) and the condition for separation of the products of transglycosylation was a gradient from 0.1% formic acid in water (HPLC grade) to 0.1% formic acid in methanol (HPLC grade) according to the time frame shown in the Table 2.1. The reaction products were separated at a flow rate of 1.0 ml/min and detected by absorbance on a diode array detector (DAD) at 254 nm wavelength.

Table 2.1 The gradient for HPLC separation of the products of transglycosylation.

Time (min)	0.1% formic acid in water (%)	0.1% formic acid in methanol (%)
0	90	10
20	20	80
25	0	100
30	0	100

CHAPTER III

RESULTS

3.1 Recombinant expression and purification of BGlu1 E176Q

BGlu1 E176Q fusion protein containing N-terminal thioredoxin and His₆ fusion tags was expressed in recombinant *E.coli* stain Origami(DE3). The expressed protein was purified by 2 steps of IMAC on Co²⁺ resin. In the first step, the recombinant BGlu1 E176Q protein containing the His₆ tag was loaded on the resin and washed, then eluted with 150 mM imidazole in equilibration buffer. The protein was checked by SDS-PAGE, which showed the major band of the fusion protein at 66 kDa (Figure 3.1). The BGlu1 E176Q protein was pooled, the buffer changed to 20 mM Tris-HCl, pH 8.0, and the N-terminal thioredoxin and His₆ tag were cleaved from BGlu1 E176Q with enterokinase. After cleavage, the free BGlu1 E176Q protein was purified by adsorbing the thioredoxin and His₆ tags on the same IMAC column. The free BGlu1 E176Q protein, which had an apparent mass of 55 kDa on SDS-PAGE, eluted in equilibration buffer, while the thioredoxin and His₆ could later be eluted with 150 mM imidazole in equilibration buffer (Figure 3.2). After concentration of the free BGlu1 E176Q protein by centrifugal filtration, it was further purified by gel filtration on a Superdex S-200 column. In a typical purification is shown analyzed by SDS-PAGE in Figure 3.3. In this preparation, fractions 31-37 had high absorbance and activity, and the pool of these fractions showed the same pattern after it was concentrated by

centrifugal filtration until the protein concentration reached about 10 mg/ml, which was used as the stock for crystallization experiments.

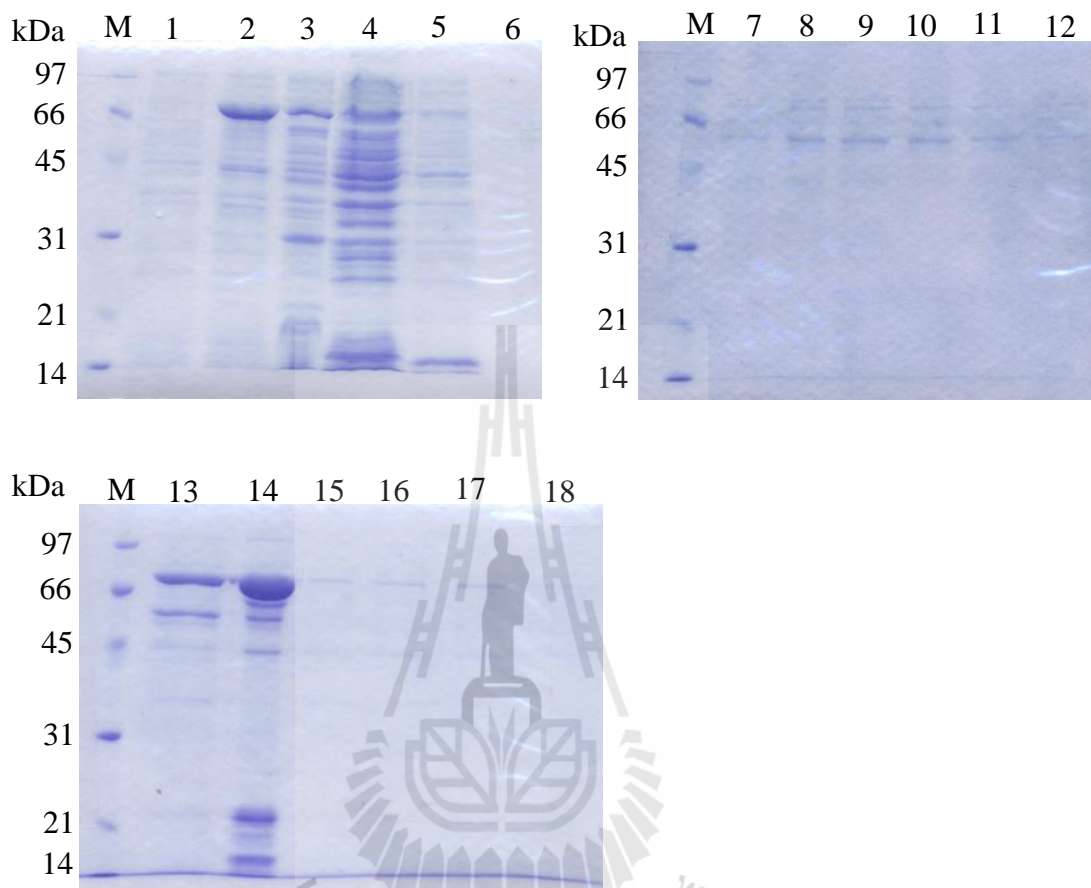


Figure 3.1 SDS-PAGE of recombinant thioredoxin and His₆ tagged BGlul E176Q protein IMAC purification fractions. Lane M, protein molecular weight marker. Lane 1, extract of uninduced *E. coli* cells containing pET32(a+)/DEST-BGlul E176Q. Lane 2, extract of *E. coli* cells containing pET32(a+)/DEST-BGlul E176Q after induction. Lane 3, soluble protein from induced cell extract. Lane 4, flowthrough of IMAC column. Lane 5, protein washed from IMAC column with equilibration buffer. Lane 6, protein washed from IMAC column with 5 mM imidazole. Lanes 7-12, protein fractions 1-6 washed from IMAC column with 10 mM imidazole. Lanes 13-18, protein in fractions 1-6 eluted with 150 mM imidazole.

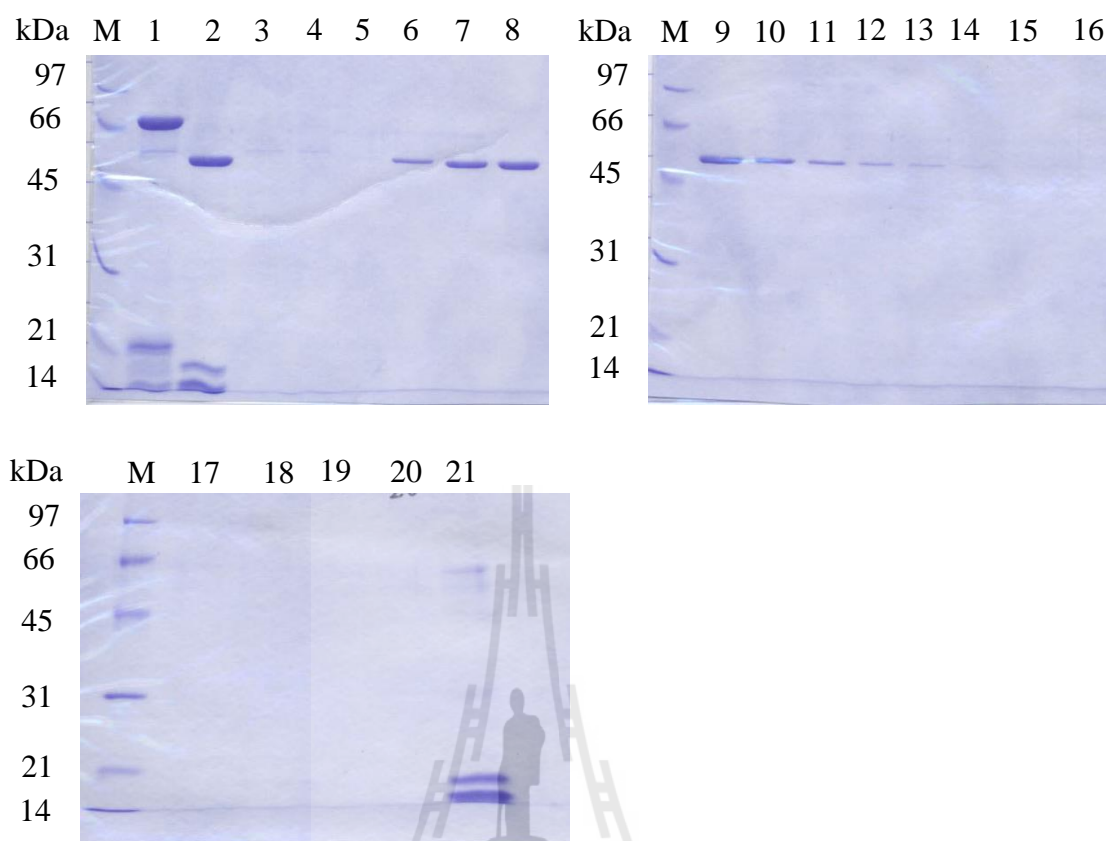
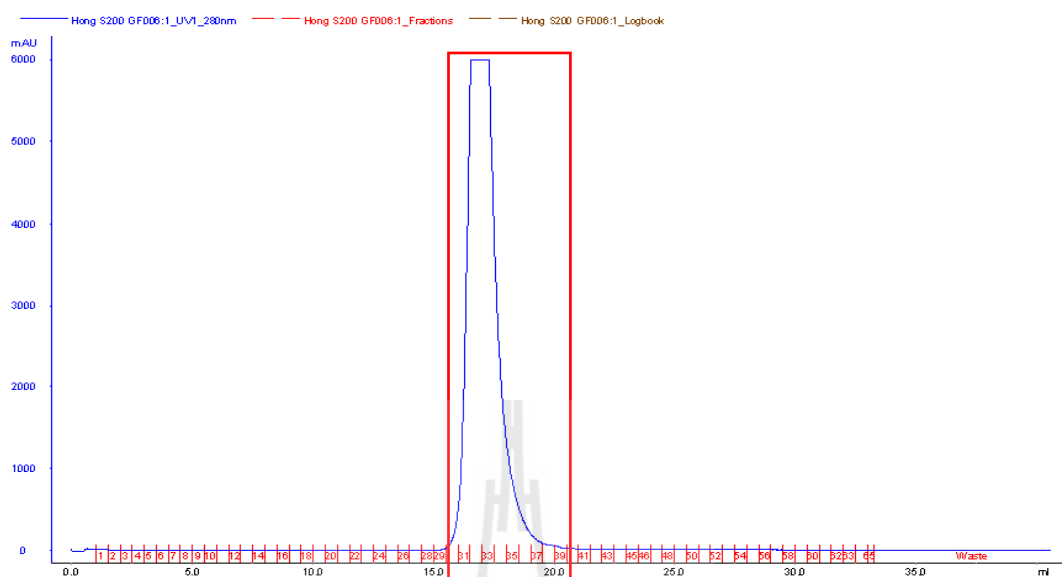


Figure 3.2 SDS-PAGE of fractions from purification of BGlul E176Q by cleavage with enterokinase and adsorption of tag protein with a second IMAC step. Lane M, low molecular weight protein marker. Lane 1, BGlul E176Q fusion protein preparation before cleavage with enterokinase. Lane 2, BGlul E176Q fusion protein after cleavage with enterokinase. Lane 3, flow-through fraction of 2nd IMAC step. Lanes 4-15, fractions 1 to 12 of BGlul E176Q protein eluted in the wash with equilibration buffer collected to contain 1 column volume per fraction. Lanes 16-17, protein eluted in the wash with 5 mM imidazole collecting 1 column volume per fraction. Lanes 18-19, protein eluted in fractions 1 and 2 of the wash with 10 mM imidazole. Lanes 20-21, elution fractions 1 and 2 containing N-terminal thioredoxin and His₆ tag eluted with 150 mM imidazole.

A



B

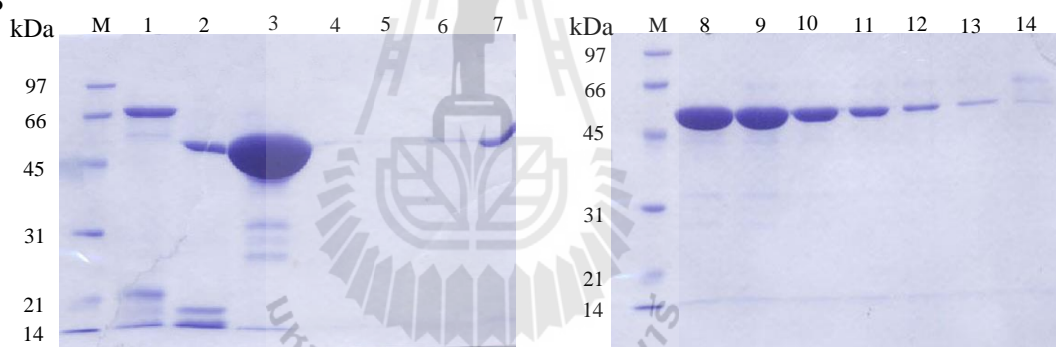


Figure 3.3 Elution profile of the BGlul E176Q protein without fusion tag obtained from Superdex S-200 gel filtration chromatography and SDS-PAGE of the protein peak fractions. A, The 280 nm absorbance profile of the protein elution from the Superdex S-200 column. The separation was done in a Superdex S-200 column on an ÄKTA purifier system. The protein was eluted with 20 mM Tris-HCl, pH 8.0, and 150 mM NaCl, at a flow rate of 1 ml/min. B. The SDS analysis of the purification fractions. Lane M, molecular weight markers; Lane 1, BGlul E176Q fusion protein preparation before cleavage with enterokinase; Lane 2, BGlul E176Q fusion protein after cleavage with enterokinase; Lane 3, BGlul E176Q after purification over the

2nd Co²⁺ IMAC column; Lanes 4-14, BGlu1 E176Q fractions separated by Superdex S-200 column. The fractions of BGlu1 E176Q in lanes 7-13 were pooled and concentrated in a 10 kDa molecular weight cut-off (MWCO) Centricon centrifugal filter to 10 mg/ml for crystallization.

3.2 Crystallization of BGlu1 E176Q

3.2.1 Crystallization by hanging drop

The BGlu1 E176Q protein was crystallized by the hanging drop vapor diffusion method, in which each drop contained 2 μ l of protein and 1 μ l of precipitant solution. As described in section 2.4.1, the concentrations of PEG 5000 MME, (NH₄)₂SO₄ and BGlu1 E176Q protein were varied and the initial crystals were used for microseeding to produce high quality crystals. Figure 3.4 A shows the crystal of BGlu1 E176Q co-crystallized with 10 mM DNP2FM produced after 2 months in 23% PEG MME 5000, 0.19 M (NH₄)₂SO₄, 0.1 M MES, pH 6.7. Figure 3.4 B shows the crystal of BGlu1 E176Q co-crystallized with 10 mM *p*NPMan produced after 2 months in 23% PEG MME 5000, 0.18 M (NH₄)₂SO₄, 0.1 M MES, pH 6.7. Figures 3.4 C, D, E, and F show crystals soaked with 100 mM *p*NPMan for 10, 20, 30, and 60 min, respectively, at 15°C.

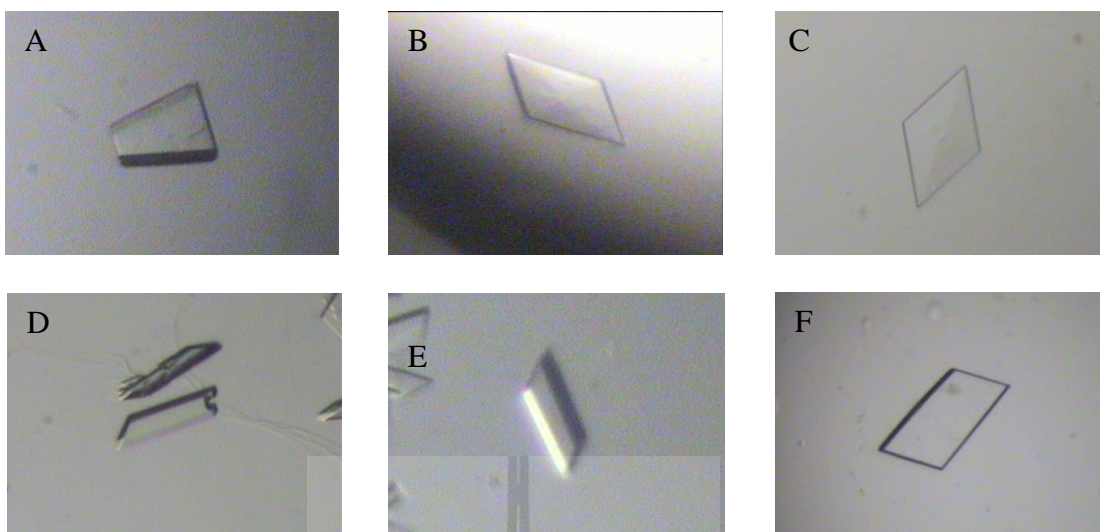


Figure 3.4 Crystals of BGluc1 E176Q. (A) Crystal produced by co-crystallization with 10 mM 2-deoxy-2-fluoro- β -D-mannoside (DNP2FM) in 23% PEG MME 5000, 0.19 M $(\text{NH}_4)_2\text{SO}_4$, 0.1 M MES, pH 6.7, with dimensions of 60 x 90 x 10 μm ; (B) Crystal produced by co-crystallization with 10 mM *p*-nitrophenol β -D-mannopyranoside (*p*NPMan) in 23% PEG MME 5000, 0.18 M $(\text{NH}_4)_2\text{SO}_4$, 0.1 M MES, pH 6.7, with dimensions of 60 x 90 x 10 μm ; (C-F) Crystals soaked with 100 mM *p*NPMan in 10, 20, 30 and 60 min, respectively. The crystal in C had dimensions of 90 x 90 x 10 μm and was produced in 20% PEG MME 5000, 0.22 M $(\text{NH}_4)_2\text{SO}_4$, 0.1 M MES, pH 6.7; the crystal in D had dimensions of 50 x 100 x 10 μm and was produced in 23% PEG MME 5000, 0.20 M $(\text{NH}_4)_2\text{SO}_4$, 0.1 M MES, pH 6.7; The crystal in (E) had dimensions of 60 x 120 x 10 μm and was produced in 22% PEG MME 5000, 0.22 M $(\text{NH}_4)_2\text{SO}_4$, 0.1 M MES, pH 6.7; and the crystal in (F) had dimensions of 100 x 160 x 10 μm , and was produced in 20% PEG MME 5000, 0.22 M $(\text{NH}_4)_2\text{SO}_4$, 0.1 M MES, pH 6.7. All crystals were produced by the hanging drop vapor diffusion method.

3.2.2 Datasets collected for crystals produced for mannoside complexes.

Crystals of BGlu1 E176Q cocrystallized or soaked with mannosides were used to X-ray diffraction, the crystal cocrystallized with 10 mM *p*NPMan and soaked with 100 mM *p*NPMan from diffraction data showed the crystal of both BGlu1 E176Q cocrystallized with 10 mM *p*NPMan and soaked with 100 mM *p*NPMan belong to the $P2_12_12_1$ space group, with very similar unit cell parameters of $a = 79.5 \text{ \AA}$, $b = 101.3 \text{ \AA}$, $c = 127.9 \text{ \AA}$ ($\alpha = \beta = \gamma = 90^\circ$) and $a = 79.4 \text{ \AA}$, $b = 101.7 \text{ \AA}$, $c = 127.7 \text{ \AA}$ ($\alpha = \beta = \gamma = 90^\circ$), respectively. The statistics of data collection are listed in Table 3.1. The BGlu1 E176Q crystal cocrystallized with *p*NPMan were collected to 98.3% completeness in the resolution range of 30-1.95 \AA , with the number of unique reflections of 74,582 and R_{sym} value of 11.4%. The crystal of BGlu1 E176Q soaked with *p*NPMan was collected to the 99.9% completeness in the resolution range of 30-1.69 \AA , with 116,261 unique reflections and an R_{sym} value of 7.9%. The data set of BGlu1 E176Q cocrystallized with *p*NPMan and soaked with *p*NPMan was solved with the apo BGlu1 E176Q structure as a search model by rigid body refinement. The solution indicated the presence of two molecules per asymmetric unit, a solvent content was 47.63% and Matthews coefficient $V_M = 2.35 \text{ \AA}^3 \text{ Da}^{-1}$. In the active site of the structure of BGlu1 E176Q cocrystallized with *p*NPMan, the electron density appeared to represent a glycerol molecule rather than the pyranose ring of hexose sugar, but the structure and electron density map of BGlu1 E176Q soaked with 100 mM *p*NPMan for 60 min showed the electron density of sugar in the active site, as shown in the Figure 3.5.

Table 3.1 Data collection statistics for crystals not used for final structure solution.

dataset	BGlu1E176Q_	BGlu1 E176Q-
	<i>p</i> NPMan	<i>p</i> NPMan
Beamline	BL13B1	BL13B1
Date of data collection	21/8/2009	21/8/2009
Wavelength (Å)	1.00	1.00
Space group	P2 ₁ 2 ₁ 2 ₁	P2 ₁ 2 ₁ 2 ₁
Unit cell parameters (Å)	a = 79.5	a = 79.4
	b = 101.3	b = 101.7
	c = 127.8	c = 127.7
Resolution range (Å)	30-1.95	30-1.69
Resolution of outer shell (Å)	1.95-2.02	1.75-1.69
No. Unique reflections	74,582	88,886
No. Observed reflections	541,594	749,091
Completeness (%)	99.1 (98.3)	100 (99.9)
Average redundancy	7.2 (7.0)	6.8 (6.2)
<i>I</i> / σ (<i>I</i>)	16.9 (3.84)	21.8 (3.87)
R _(merge) (%)	11.4 (53.6)	7.9 (45)
Intended ligand in active site	α -mannoside	α -mannoside
Ligand in active site	glycerol	mannose

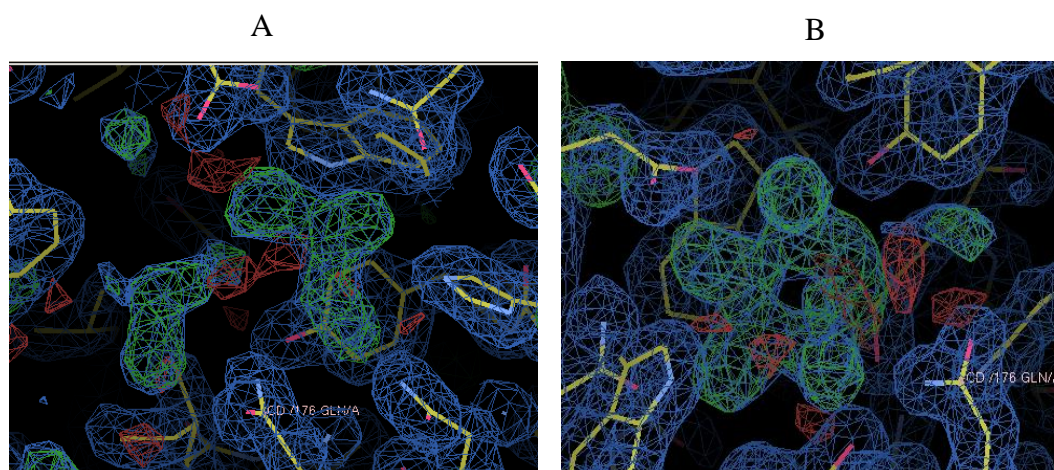


Figure 3.5 The electron density in the active site of BGLu1 E176Q cocrystallized with 10 mM *p*NPMAN (A) and BGLu1 E176Q soaked with 100 mM *p*NPMAN for 60 min (B). The figures were drawn with Coot (Emsley and Cowtan, 2004).

3.2.3 Preliminary structures of BGLu1 E176Q in complexes with DNP2FM and *p*NPMAN by X-ray diffraction.

Crystals of BGLu1 E176Q cocrystallized or soaked with mannosides were used to diffract X-ray beams from synchrotron radiation at the National Synchrotron Radiation Research Center, Hsinchu, Taiwan. Diffraction data collection of BGLu1 E176Q in complexes with α -D-2-fluoromannoside from DNP2FM and mannose from *p*NPMAN were isomorphous with previously published BGLu1 and BGLu1 E176Q mutant structures (Chuenchor *et al.*, 2006; 2008; 2011) in space group $P2_12_12_1$ with the unit cell parameters shown in Table 3.2.

The crystals of BGLu1 E176Q with DNP2FM diffracted X-rays to 1.95 Å resolution with a completeness of 99.7% and crystals with *p*NPMAN diffracted X-rays to 1.69 Å resolution with 99.9% completeness. Analysis of the diffraction patterns showed that the crystals of both BGLu1 E176Q complexes with DNP2FM and

*p*NPMan belong to the $P2_12_12_1$ space group, with very similar unit cell parameters of $a = 79.5 \text{ \AA}$, $b = 101.6 \text{ \AA}$, $c = 127.9 \text{ \AA}$ ($\alpha = \beta = \gamma = 90^\circ$) and $a = 79.4 \text{ \AA}$, $b = 101.7 \text{ \AA}$, $c = 127.7 \text{ \AA}$ ($\alpha = \beta = \gamma = 90^\circ$), respectively. The statistics of data collection are listed in Table 3.2. The data set of BGlu1 E176Q with DNP2FM was solved with the native BGlu1 structure as a search model by rigid body refinement. The solution indicated the presence of two molecules per asymmetric unit, a solvent content was 47.63% and Matthews coefficient (V_M) = $2.35 \text{ \AA}^3 \text{ Da}^{-1}$. The data set of BGlu1 E176Q with *p*NPMan was isomorphous with two molecules per asymmetric unit, a solvent content of 47.63% and $V_M = 2.35 \text{ \AA}^3 \text{ Da}^{-1}$. Diffraction data parameters are shown in Table 3.2.

3.2.4 Overall structure and quality of models

The structures of the BGlu1 E176Q complexes were solved by molecular replacement with the apo structure of rice BGlu1 E176Q (3AHT, Chuenchor *et al.*, 2011) as a search model. The overall structure of the rice BGlu1 E176Q complex with *p*NPMan and DNP2FM has a $(\beta/\alpha)_8$ barrel fold, as found in other structures of rice BGlu1 and related glycoside hydrolase family 1 (GH1) glycosidases. The asymmetric unit of the BGlu1 E176Q complex with *p*NPMan and DNP2FM crystals contains a dimer, whereas gel filtration and dynamic light scattering of the BGlu1 E176Q were consistent with the presence of a monomer (Figure 3.3). Crystals of BGlu1 E176Q belong to the space group $P2_12_12_1$, and were isomorphous with BGlu1 E176Q crystals (Chuenchor *et al.*, 2011). The model of BGlu1 E176Q complex with *p*NPMan was refined at 1.69 \AA resolution to an R_{factor} of 18.24% and R_{free} of 21.78% for 7964 protein atoms (476 amino acid residues for each of two molecules in the asymmetric unit). The structure of the DNP2FM complex was refined at 1.95 \AA to an R_{factor} of

18.01% and R_{free} of 21.30% for 7882 protein atoms in the asymmetric unit (Table 3.3). A 2-fluoro-mannoside molecule is bound within the -1 subsite of the BGlu1 E176Q structure from the crystal soaked with DNP2FM (Figure 3.6 A) and the structure of the BGlu1 E176Q complex with *p*NPMan show mannose binding in -1 subsite (Figure 3.6 B). BGlu1 E176Q with ligands derived from DNP2FM and *p*NPMan showed sugars apparently bound in relaxed 4C_1 chair conformations, in the same position as the 2-deoxy-2-fluoro- α -D-glucosyl moiety (G2F) in its covalent complex with BGlu1 (Chuenchor *et al.*, 2008).



Table 3.2 Data collection statistics for the datasets used to solve the structures of BGlu1 E176Q in covalent complexes with α -D-2-fluoromannoside and D-mannose.

dataset	BGlu1	BGlu1 E176Q- <i>p</i> NPM
	E176Q_DNP2FM	
Beamline	BL13B1	BL13B1
Date of data collection	21/8/2009	21/8/2009
Wavelength (Å)	1.00	1.00
Space group	P2 ₁ 2 ₁ 2 ₁	P2 ₁ 2 ₁ 2 ₁
Unit cell parameters (Å)	a = 79.5	a = 79.4
	b = 101.6	b = 101.7
	c = 127.9	c = 127.7
Resolution range (Å)	30-1.95	30-1.69
Resolution of outer shell (Å)	2.02-1.95	1.75-1.69
No. Unique reflections	75,540	88,886
No. Observed reflections	505,669	749,091
Completeness (%)	99.4 (99.7)	100 (99.9)
Average redundancy	6.7 (6.6)	6.8 (6.2)
$I/\sigma(I)$	17.6 (4.41)	21.8 (3.87)
R _(merge) (%)	10.5 (46.5)	7.9 (45)

Table 3.3 Refinement statistics for the structural models of BGlu1 E176Q with α -D-fluoromannopyranoside and α -D-mannopyranoside.

Structure:	BGlu1 E176Q_DNP2FM	BGlu1 E176Q-pNPM
Resolution range	30-1.95	30-1.69
Resolution in outer shell	2.02-1.95	1.75-1.69
R _{factor} (%)	18.01	18.24
R _{free} (%)	21.30	21.78
No. of amino-acid residues	1156	1244
No. protein atom	7882	7964
No. Ligand atom	14 (M2F)	12 (BMA)
No. of water molecules	199	293
B-Factors		
Protein	16.67	16.21
Ligand	13.28 (M2F)	11.48 (BMA)
Waters	19.84	20.66
r.m.s. bond deviations (length)	0.021	0.022
r.m.s. angle deviations (degree)	1.896	1.988

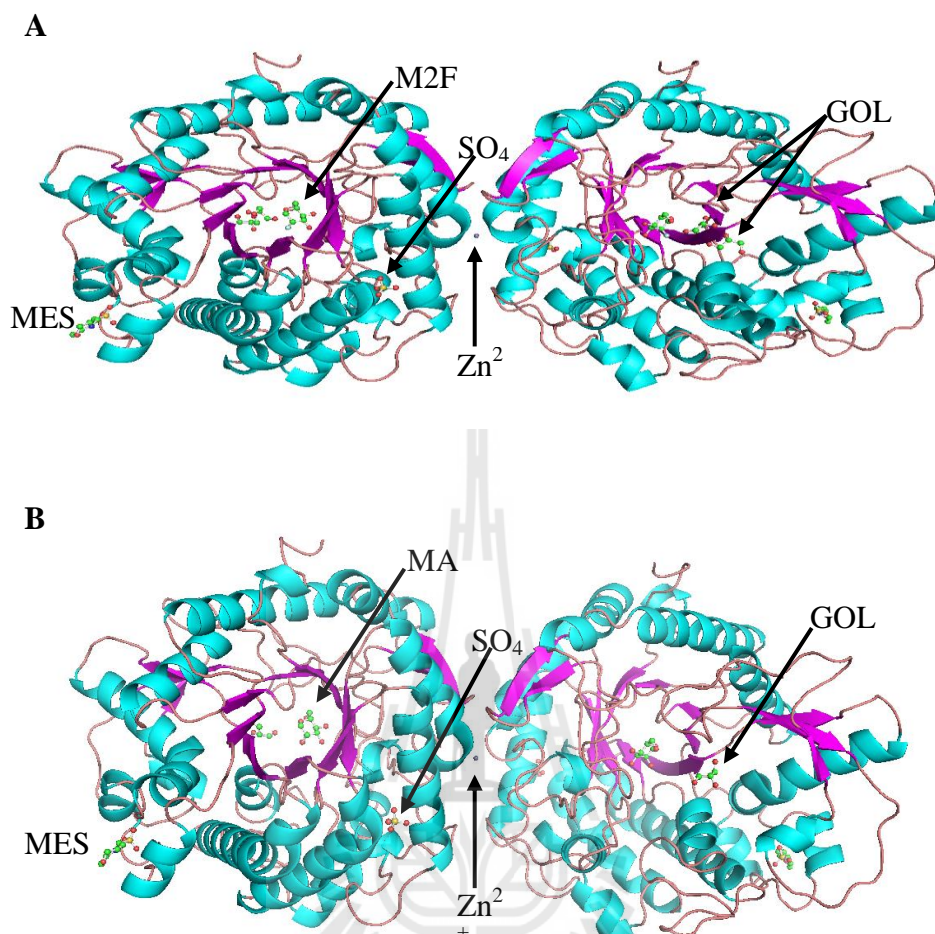


Figure 3.6 Ribbon diagram representation of the dimeric structure of BGLu1 E176Q complex with DNP2FM (M2F) (A) and *p*NPMAN (MAN) complex (B). The β -strands are colored purple and α -helices are in cyan. The loops are depicted in pink. The Zn²⁺ ion between the two molecules in the asymmetric unit is labeled. The M2F molecule in the complex (A) is represented by balls and sticks with carbon in green, oxygen in red, and fluoride in blue. The MAN molecule in the complex (B) is represented by balls and sticks with carbon in green and oxygen in red. The figure was generated by Pymol (Schrödinger LLC).

In the active sites of the BGlu1 E176Q complexes with DNP2FM and *p*NPMan, the ligand electron densities were similar in the two protein molecules in the asymmetric units, and the $F_{\text{obs}} - F_{\text{calc}}$ electron density map was relatively clean, as shown in Figure 3.7.

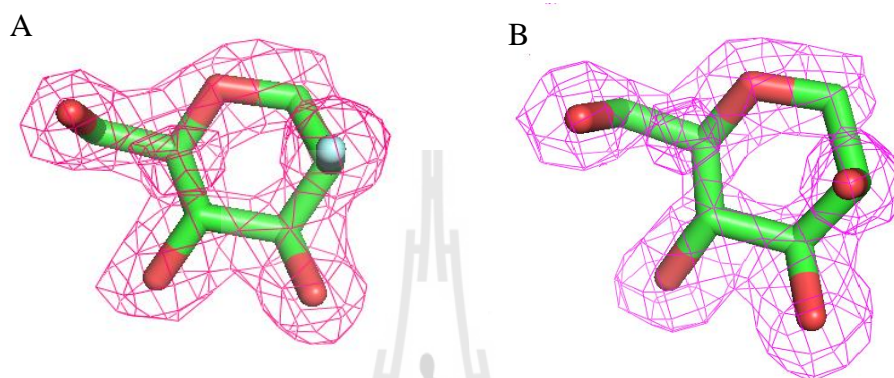


Figure 3.7 The electron densities of M2F (A) and MAN (B) in the -1 subsite of BGlu1E176. The electron density ($F_{\text{obs}} - F_{\text{calc}}$) maps were calculated for each structure with all heteroatoms omitted from the active site, and are shown in pink mesh at an electron density equivalent to $+3\sigma$. Oxygen is shown in red and fluorine in green. The figures were generated with Pymol (Schrödinger LLC).

Several hydrogen-bonding interactions with the ligands in the active sites of BGlu1 E176Q complexes with M2F and MAN were observed and found to be the same for the two structures (Figure 3.8 A, B). The comparison of the structures of BGlu1 E176Q in complexes with DNP2FM and *p*NPMan with those of the BGlu1 E176Q mutant in complex with 2,4-dinitrophenyl 2-deoxy-2-fluoro- β -D-glucopyranoside (DNP2GF) (PDB: 3AHV, Chuenchor *et al.*, 2011) in Figure 3.8 C reveals that the positions of the active site amino acid residues are similar, except the catalytic nucleophile, E386, has moved in the covalent intermediates with M2F and

G2F, while it is in a position similar to apo enzyme in the MAN complex. The pyranose rings of the sugars appeared to have the same 4C_1 relax chair conformation.

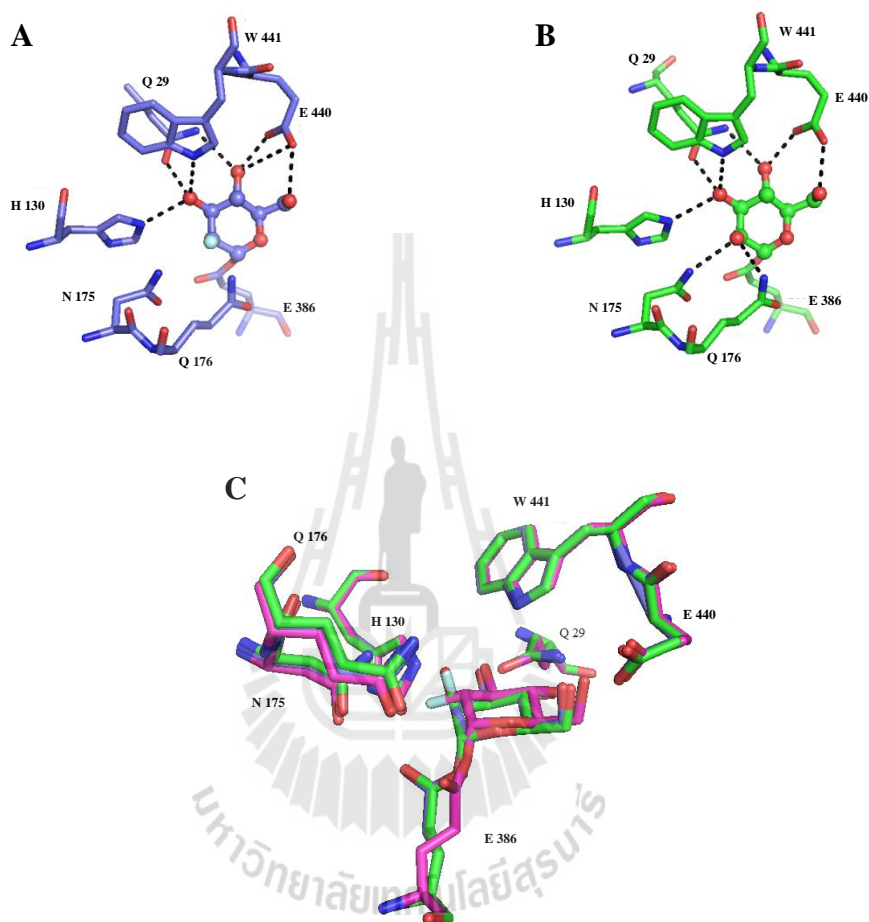


Figure 3.8 Comparison of the active sites of BGLu1 E176Q complex with M2F, MAN and G2F. An active site sugar molecule is seen in a covalent intermediate in the complexes with M2F and G2F. This water occupies a very similar position in BGLu1 E176Q complex with M2F (A) and BGLu1 E176Q complex with MAN (B). The superimposition of BGLu1 E176Q complex with M2F (purple carbons), BGLu1 E176Q complex with MAN (green carbons) and the complex of G2F with BGLu1 E176Q

(pink carbons, PDB code; 3AHV) is shown in C The figure was produced with Pymol (Schrödinger LLC).

3.3 Rescue of *p*NPMan and *p*NPGlc hydrolysis by small nucleophiles

Since α -D-mannoside from *p*NPMan initially appeared to be stably bonded to the catalytic nucleophile of the BGl1 E176Q enzyme, it was of interest to see whether the enzyme could be rescued with small nucleophiles, as seen with *p*NPGlc (Chuenchor *et al.*, 2011). To test the rescue activity of small nucleophiles, reactions of BGl1 E176Q were set-up with 1 mM *p*NPMan and 50 mM nucleophiles, including azide, acetate, formate, fluoride (KF), ascorbate, dithiothreitol (DTT), pyridine, imidazole, β -mercaptoethanol, sulphite, cyanide, thiocyanate and benzoic acid in 50 mM MES buffer, pH 5.0, which has not been observed to act as a nucleophile, and 50 mM sodium acetate buffer, pH 5.0, which can compete with the added compounds as a nucleophile with *p*NPGlc. Reactions of *p*NPMan with and without azide were analyzed by TLC at time points of 18 h (Figure 3.9), 24 h (Figure 3.10), 36 h (Figure 3.11) and 48 h (Figure 3.12). The reactions with *p*NPMan were compared with the reaction of *p*NPGlc. After 18 h, the TLC of the reaction with *p*NPMan showed an unknown product in the reaction with azide, while in the reaction without azide no product was observed (Figure 3.9). The reaction of *p*NPGlc with azide also showed an unknown compound in the reaction, likely to be azo- β -D-glucoside (Wang *et al.*, 1994), while in the reaction without azide a spot with the same R_f as glucose was seen in the product.

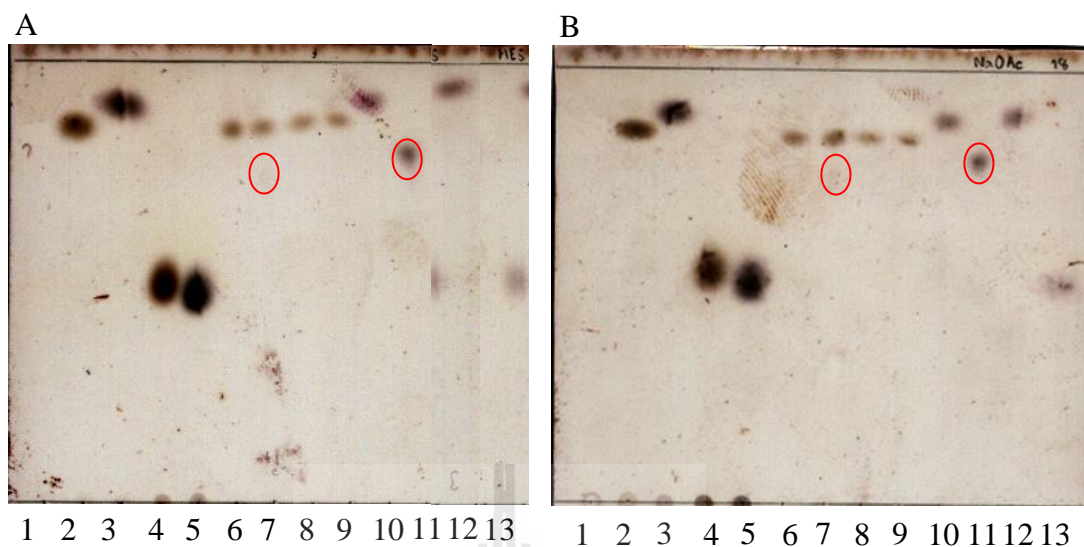


Figure 3.9 TLC of reactions of BGluc1 E176Q with *p*NPMannan and *p*NPGlucose rescued with azide at 18 h. Reactions of BGluc1 E176Q with *p*NPMannan and *p*NPGlucose with and without azide were done in 50 mM MES buffer, pH 5.0 (A), and 50 mM acetate buffer, pH 5.0 (B). Reaction products were analyzed by TLC on silica gel 60 F₂₅₄ plates with ethyl acetate: acetic acid: water (2:1:1 v/v/v) as solvent, and detection by charring with sulfuric acid. Lane 1, *p*NP; Lane 2, *p*NPMannan; Lane 3, *p*NPGlucose; Lane 4, mannose; Lane 5, glucose; Lane 6, reaction of *p*NPMannan with azide, without enzyme; Lane 7, reaction of *p*NPMannan with azide and BGluc1 E176Q; Lane 8, *p*NPMannan without azide, without enzyme; Lane 9, *p*NPMannan without azide with BGluc1 E176Q; Lane 10, *p*NPGlucose with azide, without enzyme; Lane 11, *p*NPGlucose with azide and BGluc1 E176Q; Lane 12, *p*NPGlucose without azide and without enzyme; Lane 13, *p*NPG with BGluc1 E176Q without azide.

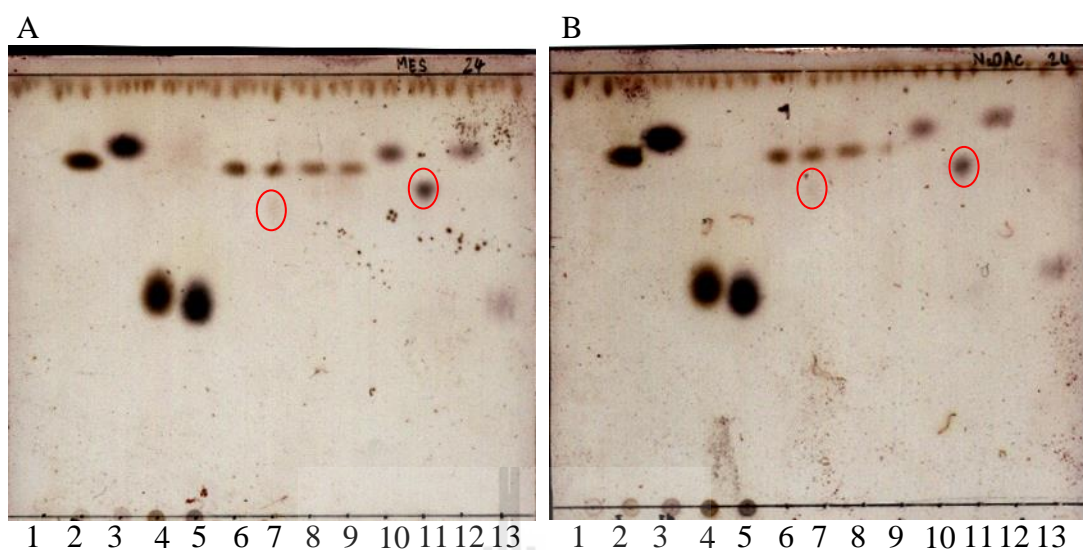


Figure 3.10 TLC of reactions of BGlucanase E176Q with *pNPMan* and *pNPGlc* rescued with azide at 24 h. Reactions of BGlucanase E176Q with *pNPMan* and *pNPGlc* with and without azide were set-up in 50 mM MES buffer, pH 5.0 (A), and 50 mM acetate buffer, pH 5.0 (B). Reaction products were analyzed by TLC on silica gel 60 F₂₅₄ plates with ethyl acetate: acetic acid: water (2:1:1 v/v/v) as solvent, and detection by charring with sulfuric acid. Lane 1, *pNP*; Lane 2, *pNPMan*; Lane 3, *pNPGlc*; Lane 4, mannose; Lane 5, glucose; Lane 6, reaction of *pNPMan* with azide, without enzyme; Lane 7, reaction of *pNPMan* with azide and BGlucanase E176Q; Lane 8, *pNPMan* without azide, without enzyme; Lane 9, *pNPMan* without azide with BGlucanase E176Q; Lane 10, *pNPGlc* with azide, without enzyme; Lane 11, *pNPGlc* with azide and BGlucanase E176Q; Lane 12, *pNPGlc* without azide and without enzyme; Lane 13, *pNPGlc* with BGlucanase E176Q without azide.

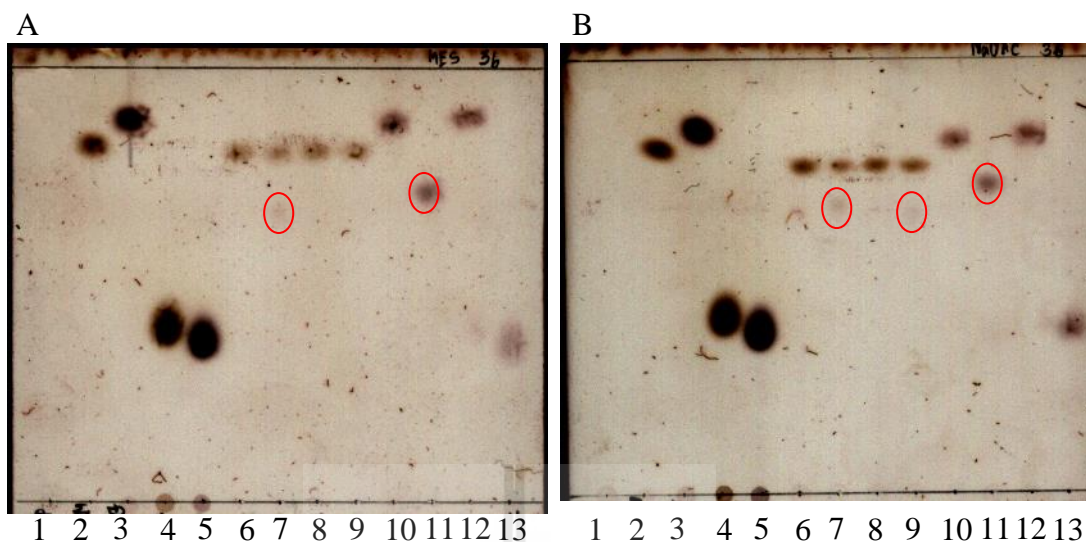


Figure 3.11 TLC of reactions of BGluc1 E176Q with *pNPMannan* and *pNPGlucose* rescued with azide at 36 h. Reactions of BGluc1 E176Q with *pNPMannan* and *pNPGlucose* with and without azide were set in 50 mM MES buffer, pH 5.0 (A), and 50 mM acetate buffer, pH 5.0 (B). Reaction products were analyzed by TLC on silica gel 60 F₂₅₄ plates with ethyl acetate: acetic acid: water (2:1:1 v/v/v) as solvent, and detection was achieved by charring with sulfuric acid. Lane 1, *pNP*; Lane 2, *pNPMannan*; Lane 3, *pNPGlucose*; Lane 4, mannose; Lane 5, glucose; Lane 6, reaction of *pNPMannan* with azide, but without enzyme; Lane 7, *pNPMannan* reaction with azide and BGluc1 E176Q; Lane 8, control reaction of *pNPMannan* without azide or enzyme; Lane 9, *pNPMannan* reaction without azide with BGluc1 E176Q; Lane 10, control *pNPGlucose* reaction with azide, without enzyme; Lane 11, *pNPGlucose* reaction with azide and BGluc1 E176Q; Lane 12, control reaction of *pNPGlucose* without azide or enzyme; Lane 13, *pNPGlucose* reaction with BGluc1 E176Q without azide.

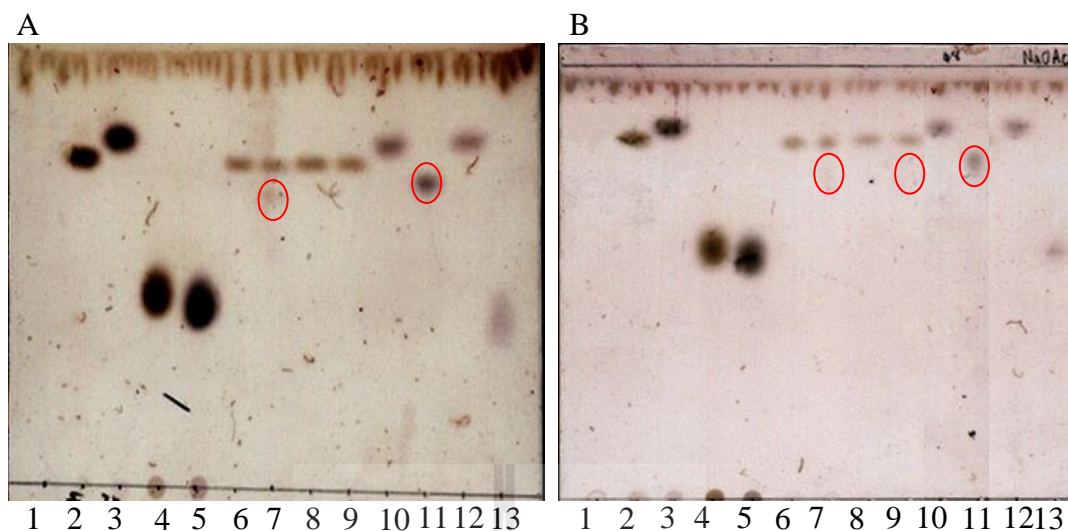


Figure 3.12 TLC of reactions of BGlucanase E176Q with *p*NPMan and *p*NPGlc rescued with azide at 48 h. Reactions of BGlucanase E176Q with *p*NPMan and *p*NPGlc with and without azide were set in 50 mM MES buffer, pH 5.0 (A), and 50 mM acetate buffer, pH 5.0 (B). Reaction products were analyzed by TLC on silica gel 60 F₂₅₄ plates with ethyl acetate: acetic acid: water (2:1:1 v/v/v) as solvent, and detection by charring with sulfuric acid. Lane 1, *p*NP; Lane 2, *p*NPMan; Lane 3, *p*NPGlc; Lane 4, mannose; Lane 5, glucose; Lane 6, control reaction of *p*NPMan with azide without enzyme; Lane 7, *p*NPMan reaction with azide and BGlucanase E176Q; Lane 8, control reaction of *p*NPMan without azide without enzyme; Lane 9, *p*NPMan reaction without azide with BGlucanase E176Q; Lane 10, control reaction of *p*NPGlc reaction with azide without enzyme; Lane 11, *p*NPGlc reaction with azide with BGlucanase E176Q; Lane 12, control reaction of *p*NPGlc without azide or enzyme; Lane 13, *p*NPG reaction with BGlucanase E176Q without azide.

Furthermore, the effect of the amount of enzyme was tested by comparing the product from reactions with and without azide in 50 mM MES buffer, pH 5.0, for 18 h at 30°C, with BGlu1 E176Q protein concentrations of 0.5, 1, 2, 3, and 4 mg/ml. After 18 h the reaction with 1 mg/ml or more BGlu1 E176Q protein could convert all the *p*NPMan to a product compound in the reaction with azide in 50 mM MES buffer, pH 5.0, as shown in Figure 3.13, while no product was seen in the reaction without azide.

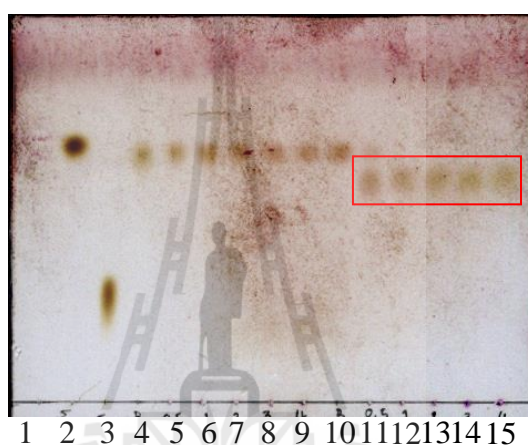
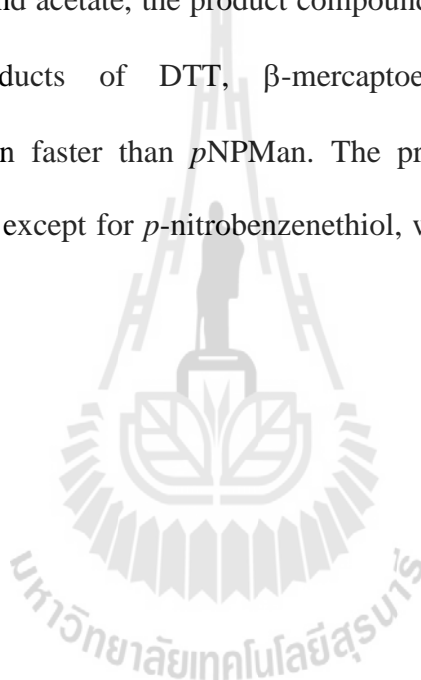


Figure 3.13 Products of reactions of BGlu1 E176Q with *p*NPMan with and without azide at different enzyme concentrations. Reactions were set in 50 mM MES buffer, pH 5.0, at 30°C for 18 h, and products detected by TLC on silica gel 60 F254 plates. Lane 1, *p*NP standard. Lane 2, *p*NPMan standard, Lane 3, mannose, Reactions were set up without azide (Lanes 4-9) or with 50 mM sodium azide (Lanes 10-15) and 0 (Lanes 4 and 10), 0.5 mg/ml (Lanes 5 and 11), 1 mg/ml (Lanes 6 and 12), 2 mg/ml (Lanes 7 and 13), 3 mg/ml (Lanes 8 and 14), and 4 mg/ml (Lanes 9 and 15) BGlu1 E176Q as catalyst.

To test the abilities of possible nucleophiles to rescue the reaction of BGlul E176Q with *p*NPMan, reactions of 1 mM *p*NPMan were set-up with 50 mM nucleophiles, including azide, acetate, formate, fluoride (KF), ascorbate, dithiothreitol (DTT), pyridine, imidazole, β -mercaptoethanol, sulphite, cyanide, thiocyanate and benzoic acid in 50 mM MES buffer, pH 5.0. Product compounds could be detected with azide, acetate, DTT, β -mercaptoethanol, benzoic acid and *p*-nitrobenzenethiol. In the cases of azide and acetate, the product compounds ran slower than *p*NPMan on TLC, but the products of DTT, β -mercaptoethanol, benzoic acid, and *p*-nitrobenzenethiol ran faster than *p*NPMan. The products of these reactions are shown in Figure 3.14, except for *p*-nitrobenzenethiol, which is considered in the next section.



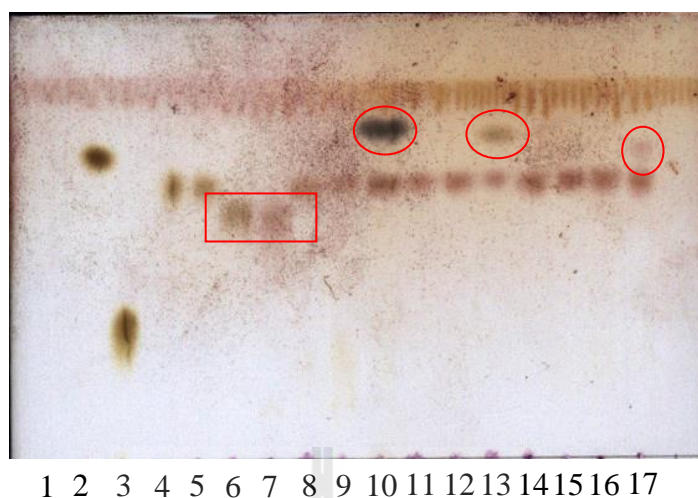


Figure 3.14 TLC analysis of products of reactions of *p*NPMAN with nucleophiles catalyzed by BGlu1 E176Q. The reactions contained 1 mM *p*NPMAN, 50 mM nucleophile and 1 mg/ml BGlu1 E176Q protein in 50 mM MES buffer, pH 5.0. Lane 1, *p*NP standard; Lane 2, *p*NPMAN standard; Lane 3, mannose standard; Lane 4, control reaction of *p*NPMAN without enzyme. Lanes 5-17, reactions catalyzed by BGlu1 E176Q for *p*NPMAN with: no nucleophile (Lane 5), azide (Lane 6), acetate (Lane 7), formate (Lane 8), fluoride (Lane 9), dithiothreitol (Lane 10), pyridine (Lane 11), imidazole (Lane 12), β -mercaptoethanol (Lane 13), sulphite (Lane 14), cyanide (Lane 15), thiocyanate (Lane 16), and benzoic acid (Lane 17).

3.4 Transglycosylation of *p*-nitrobenzenethiol

One nucleophile of interest was *p*-nitrobenzenethiol, since the expected reaction product would be *p*-nitrophenyl- β -thioglycoside, a *p*NP-glycoside analogue and β -glycosidase inhibitor. Although such compounds can be synthesized chemically, the β -D-thiomannoside is particularly difficult, since the axial 2-hydroxyl group provides a steric hindrance to nucleophilic attack from the beta side. Therefore, it was of interest to see if BGlu1 E176Q could be used to catalyze such reactions to make thioglycoside and thiomannoside inhibitors.

Transglycosylation reactions for *p*-nitrobenzenethiol (NBT) with *p*NP β Glc were initially set up in water, 10 mM sodium acetate buffer, pH 5.0, 50 mM sodium acetate buffer, pH 5.0, 10 mM MES buffer, pH 5.0, and 50 mM MES buffer, pH 5.0, with the NBT concentrations of 2, 5, and 10 mM for 18 h. In the reactions of *p*NP β Glc with 2 mM and 5 mM NBT, the donor substrate was completely converted to products after 18 h and 3 product spots were observed on TLC under UV light for each reaction, corresponding to *p*NP- β -D-thioglycoside, *p*NP, and an unknown compound. After staining with 10% H₂SO₄ in ethanol and heating, 3 spots of glucose-containing reaction products were observed, *p*NP- β -D-thioglycoside, glucose, and an unknown compound with the same R_f as the unknown product in the UV visualization (Figure 3.15 A and B for the reaction with 2 mM NBT, and C and D for the reaction with 5 mM NBT). In the reaction with 10 mM NBT the *p*NP β Glc substrate was also completely converted to products after 18 h, but only the 2 product spots corresponding to *p*NP β -D-thioglycoside and *p*NP were clearly visible under UV light, and after staining with 10% H₂SO₄ in ethanol, only the 2 spots of *p*NP β -D-thioglycoside and glucose were evident (Figure 3.15 E, F). The product compound

that comigrated with *p*NP β -D-thioglucoiside was observed in higher amounts as the concentrations of *p*NPGlc and NBT increased and appeared to be produced in a higher amount in 50 mM MES buffer, pH 5.0 than in 10 mM or 50 mM sodium acetate buffer, pH 5.0 or in 10 mM MES buffer, pH 5.0.



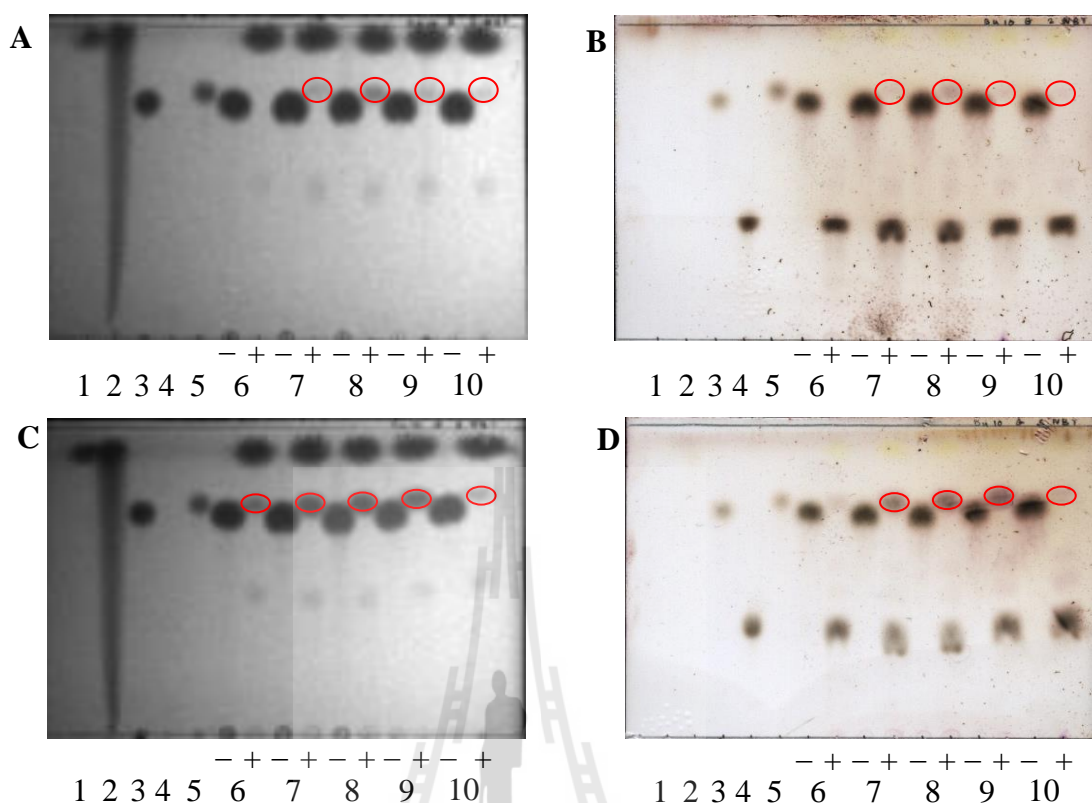


Figure 3.15 TLC analysis of the transglycosylation products of *p*-nitrobenzenethiol with *p*NPGlc in various buffers. Reactions of 10 mM *p*NPGlc with 2, 5 or 10 mM NBT and with (+) or without (-) 1 mg/ml BGlul E176Q were incubated at 30°C for 18 h. (A, B) 2 mM NBT, (C, D) 5 mM NBT, (E, F) 10 mM NBT. Lane 1, *p*NP standard; Lane 2, NBT standard; Lane 3, *p*NPGlc standard; Lane 4, glucose standard; Lane 5, *p*NP β -D-thioglucoside standard; Lane 6, reaction in water; Lane 7, reaction in 10 mM sodium acetate buffer, pH 5.0; Lane 8, reaction in 50 mM sodium acetate buffer, pH 5.0; Lane 9, reaction in 10 mM MES buffer, pH 5.0; and Lane 10, reaction in 50 mM MES buffer, pH 5.0. In frames A, C, and E the TLC plates were photographed under UV light and in frames B, D, and F the same TLC plates were photographed after staining with 10% H₂SO₄ in ethanol and charring at 120°C for 10 min.

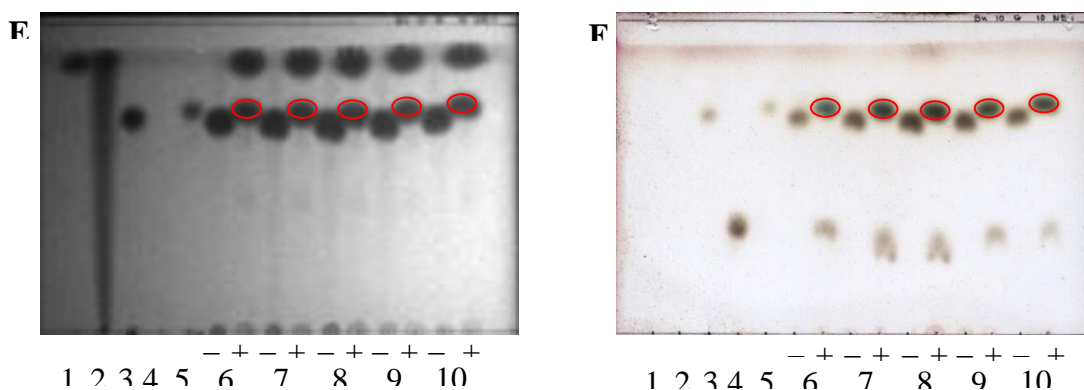


Figure 3.15 TLC analysis of the transglycosylation products of *p*-nitrobenzenethiol with *p*NPGlc in various buffers. Reactions of 10 mM *p*NPGlc with 2, 5 or 10 mM NBT and with (+) or without (-) 1 mg/ml BGlu1 E176Q were incubated at 30°C for 18 h. (A, B) 2 mM NBT, (C, D) 5 mM NBT, (E, F) 10 mM NBT. Lane 1, *p*NP standard; Lane 2, NBT standard; Lane 3, *p*NPGlc standard; Lane 4, glucose standard; Lane 5, *p*NP β-D-thioglucoside standard; Lane 6, reaction in water; Lane 7, reaction in 10 mM sodium acetate buffer, pH 5.0; Lane 8, reaction in 50 mM sodium acetate buffer, pH 5.0; Lane 9, reaction in 10 mM MES buffer, pH 5.0; and Lane 10, reaction in 50 mM MES buffer, pH 5.0. In frames A, C, and E the TLC plates were photographed under UV light and in frames B, D, and F the same TLC plates were photographed after staining with 10% H₂SO₄ in ethanol and charring at 120°C for 10 min (Continued).

Transglycosylation reactions of *p*-nitrobenzenethiol (NBT) with *p*NPMan were initially set-up in water, 10 mM sodium acetate buffer, pH 5.0, 50 mM sodium acetate buffer, pH 5.0, 10 mM MES buffer, pH 5.0, and 50 mM MES buffer, pH 5.0, and reacted for 18 h. In the reactions with 2 mM NBT and 5 mM NBT, inspection under UV light demonstrated that the *p*NPMan substrate was not completely converted to

products after 18 h, and 3 spots, corresponding to *p*NP, *p*NPMan, and *p*NP β-D-thiomannoside, were present. When stained with 10% H₂SO₄ in ethanol followed by charring to detect carbohydrates, the reactions in water, 10 mM MES buffer, pH 5.0, and 50 mM MES buffer, pH 5.0, showed 3 spots that migrated at positions corresponding to *p*NPMan, *p*NP β-D-thiomannoside, and mannose. In contrast, the reactions in 10 mM sodium acetate buffer, pH 5.0, and 50 mM sodium acetate buffer, pH 5.0, gave 4 spots of substrate and products, which migrated at positions corresponding to *p*NPMan, *p*NP β-D-thiomannoside, mannose, and an unknown compound under the spot of *p*NPMan (Figure 3.16 A and B for the reactions with 2 mM NBT, C and D for the reactions with 5 mM NBT). In the reactions with 10 mM NBT, the *p*NPMan substrate was also not completely converted to the products of *p*NP, *p*NPMan, and *p*NP β-D-thiomannoside, which could be seen under UV light (Figure 3.16 E) and only the spots corresponding to *p*NPMan and *p*NP β-D-thiomannoside, but not free mannose, could be seen after staining for carbohydrate with 10% H₂SO₄ in ethanol and charring (Figure 3.16 F).

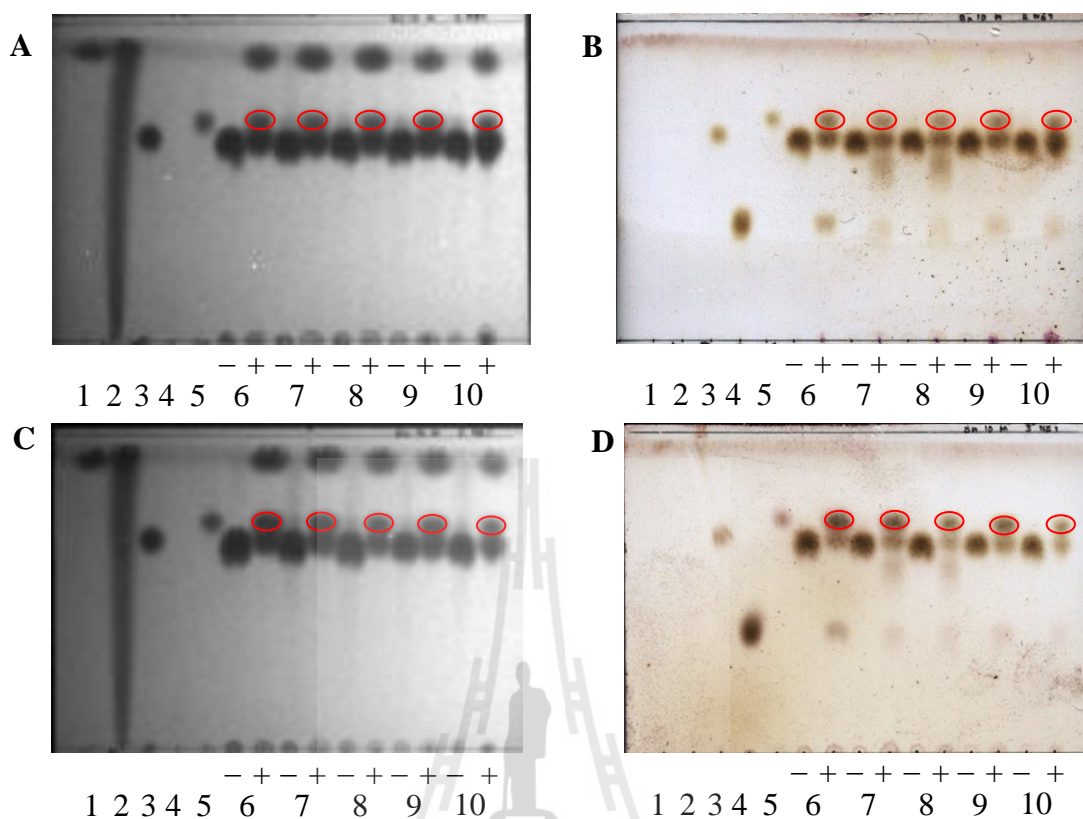


Figure 3.16 TLC analysis of transglycosylation product of *p*-nitrobenzenethiol with *p*NPMAN in various buffers. Reactions of 10 mM *p*NPMAN with 2, 5 or 10 mM NBT with (+) or without (-) 1 mg/ml BGLu1 E176Q were incubated at 30°C for 18 h. The acceptor substrates for the various plates were: (A, B) 2 mM NBT, (C, D) 5 mM NBT, and (E, F) 10 mM NBT. The lanes contain: Lane 1, *p*NP standard; Lane 2, NBT standard; Lane 3, *p*NPMAN standard; Lane 4, glucose standard; Lane 5, *p*NP β-D-thiomannoside standard; Lane 6, reaction in water; Lane 7, reaction in 10 mM sodium acetate buffer, pH 5.0; Lane 8, reaction in 50 mM sodium acetate buffer, pH 5.0; Lane 9, reaction in 10 mM MES buffer, pH 5.0; and Lane 10, reaction in 50 mM MES buffer, pH 5.0. In frames A, C, and E, the TLC plates were photographed under UV light, while in frames B, D, and F the same TLC plates were photographed after staining with 10% H₂SO₄ in ethanol and charring at 120°C for 10 min.

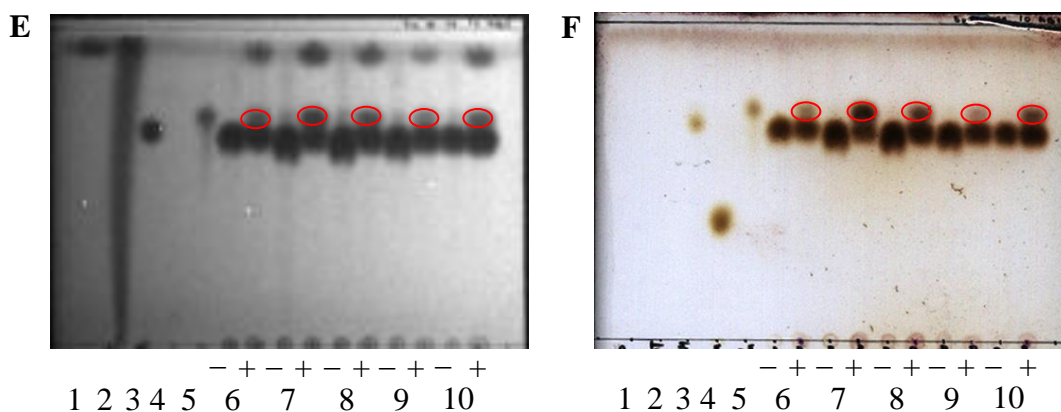
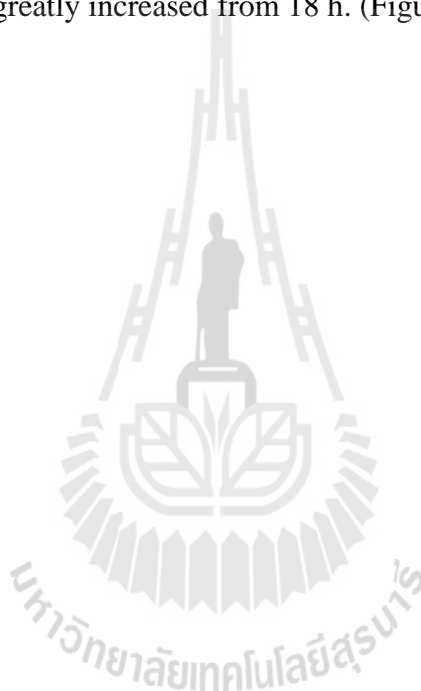


Figure 3.16 TLC analysis of transglycosylation product of *p*-nitrobenzenethiol with *p*NPMAN in various buffers. Reactions of 10 mM *p*NPMAN with 2, 5 or 10 mM NBT with (+) or without (-) 1 mg/ml BGluc1 E176Q were incubated at 30°C for 18 h. The acceptor substrates for the various plates were: (A, B) 2 mM NBT, (C, D) 5 mM NBT, and (E, F) 10 mM NBT. The lanes contain: Lane 1, *p*NP standard; Lane 2, NBT standard; Lane 3, *p*NPMAN standard; Lane 4, glucose standard; Lane 5, *p*NP β -D-thiomannoside standard; Lane 6, reaction in water; Lane 7, reaction in 10 mM sodium acetate buffer, pH 5.0; Lane 8, reaction in 50 mM sodium acetate buffer, pH 5.0; Lane 9, reaction in 10 mM MES buffer, pH 5.0; and Lane 10, reaction in 50 mM MES buffer, pH 5.0. In frames A, C, and E, the TLC plates were photographed under UV light, while in frames B, D, and F the same TLC plates were photographed after staining with 10% H₂SO₄ in ethanol and charring at 120°C for 10 min (Continued).

Because the transglycosylation reactions of NBT with *p*NPMAN were not complete after 18 h, the concentration of BGluc1 E176Q protein was varied from 1 mg/ml to 5 mg/ml of BGluc1 E176Q and the time varied at 18 h., 2, 3, and 4 days at 30°C in water, 10 mM sodium acetate buffer, pH 5.0, 50 mM sodium acetate buffer, pH 5.0, 10 mM MES buffer, pH 5.0, and 50 mM MES buffer, pH 5.0, with 10 mM

*p*NPMan and 10 mM NBT. After 18 h, the reaction did not completely convert the *p*NPMan substrate to products, but reactions with high concentrations of protein produced more *p*NP and *p*NP β-D-thiomannoside and the *p*NPMan substrate remaining decreased, as seen under UV light to detect the *p*NP and with 10% H₂SO₄ in ethanol and charring to detect the carbohydrate. After 4 days of reactions in the various buffers, the substrate still could not be completely converted to product and the products were not greatly increased from 18 h. (Figure 3.17).



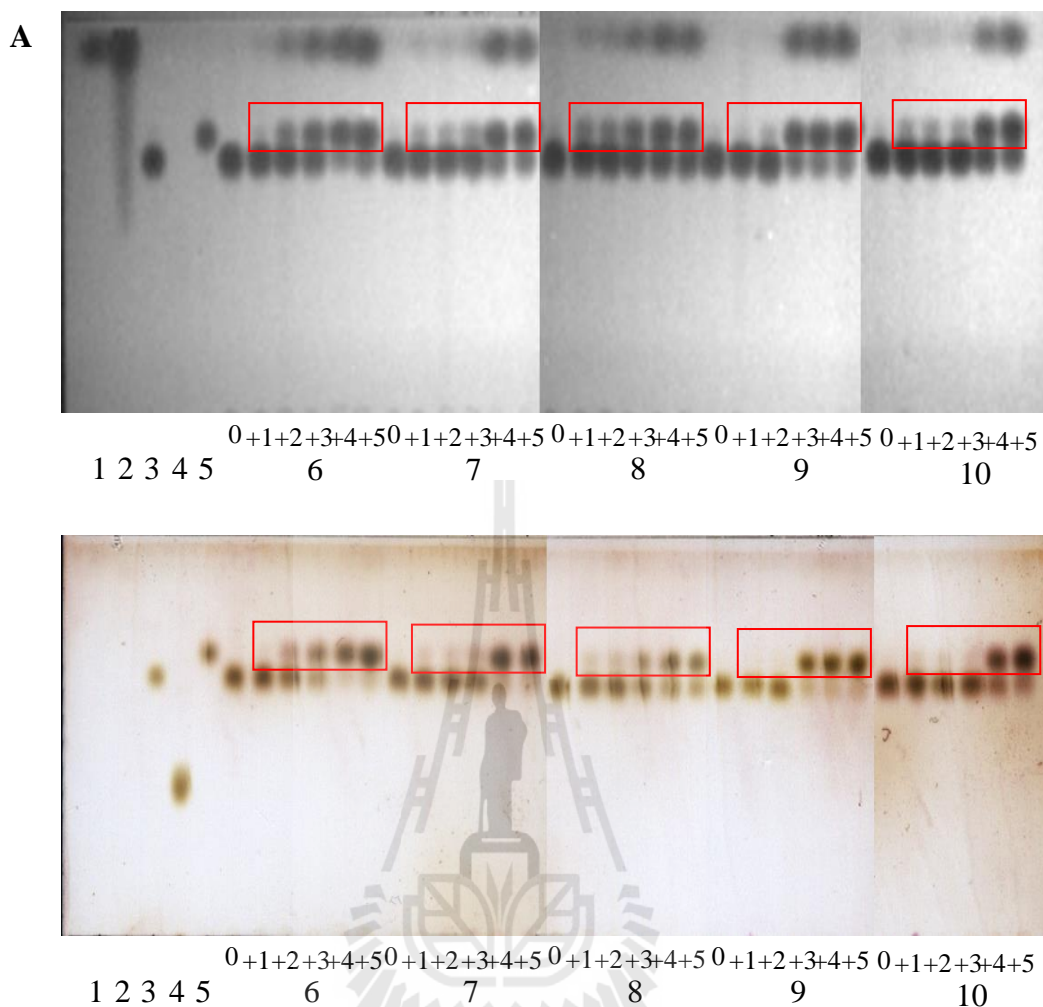


Figure 3.17 TLC analysis of transglycosylation reactions of *p*-nitrobenzenethiol (NBT) with *p*NPMan with various concentrations of BGlu1 E176Q for various times. The reactions contained BGlu1 E176Q at 1 (+1), 2 (+2), 3 (+3), 4 (+4) and 5 (+5) mg/ml or control reactions without enzyme (0), as indicated at the bottom of the TLC. Reaction times were 18 h. (A) and 4 days (B). The numbers for the standard lanes and sets of lanes are: Lane 1, *p*NP standard; Lane 2, NBT standard; Lane 3, *p*NPMan standard; Lane 4, mannose standard; Lane 5, *p*NP β -D-thiomannoside standard; Set 6, reactions in water; Set 7, reactions in 10 mM sodium acetate buffer, pH 5.0; Set 8, reactions in 50 mM sodium acetate buffer, pH 5.0; Set 9, reactions in 10 mM MES buffer, pH 5.0; and Set 10, reactions in 50 mM MES buffer, pH 5.0.

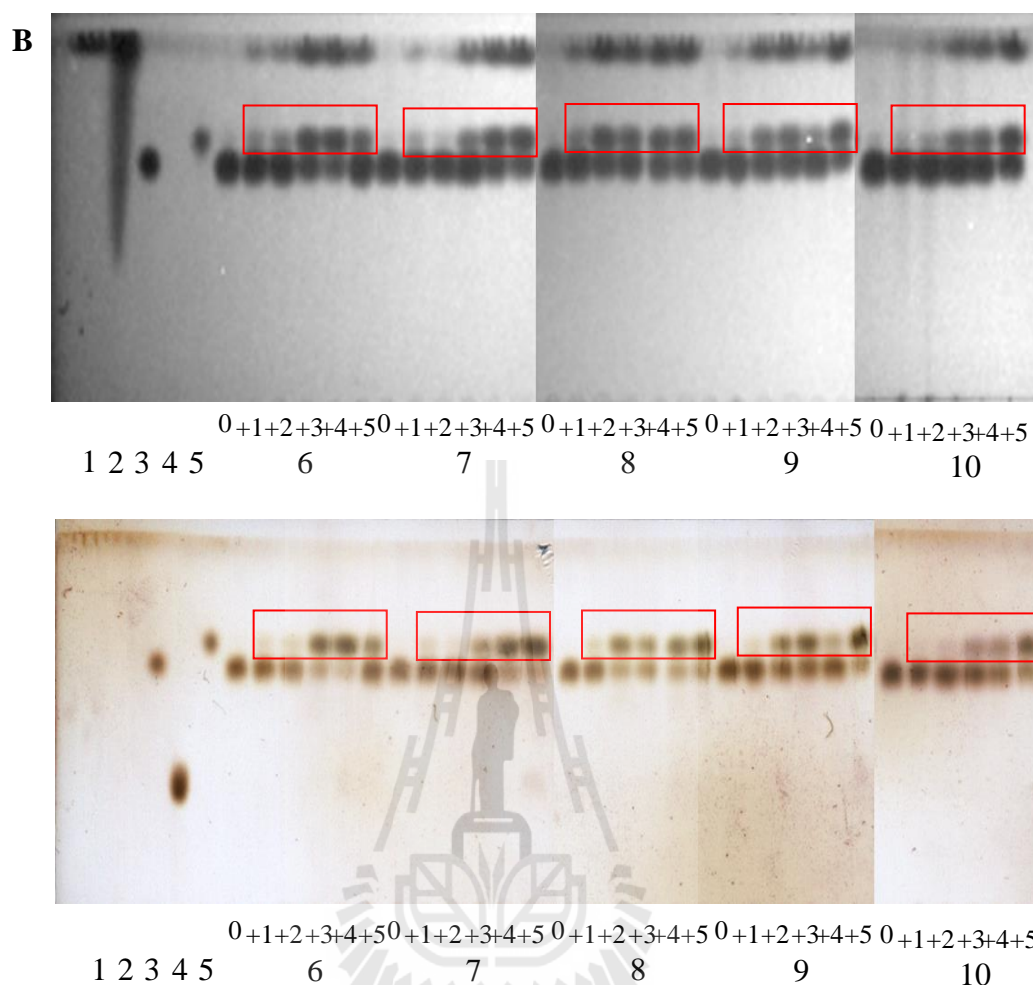


Figure 3.17 TLC analysis of transglycosylation reactions of *p*-nitrobenzenethiol (NBT) with *p*NPMan with various concentrations of BGlu1 E176Q for various times. The reactions contained BGlu1 E176Q at 1 (+1), 2 (+2), 3 (+3), 4 (+4) and 5 (+5) mg/ml or control reactions without enzyme (0), as indicated at the bottom of the TLC. Reaction times were 18 h. (A) and 4 days (B). The numbers for the standard lanes and sets of lanes are: Lane 1, *p*NP standard; Lane 2, NBT standard; Lane 3, *p*NPMan standard; Lane 4, mannose standard; Lane 5, *p*NP β -D-thiomannoside standard; Set 6, reactions in water; Set 7, reactions in 10 mM sodium acetate buffer, pH 5.0; Set 8, reactions in 50 mM sodium acetate buffer, pH 5.0; Set 9, reactions in 10 mM MES buffer, pH 5.0; and Set 10, reactions in 50 mM MES buffer, pH 5.0 (Continued).

3.5 Analysis of transglycosylation products by HPLC

The products of transglycosylation reactions with 10 mM *p*NPGlc and 2, 5, and 10 mM NBT in 50 mM MES buffer, pH 5.0, for 0 and 18 h with 4 mg/ml of BGlul E176Q were separated by reverse-phase HPLC. The standard solutions of 10 mM *p*NP (Figure 3.18 A), 10 mM *p*NPGlc (Figure 3.18 B), 10 mM *p*NP β -D-thioglucoside (Figure 3.18 C), 100 mM NBT (Figure 3.18 D) had major peaks with retention times of 22.90, 6.25, 11.37, 29.78 min, respectively.



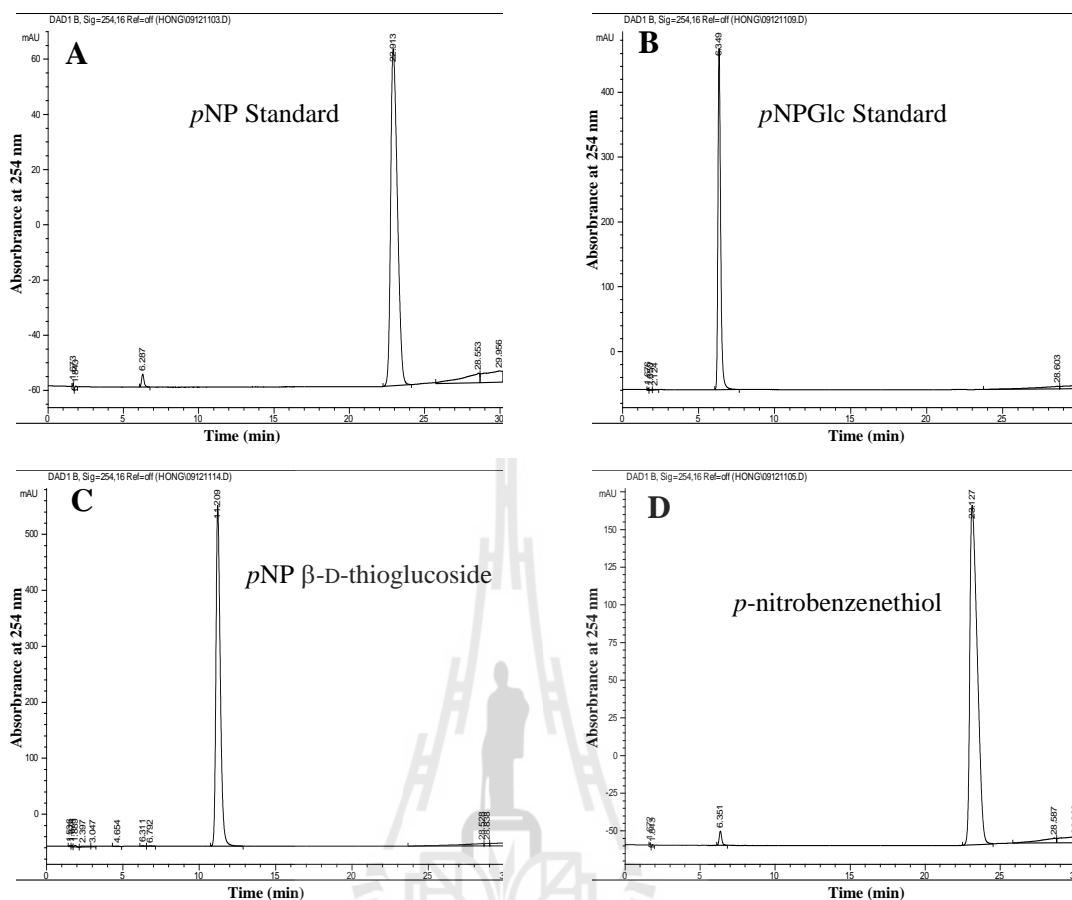


Figure 3.18 Reverse phase HPLC analysis of 10 mM *p*NP, 10 mM *p*NPGlc, 10 mM *p*NP β-D-thioglucoside, and 100 mM NBT standard. The standard solutions were run on a ZORBAX Eclipse XDB-C18 analytical column (4.6 x 150 mm) with elution with a gradient from 10 to 100% of methanol in 0.1% formic acid in 30 min at a flow rate of 1 ml/min. (A) 10 mM *p*NP standard. (B) 10 mM *p*NPGlc standard. (C) 10 mM *p*NP β-D-thioglucoside. (D) 100 mM NBT.

The transglycosylation reaction of 10 mM *p*NPGlc without NBT for 0 h had a 254 nm absorbance peak corresponding to *p*NPGlc with a retention time of 6.1 min (Figure 3.19 A), which was calculated to have a concentration of 10 mM, based on the standard curve. After 18 h of reaction, this same reaction exhibited peaks corresponding to *p*NPGlc and *p*NP with retention times at 6.1 and 21.8 min, and the peak areas were 0.050 and 2.23 AU (Figure 3.19 B). This confirmed that no compound with a retention time similar to *p*NP β -D-thioglucoside was found in the reaction without NBT. The reaction of 10 mM *p*NPGlc and 2 mM NBT for 0 h had a peaks for *p*NPGlc (retention time 6.1 min, Figure 3.19 C), while after 18 h peaks corresponding to *p*NPGlc, *p*NP, and *p*NP β -D-thioglucoside were observed at retention times of 6.1, 21.6, and 11.2 min, respectively (Figure 3.19 D). Reaction of 10 mM *p*NPGlc and 5 mM NBT showed only *p*NPGlc (retention time 6.06 min) at 0 h (Figure 3.19 E), and after 18 h showed peaks for *p*NP and *p*NP β -D-thioglucoside at retention times of 23.2 and 11.9 min, respectively (Figure 3.19 F). The reaction of 10 mM *p*NPGlc and 10 mM NBT showed only *p*NPGlc (retention time at 6.07 min) at 0 h (Figure 3.19 G) and peaks of *p*NP and *p*NP β -D-thioglucoside (retention times of 23.25 and 11.86 min, respectively) at 18 h (Figure 3.19 H). This confirmed the reaction with NBT produced the product of *p*NP β -D-thioglucoside and the relative amounts of *p*NP β -D-thioglucoside increased with the concentration of NBT, as shown in the Table 3.4.

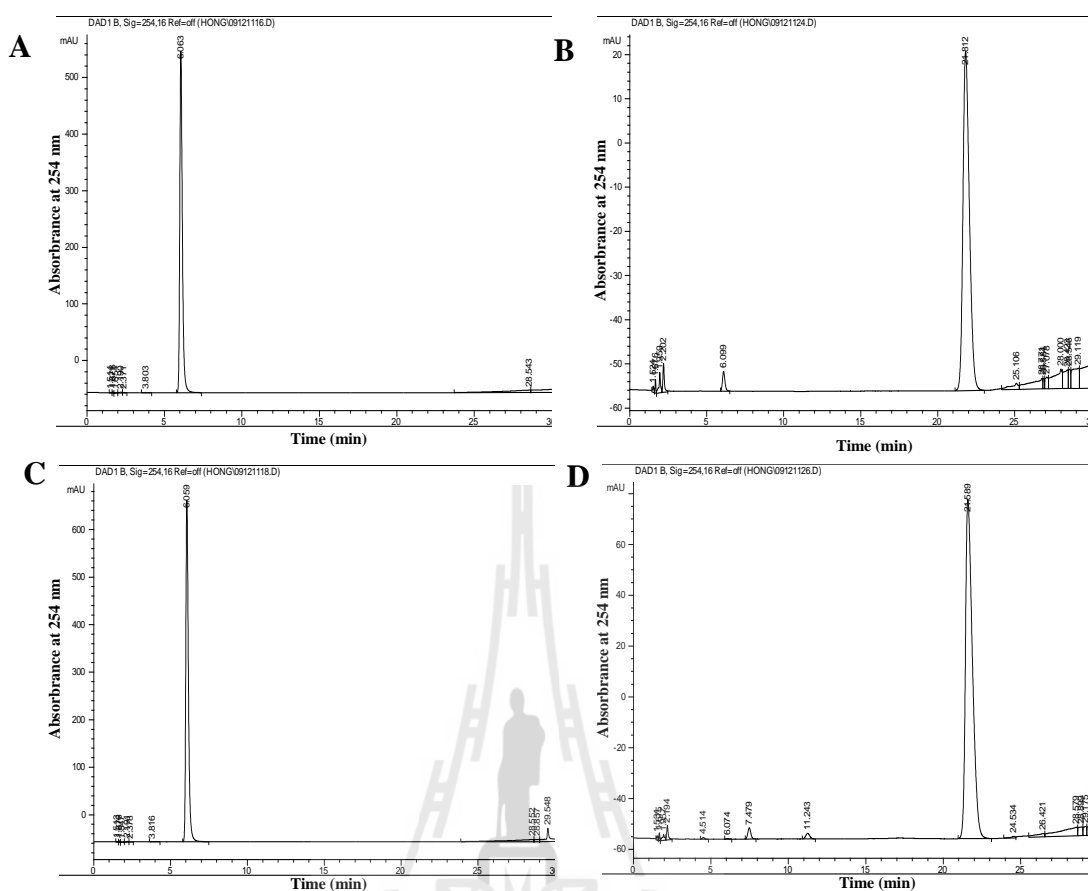


Figure 3.19 Reverse phase HPLC analysis of transglycosylation products of BGluc1 E176Q with *p*NPGlc and NBT as substrates. The reactions were done with 10 mM *p*NPGlc in MES buffer, pH 5.0, for 18 h with 1 mg/ml BGluc1 E176Q. HPLC analysis was done on a ZORBAX Eclipse XDB-C18 analytical column (4.6 x 150 mm) with elution with a gradient from 10 to 100% methanol in 0.1% formic acid over 30 min at 1 ml/min. The chromatographs are (A) reaction without NBT at 0 h; (B) reaction without NBT at 18 h; (C) reaction with 2 mM NBT at 0 h; (D) reaction with 2 mM NBT at 18 h; (E) reaction with 5 mM NBT at 0 h; (F) reaction with 5 mM NBT at 18 h; (G) reaction with 10 mM NBT at 0 h; and (H) reaction with 10 mM NBT at 18 h.

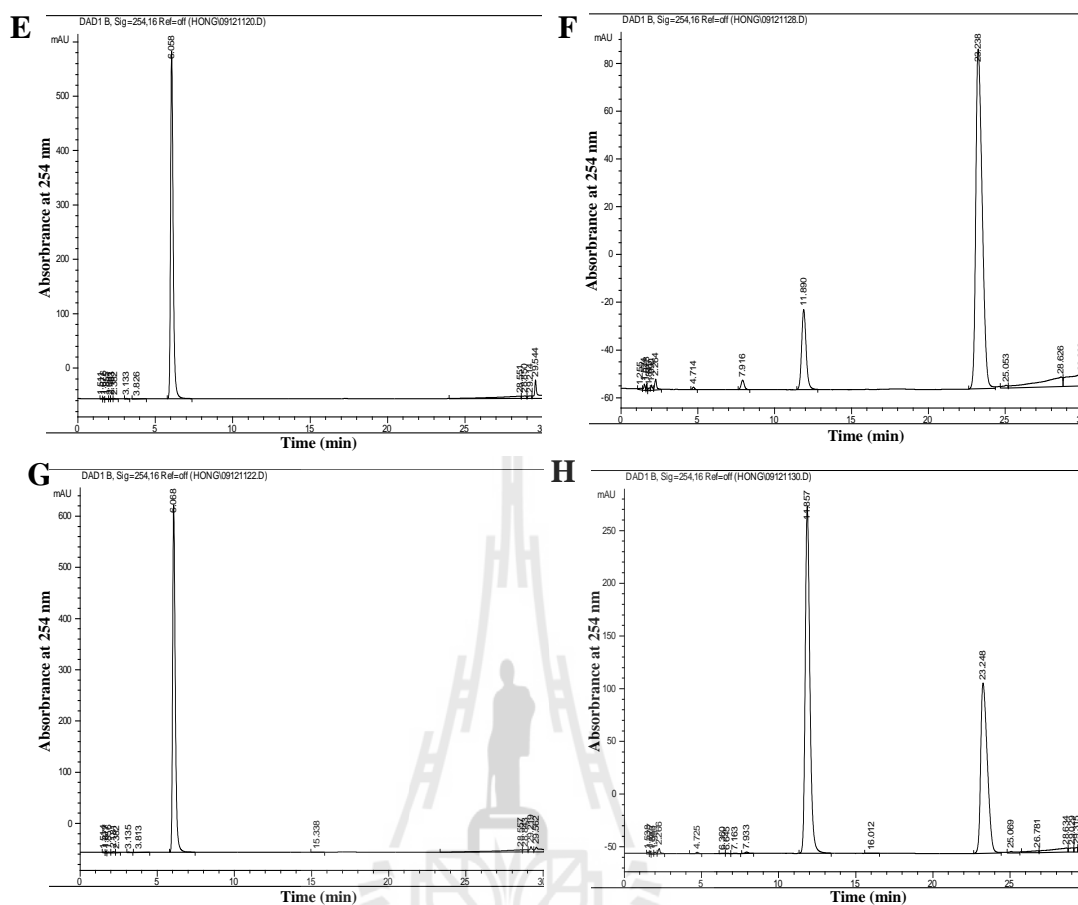


Figure 3.19 Reverse phase HPLC analysis of transglycosylation products of BGluc1 E176Q with *p*NPGlc and NBT as substrates. The reactions were done with 10 mM *p*NPGlc in MES buffer, pH 5.0, for 18 h with 1 mg/ml BGluc1 E176Q. HPLC analysis was done on a ZORBAX Eclipse XDB-C18 analytical column (4.6 x 150 mm) with elution with a gradient from 10 to 100% methanol in 0.1% formic acid over 30 min at 1 ml/min. The chromatographs are (A) reaction without NBT at 0 h; (B) reaction without NBT at 18 h; (C) reaction with 2 mM NBT at 0 h; (D) reaction with 2 mM NBT at 18 h; (E) reaction with 5 mM NBT at 0 h; (F) reaction with 5 mM NBT at 18 h; (G) reaction with 10 mM NBT at 0 h; and (H) reaction with 10 mM NBT at 18 h (Continued).

The quantification of the products of the transglycosylation reactions after 18 h, including *p*NP β -D-thioglucoside and *p*NP determined by comparison of the peak areas of absorbance at 254 nm with the standard peaks, are shown in Table 3.4. The reaction of 10 mM *p*NPGlc without NBT produced about 3.92 mM *p*NP as the one visible product, while the reaction with 2 mM NBT produced the products of 7.31 mM *p*NP and 0.07 mM *p*NP β -D-thioglucoside, the reaction with 5 mM NBT produced 7.23 mM *p*NP and 1.20 mM *p*NP β -D-thioglucoside, and the reaction with 10 mM NBT produced peaks that corresponded to the apparent concentrations of 8.42 mM *p*NP and 12.08 mM β -D-thioglucoside. The apparent percentages of substrate converted to *p*NP β -D-thioglucoside per *p*NP produced in the reactions with 2, 5, and 10 mM NBT are 0.96, 16.6, and 143%, respectively.

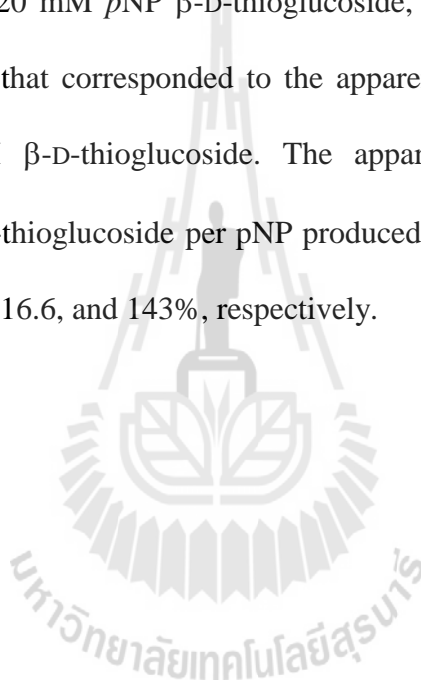
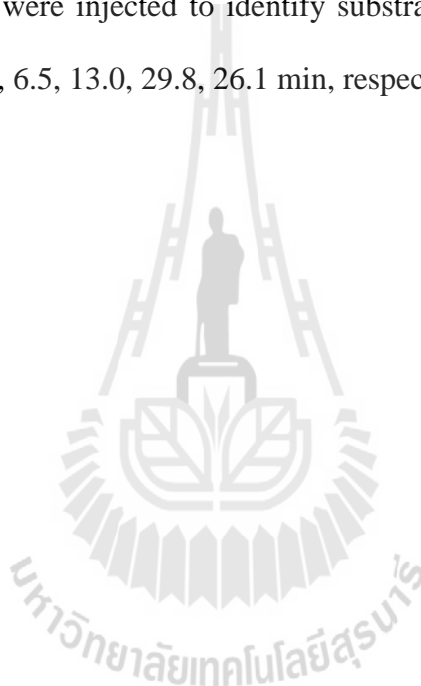


Table 3.4 The apparent concentrations of products in transglycosylation reactions with 10 mM pNPGlc and NBT determined by reverse phase HPLC.

Concentration of NBT (mM)	Concentration of pNPGlc (mM)	Concentration of pNP (mM)	Concentration of pNP β -D-thioglucoside (mM)	Apparent Percent of substrate converted to pNP β -D-thioglucoside*
0	0.09	3.92	0.00	0.00
2	0.11	7.31	0.07	0.96
5	0.11	7.23	1.20	16.6
10	0.00	8.42	12.1	143

* Calculated from the amount of pNP β -D-thioglucoside produced per pNP released from pNPGlc.

The components of the transglycosylation reactions with 2, 5, and 10 mM *p*NPMan with 2, 5, and 10 mM NBT after 0 and 18 h. with 4 mg/ml of BGlu1 E176Q. The product of transglycosylation reactions of *p*NPMan were separated by reverse phase HPLC similar to the reaction with *p*NP_{Glc} and the standard solutions of 10 mM *p*NP (Figure 3.18 A), 10 mM *p*NPMan (Figure 3.20 A), 10 mM *p*NP β-D-thiomannoside (Figure 3.20 B), *p*NP α-D-thiomannoside (Figure 3.20 C), and 100 mM NBT (Figure 3.20 D) were injected to identify substrate and product peaks and had retention times of 22.9, 6.5, 13.0, 29.8, 26.1 min, respectively.



Transglycosylation reactions of NBT with *p*NPMan were done with varying concentrations of *p*NPMan and NBT to see what was the most efficient set of concentrations to convert substrates to products. In each case, reactions at 0 h showed only the *p*NPMan substrate peak. In the reaction of 2 mM *p*NPMan without NBT for 18 h, the peaks of *p*NPMan and *p*NP (retention times of 6.38 and 23.22 min) had the peak areas of 1.08 and 0.18 AU, which corresponded to 1.90 *p*NPMan and 0.42 mM *p*NP, respectively, as calculated from the respective standard curves (Figure 3.21 B). In the reaction of 2 mM *p*NPMan and 2 mM NBT after 18 h peaks of *p*NPMan, *p*NP, and *p*NP β -D-thiomannoside (retention times of 6.39, 23.24, and 12.96 respectively) were seen (Figure 3.21 D). The reaction of 2 mM *p*NPMan and 5 mM NBT showed peaks of *p*NPMan, *p*NP, and *p*NP β -D-thiomannoside (at 6.30, 23.30, and 14.00 min, (the latter of which is shifted compared to the standard, because the standard was contaminated with another compound that gave a nearby peak), respectively, after 18 h (Figure 3.21 F). The reaction of 2 mM *p*NPMan and 10 mM NBT after 18 h (Figure 3.21 H) showed peaks of *p*NPMan, *p*NP, and *p*NP β -D-thiomannoside at retention times of 6.40, 23.19, and 13.94 min, respectively. The reaction of transglycosylation without NBT confirmed that no peaks eluting with *p*NP β -D-thiomannoside were present, nor could any such peak be seen in reactions with NBT at 0 h, while reactions with NBT for 18 h produced *p*NP β -D-thiomannoside.

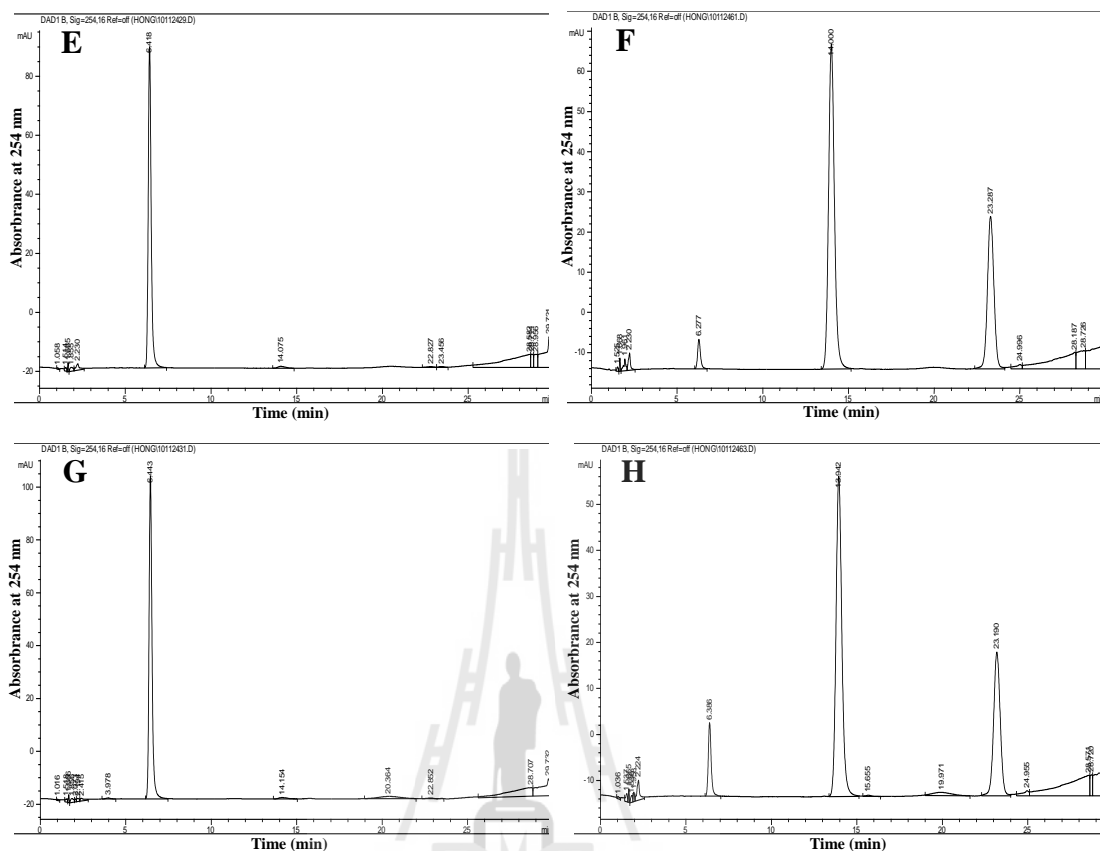


Figure 3.21 Reverse phase HPLC analysis of transglycosylation products of BGlul E176Q with 2 mM *p*NPMan and NBT as substrates. The reaction was done in MES buffer, pH 5.0, for 18 h with 4 mg/ml BGlul E176Q. HPLC analysis was done on a ZORBAX Eclipse XDB-C18 analytical column (4.6x150 mm) eluted with a gradient from 10 to 100% methanol in 0.1% formic acid. The chromatographs are (A) reaction without NBT at 0 h; (B) reaction without NBT at 18 h; (C) reaction with 2 mM NBT at 0 h; (D) reaction with 2 mM NBT at 18 h; (E) reaction with 5 mM NBT at 0 h; (F) reaction with 5 mM NBT at 18 h; (G) reaction with 10 mM NBT at 0 h; and (H) reaction with 10 mM NBT at 18 h (Continued).

The concentrations of the remaining *p*NPMan substrate and products of transglycosylation reactions of *p*NP β -D-thiomannoside and *p*NP after 18 h are shown in Table 3.5. The reaction of 2 mM *p*NPMan without NBT produced about 0.42 mM *p*NP. The reaction with 2 mM *p*NPMan and 2 mM NBT produced both *p*NP and *p*NP β -D-thiomannoside at apparent concentrations of 1.80 and 1.48 mM, respectively. The reaction with 5 mM NBT produced 2.61 mM *p*NP and 2.95 mM β -D-thiomannoside, while the reaction with 10 mM NBT produced are 2.19 mM *p*NP and 2.52 mM β -D-thiomannoside, and the apparent percent of substrate converted to *p*NP β -D-thiomannoside with 2, 5, and 10 mM NBT are 82.3, 113, and 115%, respectively.

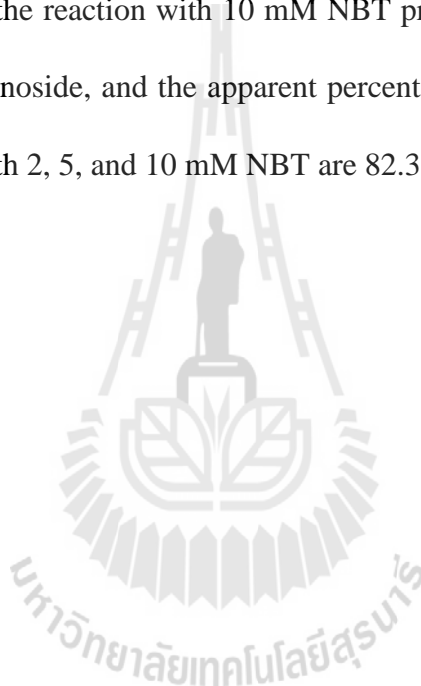


Table 3.5 The concentrations of products of reactions with 2 mM *p*NPMan and different concentrations of NBT determined by reverse phase HPLC.

Concentration of NBT (mM)	Concentration of <i>p</i> NPMan (mM)	Concentration of <i>p</i> NP (mM)	Concentration of <i>p</i> NP β-D-thiomannoside (mM)	Apparent percent of substrate converted to <i>p</i> NP β-D-thiomannoside*
0	1.90	0.42	0.00	0.00
2	0.42	1.80	1.48	82.3
5	0.16	2.61	2.95	113
10	0.33	2.19	2.52	115

* Calculated from the amount of *p*NP β-D-thiomannoside produced per *p*NP released from *p*NPMan.

In the reaction of 5 mM *p*NPMan without NBT for 18 h, peaks of *p*NPMan and *p*NP (retention times of 6.35 and 23.04 min, respectively) were seen (Figure 3.22 B). This result confirmed that the reaction with 5 mM *p*NPMan but without NBT cannot produce any products that comigrate with *p*NP β -D-thiomannoside. In the reaction of 2 mM *p*NPMan and 2 mM NBT after 18 h, peaks of *p*NPMan, *p*NP, and *p*NP β -D-thiomannoside (retention times of 6.35, 23.00, and 13.84 min, respectively) were seen (Figure 3.22 D). The reaction of 5 mM *p*NPMan and 5 mM NBT showed the product of *p*NPMan, *p*NP, and *p*NP β -D-thiomannoside (retention times of 6.33, 22.92, and 13.81 min, respectively) after 18 h (Figure 3.2 F). The reaction of 5 mM *p*NPMan with 10 mM NBT after 18 h showed peaks of *p*NPMan, *p*NP, and *p*NP β -D-thiomannoside (retention times of 6.36, 22.93, and 13.86 min, respectively, in Figure 3.22 H). The reaction of 5 mM *p*NPMan without NBT confirmed that no peaks coeluting with *p*NP β -D-thiomannoside and *p*NP were present, nor could any such peak be seen in reactions with NBT at 0 h, while reactions with NBT for 18 h produced *p*NP and *p*NP β -D-thiomannoside.

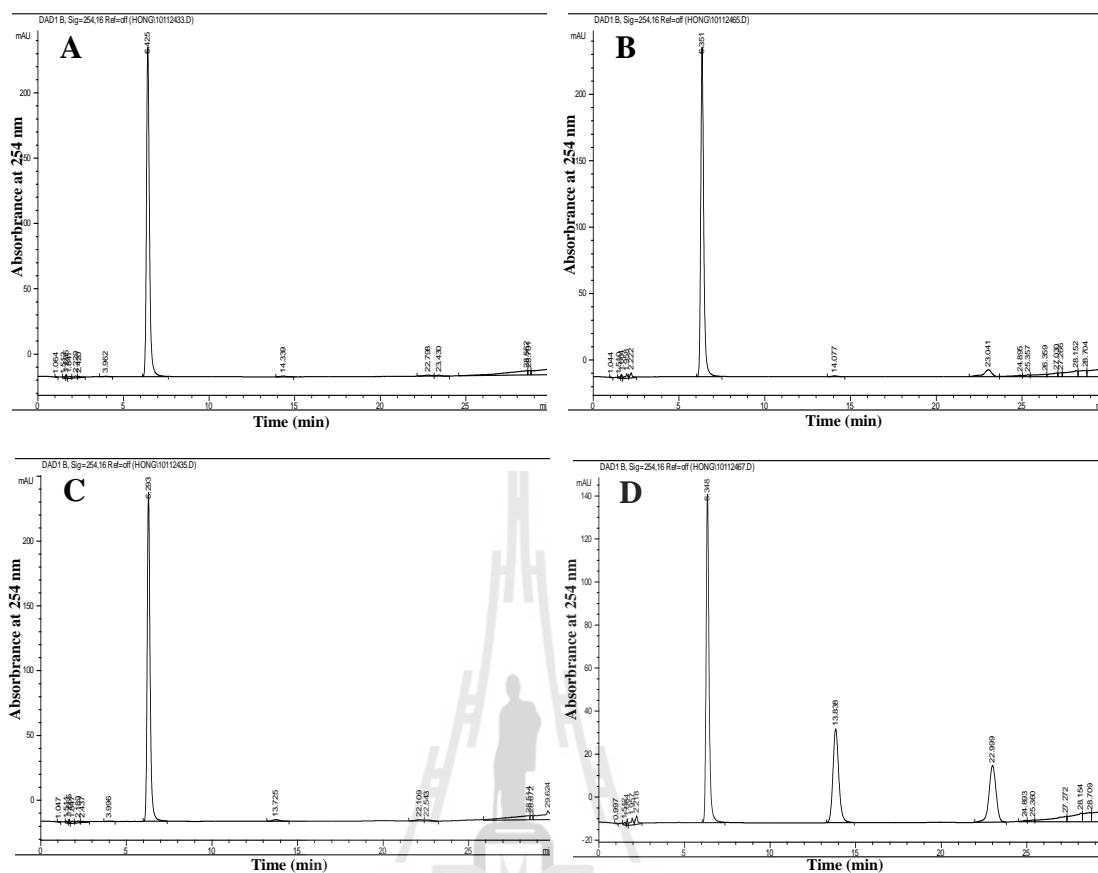


Figure 3.22 Reverse phase HPLC analysis of the products of the transglycosylation reaction of BGlu1 E176Q with 5 mM *p*NPMan and NBT as substrates. The reaction was done in MES buffer, pH 5.0, for 18 h with 4 mg/ml BGlu1 E176Q. HPLC analysis was done on a ZORBAX Eclipse XDB-C18 analytical column (4.6 x 150 mm) with elution with a gradient from 10 to 100% methanol in 0.1% formic acid. The chromatographs are (A) reaction without NBT at 0 h; (B) reaction without NBT at 18 h; (C) reaction with 2 mM NBT at 0 h; (D) reaction with 2 mM NBT at 18 h; (E) reaction with 5 mM NBT at 0 h; (F) reaction with 5 mM NBT at 18 h; (G) reaction with 10 mM NBT at 0 h; and (H) reaction with 10 mM NBT at 18 h.

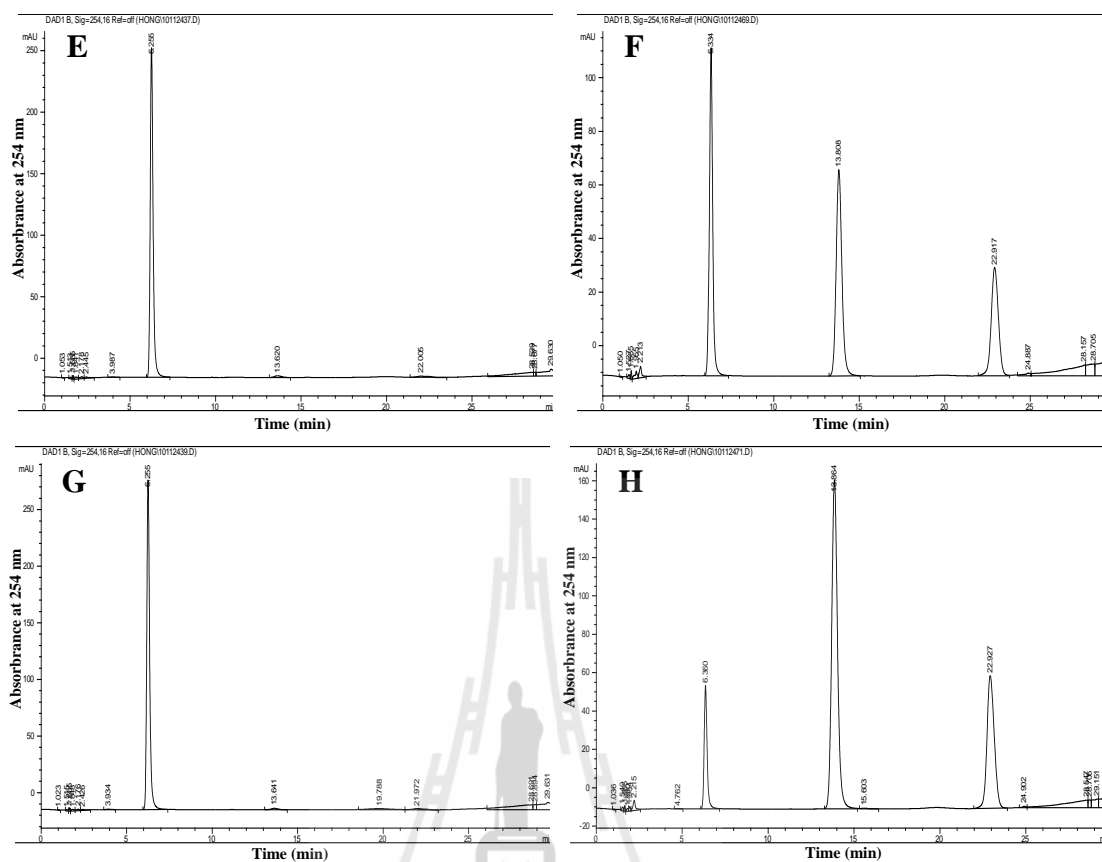


Figure 3.22 Reverse phase HPLC analysis of the products of the transglycosylation reaction of BGlu1 E176Q with 5 mM *p*NPMan and NBT as substrates. The reaction was done in MES buffer, pH 5.0, for 18 h with 4 mg/ml BGlu1 E176Q. HPLC analysis was done on a ZORBAX Eclipse XDB-C18 analytical column (4.6 x 150 mm) with elution with a gradient from 10 to 100% methanol in 0.1% formic acid. The chromatographs are (A) reaction without NBT at 0 h; (B) reaction without NBT at 18 h; (C) reaction with 2 mM NBT at 0 h; (D) reaction with 2 mM NBT at 18 h; (E) reaction with 5 mM NBT at 0 h; (F) reaction with 5 mM NBT at 18 h; (G) reaction with 10 mM NBT at 0 h; and (H) reaction with 10 mM NBT at 18 h (Continued).

The quantification of the products *p*NP β -D-thiomannoside and *p*NP produced in the transglycosylation reactions with 5 mM *p*NPMan after 18 h is shown in Table 3.6. The reaction of 5 mM *p*NPMan without NBT produced *p*NP to a concentration of about 0.44 mM, while the reaction including 2 mM NBT produced the *p*NP and *p*NP β -D-thiomannoside products to concentrations of 1.96 and 1.57 mM. When 5 mM NBT was included in the reaction, *p*NP and β -D-thiomannoside products were observed at apparent concentrations of 3.10 and 2.77 mM, respectively, while the reaction with 10 mM NBT produced the *p*NP and β -D-thiomannoside at apparent concentrations of 5.32 and 6.17 mM, respectively. The percentages of substrate converted to *p*NP β -D-thiomannoside from 5 mM *p*NPMan with 2, 5, and 10 mM NBT, as compared to the total amount of *p*NP produced from *p*NPMan, were 80.4, 89.1, and 116%, respectively.

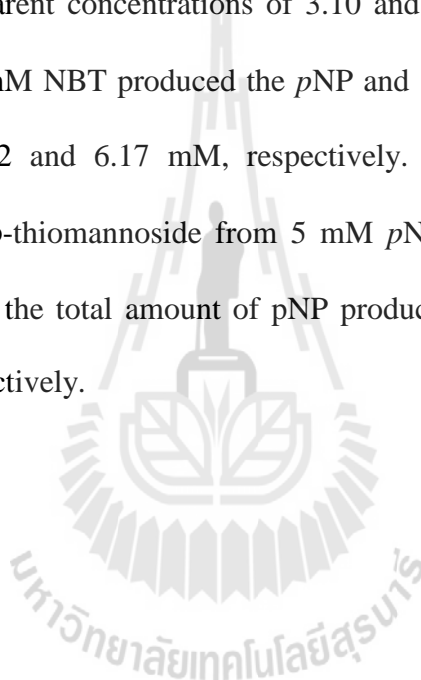


Table 3.6 The concentrations of products of reactions with 5 mM *p*NPMan with and without NBT quantified by reverse phase HPLC.

Concentration of NBT (mM)	Concentration of <i>p</i> NPMan (mM)	Concentration of <i>p</i> NP (mM)	Concentration of <i>p</i> NP β-D-thiomannoside (mM)	Percent of substrate converted to <i>p</i> NP β-D-thiomannoside*
0	5.22	0.44	0.00	0.00
2	3.20	1.96	1.57	80.4
5	2.90	3.10	2.77	89.1
10	1.35	5.32	6.17	116

* Calculated from the amount of *p*NP β-D-thiomannoside produced per *p*NP released from *p*NPMan.

In the reaction of 10 mM *p*NPMan without NBT for 18 h, peaks of *p*NPMan and *p*NP (retention times of 6.33 and 22.97 min) were seen (Figure 3.23 B). This confirmed the reaction without NBT cannot produce any product coeluting with *p*NP β -D-thiomannoside. The reaction of 10 mM *p*NPMan and 2 mM NBT showed peaks of *p*NPMan, *p*NP, and *p*NP β -D-thiomannoside (retention times of 6.33, 22.89, and 13.79 min, respectively) after 18 h (Figure 3.23 D). In reaction of 10 mM *p*NPMan and 5 mM NBT for 18 h, peaks of *p*NPMan, *p*NP, and *p*NP β -D-thiomannoside (retention times of 6.33, 22.89, and 13.81 min, respectively) were seen (Figure 3.23 F). The reaction of 10 mM *p*NPMan and 10 mM NBT for 18 h showed peaks of *p*NPMan, *p*NP, and *p*NP β -D-thiomannoside (retention times of 6.23, 21.95, and 13.45 min, respectively, in Figure 3.23 H). The transglycosylation reaction confirmed the reaction of 10 mM *p*NPMan with NBT at 18 h can produce the product of *p*NP β -D-thiomannoside.

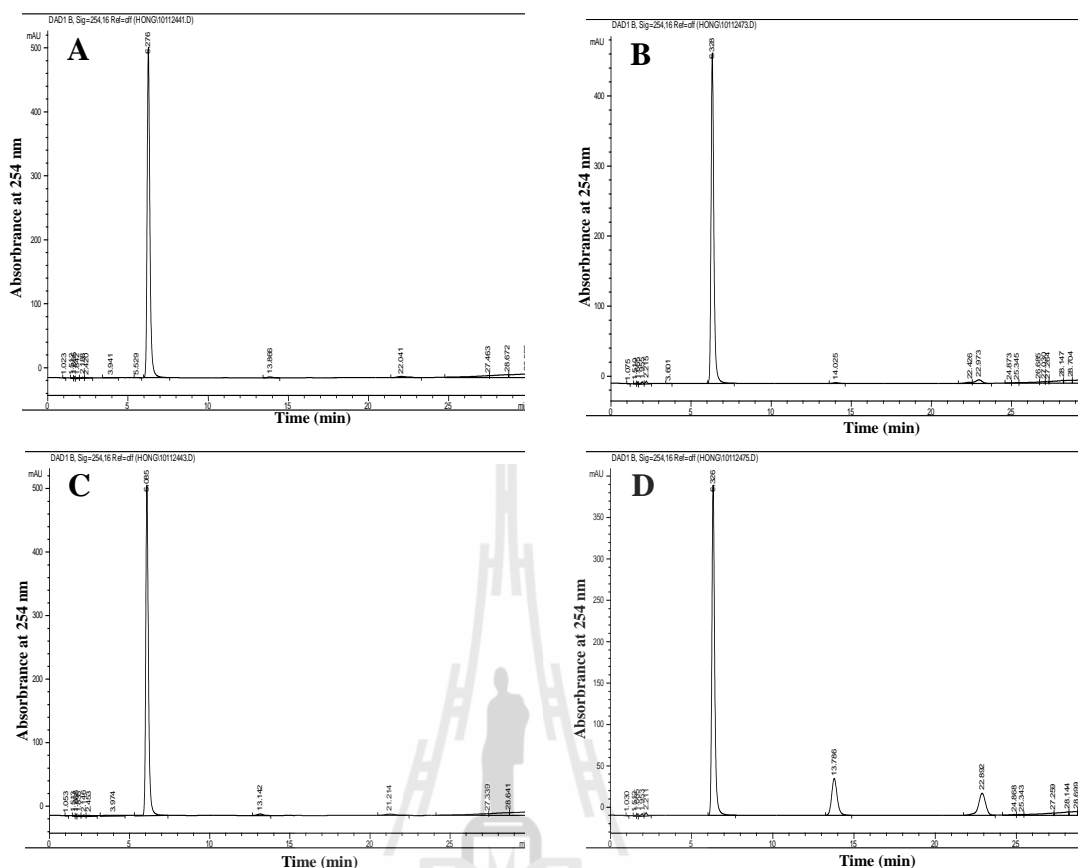


Figure 3.23 Reverse phase HPLC analysis of transglycosylation products of BGlu1 E176Q with 10 mM *p*NPMan and NBT as substrates. The reactions were done in MES buffer, pH 5.0, for 18 h with 4 mg/ml BGlu1 E176Q. HPLC analysis was done on a ZORBAX Eclipse XDB-C18 analytical column (4.6 x 150 mm) with elution with a gradient from 10 to 100% methanol in 0.1% formic acid at 1 ml/min. The chromatographs are (A) reaction without NBT at 0 h; (B) reaction without NBT at 18 h; (C) reaction with 2 mM NBT at 0 h; (D) reaction with 2 mM NBT at 18 h; (E) reaction with 5 mM NBT at 0 h; (F) reaction with 5 mM NBT at 18 h; (G) reaction with 10 mM NBT at 0 h; and (H) reaction with 10 mM NBT at 18 h.

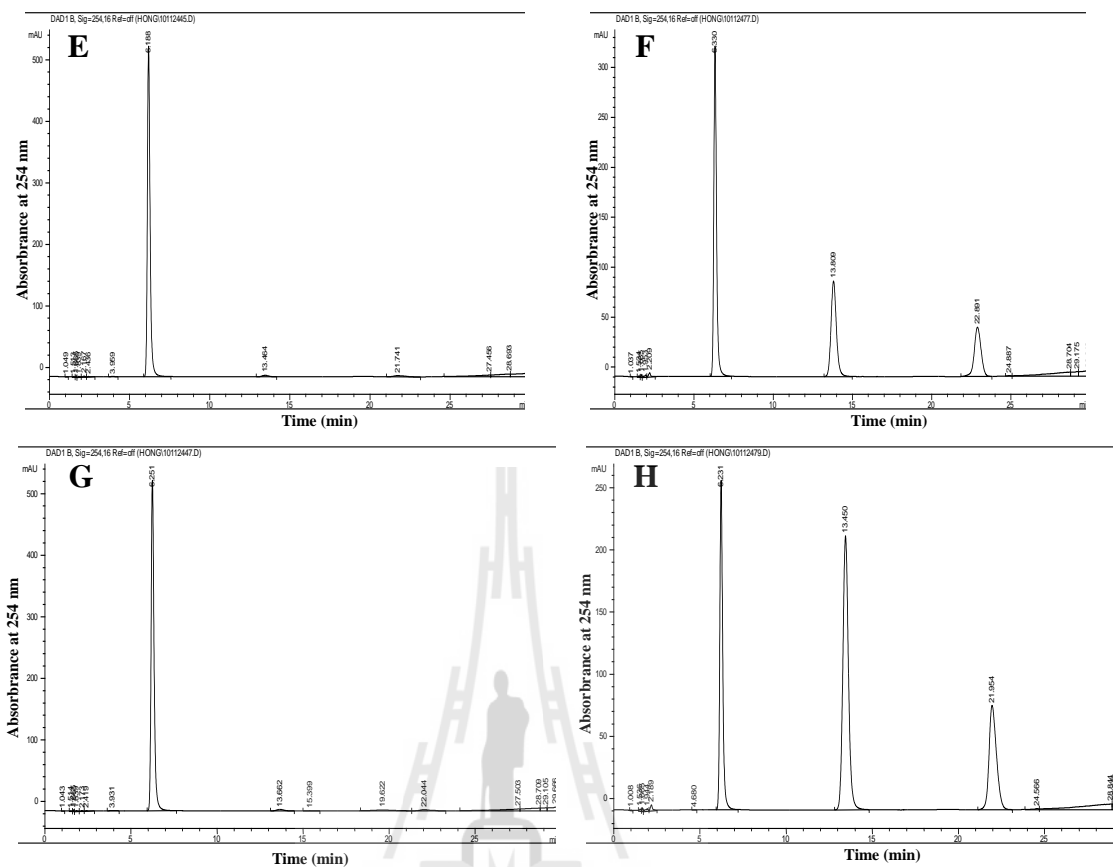


Figure 3.23 Reverse phase HPLC analysis of transglycosylation products of BGlu1 E176Q with 10 mM *p*NPMAN and NBT as substrates. The reactions were done in MES buffer, pH 5.0, for 18 h with 4 mg/ml BGlu1 E176Q. HPLC analysis was done on a ZORBAX Eclipse XDB-C18 analytical column (4.6 x 150 mm) with elution with a gradient from 10 to 100% methanol in 0.1% formic acid at 1 ml/min. The chromatographs are (A) reaction without NBT at 0 h; (B) reaction without NBT at 18 h; (C) reaction with 2 mM NBT at 0 h; (D) reaction with 2 mM NBT at 18 h; (E) reaction with 5 mM NBT at 0 h; (F) reaction with 5 mM NBT at 18 h; (G) reaction with 10 mM NBT at 0 h; and (H) reaction with 10 mM NBT at 18 h (Continued).

The apparent concentrations of the remaining substrate, *p*NPMan, and products of transglycosylation reactions, *p*NP β -D-thiomannoside and *p*NP, after 18 h reactions are shown in Table 3.7. The reaction of 10 mM *p*NPMan without NBT produced about 0.37 mM *p*NP, while the reaction with 2 mM NBT produced 2.14 mM *p*NP and 1.62 mM *p*NP β -D-thiomannoside with 8.4 mM *p*NPMan remaining. The reaction with 5 mM NBT produced 3.84 mM *p*NP and 3.45 mM β -D-thiomannoside, with 6.96 mM *p*NPMan remaining, while the reaction with 10 mM NBT produced 6.55 mM *p*NP and 7.56 mM β -D-thiomannoside with 5.44 mM *p*NPMan apparently remaining. The apparent percentages of substrate mannose converted to *p*NP β -D-thiomannoside compared to the total *p*NP produced in the reactions of 10 mM *p*NPMan with 2, 5, and 10 mM NBT were 75.7, 90.0, and 115%, respectively.

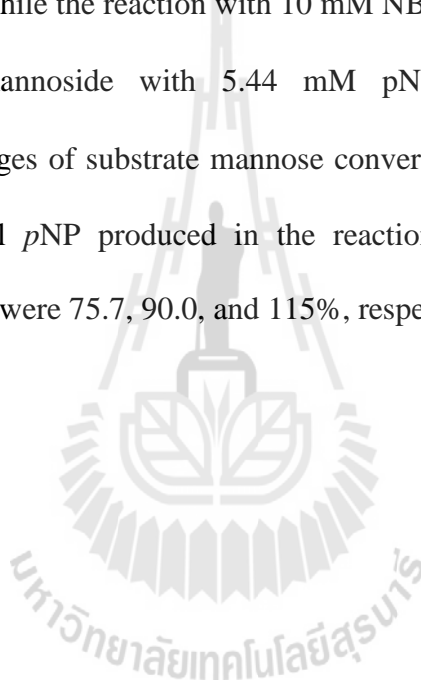
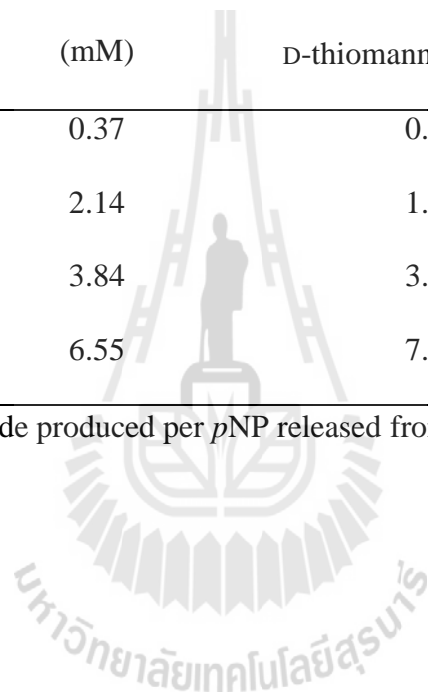


Table 3.7 The concentration of products of reactions of 10 mM *p*NPMan with and without NBT quantified by reverse phase HPLC.

Concentration of NBT (mM)	Concentration of <i>p</i> NPMan (mM)	Concentration of <i>p</i> NP (mM)	Concentration of <i>p</i> NP β-D-thiomannoside (mM)	Percent of substrate converted to <i>p</i> NP β-D-thiomannoside*
0	9.97	0.37	0.00	0.00
2	8.42	2.14	1.62	75.7
5	6.96	3.84	3.45	90.0
10	5.45	6.55	7.56	115

* Calculated from the amount of *p*NP β-D-thiomannoside produced per *p*NP released from *p*NPMan.



CHAPTER IV

DISCUSSION

4.1 Protein expression and purification

Rice BGlu1 E176Q β -glucosidase was expressed in *E. coli* strain Origami(DE3) with N-terminal thioredoxin and hexahistidine tag fusion proteins. After the first step of purification over a Co^{2+} bound IMAC resin column, a major protein band at 66 kDa was seen on SDS-PAGE (Figure 3.1), which was similar to that previously prepared by Chuenchor *et al.* (2011). This protein was used for transglycosylation reactions, since an inexpensive source of protein was desired, but further purification was needed for crystallization. The N-terminal thioredoxin and hexahistidine tags were cleaved from the fusion protein with enterokinase and the protein was passed over a second Co^{2+} IMAC column, which absorbed the histidine tag and connected thioredoxin tag, and the free BGlu1 E176Q was expected to come out in the unbound fraction. As previously observed by Chuenchor *et al.* (2008; 2011), 5-10 mM imidazole was needed to wash the rest of the nonspecifically bound tag-free BGlu1 E176Q protein from the column. On SDS-PAGE, the tag-free protein from these fractions had an apparent mass of 55 kDa of free BGlu1 E176Q, while the N-terminal thioredoxin and hexahistidine tag protein and a small amount of undigested protein were observed on SDS-PAGE of the 150 mM imidazole elution fractions (Figure 3.2). The obtained BGlu1 E176Q tag-free protein from the second Co^{2+} IMAC column was estimated to be 90-95% purity. Free BGlu1 E176Q was further purified by Superdex

S-200 gel filtration chromatography. From this step of purification, the protein purity was >95% pure. The BGlu1 E176Q obtained from the second Co²⁺ IMAC column and the final Superdex S-200 gel filtration chromatography appeared to have similar protein purity on SDS-PAGE. Since the gel filtration might eliminate impurities that were not apparent in SDS-PAGE, such as small molecules and protein aggregates, in the crystallization experiment, crystals were obtained using the protein purified with the final step of Superdex 200 gel filtration.

4.2 Protein crystallization

BGlu1 E176Q crystals could be crystallized by the hanging drop vapor diffusion method with microseeding by varying the conditions around those previously used for crystallization of BGlu1 (Chuenchor *et al.*, 2006; 2008; 2010). This included varying the precipitant concentration from 20% to 23% PEG MME 5000 and 0.17 M to 0.22 M (NH₄)₂SO₄, in 0.1 M MES, pH 6.7, and varying the BGlu1 E176Q protein concentration from 2 mg/ml to 5 mg/ml from high concentrations of freshly purified protein. The pure and fresh protein produced a good quality of crystals, but the old protein produced only poor crystals (data not shown). Moreover, when the protein preparation, precipitant or other reagents were changed, the crystallization conditions had to be finely tuned around the previously successful condition to reproduce crystals.

4.3 Structure of BGlu1 E176Q

The overall crystal structure of BGlu1 E176Q has the basic (β/α)₈ barrel fold, as previously seen for BGlu1 and other representative GH1 enzymes. The crystals of

BGlu1 E176Q included those cocrystallized with 10 mM *p*NPMan and 10 mM DNP2FM from which data was collected. The electron density of the ligand in the complex with *p*NPMan cocrystallized with BGlu1 E176Q was very weak in the active site, and appeared to be mainly represent glycerol. After the crystals were soaked with 100 mM *p*NPMan for various lengths of time, including 10, 30 and 60 min, and used for X-ray diffraction, the electron density in the active site was found to be strong in the electron density map calculated from the the crystal soaked for 60 min. The ligand electron density in the -1 subsite appeared to represent the structure of D-mannose in the active site. The crystal of BGlu1 E176Q cocrystallized with 10 mM DNP2FM for 2 months also yielded a strong electron density for the ligand in the -1 subsite, which appeared to represent the structure a 2-fluoro-D-mannosyl moiety covalently bound to the catalytic nucleophile. In the active site in the crystal structure of the BGlu1 complexed with G2F (PDB code 2RGM), the 2-F-glucosyl moiety is also covalently bound to the E386 nucleophile residue in the glycon binding pocket (Chuenchor *et al.*, 2008). The G2F inhibitor is actually a slowly hydrolyzed substrate, so the structure represents the glycosylated enzyme intermediate of the double displacement mechanism used by GH1 enzymes (Withers *et al.*, 1990). Superimposition of the BGlu1 E176Q complex with M2F, the BGlu1 E176Q complex with MAN and the complex of G2F with BGlu1 E176Q (PDB code; 3AHV, Chuenchor *et al.*, 2011) showed the same of conformation 4C_1 in a relaxed chair for both the G2F and the M2F complexes, which were found in a very similar position (Figure 3.8). The conformation of a pyranose ring has four possible forms that can fit the above mentioned requirements for coplanarity of the atoms, but only for $B_{2,5}$ and 4H_3 has strong evidence been observed by X-ray crystallography (Davies *et al.*, 2003). The

enzymatic mannoside hydrolysis appears to use a different conformation pathway. The structure of a GH26 endo- β -mannanase from *Cellvibrio japonicus* complex with 2-fluoro-2-deoxy- β -D-mannobioside revealed a 1S_5 conformation for the unhydrolysed Michaelis complex (Ducros *et al.*, 2002).

4.4 Rescue of *p*NPMan and *p*NPGlc hydrolysis by small nucleophiles

Rice BGlu1 E176Q had the highest activity toward *p*NPGlc when rescued by small nucleophiles with relative order of ascorbate > azide > acetate and low rescue activity was also observed with formate, citrate, TFA, fluoride, and cyanate (Chuenchor *et al.*, 2011). The catalytic acid/base to glutamine mutant (E170Q) with high rescue activity was also reported in *Agrobacterium* sp. β -glucosidase (Müllegger *et al.*, 2005). The glutamine mutant yielded the highest catalytic efficiency for thioglycoligase activity compared to other mutants, such as E170G, E170N, E170S, E170A, and E170T. The activities of nucleophile mutants (E386G, E386S, and E386A) of rice BGlu1 were also rescued by formate and azide (Hommalai *et al.*, 2007). When BGlu1 E176Q was rescued for release of *p*NP from *p*NPMan and *p*NPGlc a product was produced with azide and acetate in MES buffer (Figure 3.13). These products were expected to be β -glucosyl azide and β -glucosyl acetate, based on the results previously observed with Abg and rice β -glucosidase. In the *Agrobacterium* Abg β -glucosidase E170G acid/base mutant, no significant rate enhancement by azide was observed for *p*NPGlc, for which glycosylation was rate limiting. A rate increase was seen with small nucleophiles for 2,4-dinitrophenyl β -D-glucopyranoside cleavage, which was coupled with the accumulation product of β -D-glucosyl azide in the presence of azide. Other small anionic nucleophiles, such as

formate, fluoride, and cyanate also gave rate enhancements (Wang *et al.*, 1995). The product of β -glycosyl azide produced with *p*NPMan and *p*NPGlc donors could be separated by TLC. In principle, this product could be isolated by scratching the product from the TLC and eluting it from the silica with methanol. It could also be separated on HPLC by collecting the solution of the peak of the product, but when it was separated by HPLC, the solvent was dried and the compound dissolved with methanol, the product gave a smeared spot on the TLC.

4.5 Transglycosylation of *p*-nitrobenzenethiol

The barley rHv β II and rice BGlu1 (Os3BGlu7) enzymes can catalyze transglycosylation reactions to transfer glucosyl residues from cellooligosaccharide and *p*NPGlc as donor and use the same molecules as acceptors (Kuntothom *et al.*, 2009). The products from transglycosylation reactions catalyzed by rHv β II and BGlu1 appeared to be *p*NP-laminaribioside, *p*NP-cellobioside, *p*NP-gentiobioside, cellobiose, laminaritriose, and gentiobiose. However, no transglycosylation product was detected in transglycosylation reactions using *p*NPMan and mannobiose. BGlu1 E176Q showed very low levels hydrolysis of *p*NPMan in TLC, but appeared to transglycosylate it when azide and acetate acceptors were provided, as noted above. BGlu1 E176Q was tested for production of β -D-thioglycosides in transglycosylation reactions with *p*NPMan and *p*NPGlc as donors and *p*-nitrobenzenethiol as acceptor. Transglycosylation reaction with *p*NPGlc and NBT produced the product of *p*NP β -D-thioglycoside, based on the comparison with *p*NP β -D-thioglycoside standard on TLC, in which it showed the same R_f , and HPLC, in which it had the same retention time (Figure 3.19). The transglycosylation reaction with *p*NPMan and *p*-nitrobenzenethiol

gave the product that migrated with *p*NP β -D-thiomannoside on TLC and gave a similar retention time on HPLC, but the retention time of the *p*NP β -D-thiomannoside appeared to be shifted around 1 min because a nearby contaminating peak overlapped the main peak in the standard causing it to shift. This may be due to the fact that the preparation of standard had been kept a long time, resulting in breakdown to give the contaminating peak seen in the HPLC, but this contaminant was not seen as a spot on TLC. The reactions of *p*NPMAN with *p*-nitrobenzenethiol were not complete after increasing the concentration of BGlu1 E176Q and time of incubation. This is likely due to the slowness of the reaction, which would have required a higher concentration of enzyme to complete in the short time, and the stability of the enzyme in the reaction, since no further reaction was obvious between 18 and 48 hours.

The standard solutions of *p*NP β -D-thiomannoside and *p*NP β -D-thiomannoside used in HPLC were kept for a long time and may have degraded. As a result, another compound could be seen in the HPLC chromatogram with *p*NP β -D-thiomannoside, and the concentrations of the two standards were likely lower than they were supposed to be. The products of *p*NP β -D-thioglucoside and *p*NP β -D-thiomannoside at high NBT concentrations gave a higher than 100% conversion because the standard solution was kept a long time for prepared the concentration of standards were not correct. Since the lower concentrations gave lower peaks than the correct concentration in the HPLC, the standard curves were not correct, so the concentrations calculated by using this standard curve were high and showed the conversion of *p*NP glycoside to transglycosylation product was higher than 100%.

CHAPTER V

CONCLUSION

Expression and purification of the rice BGlu1 β -D-glucosidase E176Q acid-base mutant allowed its use for X-ray crystallographic analysis of mannose binding and its use as a transglycosidase to produce pNP β -D-thiogluco-side and β -D-thiomannoside. The BGlu1 E176Q was produced in *E. coli* strain Origami(DE3) from recombinant pET32a(+)*bglu1/E176Q* plasmid. The 66 kDa fusion protein was purified by IMAC, the N-terminal thioredoxin and hexahistidine fusion tag was excised from the protein with enterokinase, and the fusion tag was removed by adsorption to the IMAC resin to yield a 55 kDa tag-free protein. This free BGlu1 E176Q protein was further purified by gel filtration chromatography on a Superdex 200 column to yield >95% purify of protein.

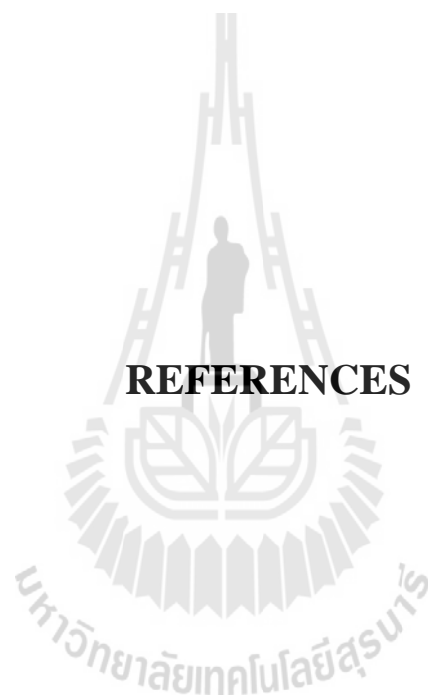
Crystallization of the BGlu1 E176Q with pNPMAN and DNP2FM was accomplished in the conditions with the precipitant concentration varied around 20%-23% PEG MME 5000 and 0.17-0.22 M $(\text{NH}_4)_2\text{SO}_4$, in 0.1 M MES, pH 6.7, by hanging drop vapor diffusion with microseeding. A crystal of the BGlu1 E176Q complex with pNPMAN produced in 20% PEG MME 5000, 0.22 M $(\text{NH}_4)_2\text{SO}_4$, 0.1 M MES, pH 6.7, with the size of 100 μm x 160 μm x 10 μm , diffracted X-rays to 1.69 \AA resolution. Crystals of the BGlu1 E176Q complex with DNP2FM were produced in the 23% PEG MME 5000, 0.19 M $(\text{NH}_4)_2\text{SO}_4$, 0.1 M MES, pH 6.7, by hanging drop vapor diffusion with microseeding. The complex crystal with dimensions of 60 μm x

90 μm x 10 μm was analyzed and diffracted X-rays to 1.95 \AA resolution. The diffraction patterns showed that the crystals of both BGlu1 E176Q complexes with DNP2FM and *p*NPMan belong to the $P2_12_12_1$ space group and had 2 molecules per asymmetric unit. The structures of BGlu1 E176Q derived from this data showed the pyranose rings in the active site were in the relax chair 4C_1 conformation, contrary to the expectation that the free mannose would be in a 1S_5 skew boat and the covalent intermediate in an 0S_2 skew boat conformation (Davies *et al.*, 2003).

The rescue of rice BGlu1 E176Q acid-base mutant by small nucleophiles in MES buffer, pH 5.0, was observed with the substrates *p*NPMan and *p*NPGlc. Inclusion of azide in the reaction with *p*NPGlc resulted in a high amount of a product that was likely to be azo β -D-glucoside (β -D-glucosyl azide), but the reaction without azide produced only relatively small amounts of *p*NP and glucose. A similar result was found with *p*NPMan, except that little mannose was released in the reaction without azide or acetate, and the unknown product with azide was likely to be azo β -D-mannoside (β -D-mannosyl azide), based on the mechanism of rescue of retaining glycoside hydrolase acid-base mutants by nucleophiles. In the transglycosylation reactions for transfer of sugars from *p*NPMan and *p*NPGlc to *p*-nitrobenzenethiol, the product spots on TLC were found at the same positions as the *p*NP β -D-thiomannoside and *p*NP β -D-thiogluconide standards, respectively, and they also had essentially the same retention times on HPLC. This confirmed that the desired β -thioglycosides were produced. Although without NBT and at low NBT concentrations hydrolysis of the *p*NPGlc and *p*NPMan was evident from the higher amounts of *p*NP than *p*NP-thioglycosides, the *p*NP- β -D-thiogluconide and *p*NP-D-thiomannoside were found at similar concentrations to the *p*NP, when the NBT acceptor was increased up to 10 mM

NBT. Thus, essentially all of the donor substrate utilized was used for transglycosylation rather than hydrolysis at 10 mM NBT acceptor concentration, although not all of the donor substrate was used for *p*NPMan. This demonstrates the potential of this enzyme for the production of *p*NP- β -D-thioglucoside and *p*NP- β -D-thiomannoside glycosidase inhibitors, the latter of which is particularly hard to synthesize chemically.





REFERENCES

REFERENCES

- Ahn, Y.O., Mizutani, M., Saino, H., and Sakata, K. (2004). Furcatin hydrolase from *Viburnum furcatum* blume is a novel disaccharide-specific acuminosidase in glycosyl hydrolase family 1. **J. Biol. Chem.** 279: 23405-23414.
- Bradford, M.M. (1976). A rapid and sensitive method for the quantification of microgram quantities of protein utilizing the principle of protein-dye binding. **Anal. Biochem.** 72: 264-273.
- Burmeister, W.P., Cottaz, S., Driguez, H., Palmieri, S., and Henrissat, B. (1997). The crystal structures of *Sinapis alba* myrosinase and of a covalent glycosyl-enzyme intermediate provide insights into the substrate recognition and active-site machinery of an S-glycosidase. **Structure.** 5: 663-675.
- Burmeister, W.P., Cottaz, S., Rollin, P., Vasella, A., and Henrissat, B. (2000). High resolution X-ray crystallography shows that ascorbate is a cofactor for myrosinase and substitutes for the function of the catalytic base. **J. Biol. Chem.** 275: 39385-39393.
- Chuankhayan, P., Hua, Y., Svasti, J., Sakdarat, S., Sullivan, P.A., and Ketudat Cairns J.R. (2005). Purification of an isoflavonoid 7-O- β -apiosyl-glucoside β -glycosidase and its substrates from *Dalbergia nigrescens* Kurz. **Phytochemistry.** 16: 1880-1889.
- Chuenchor, W., Pengthaisong, S., Yuvaniyama, J., Opassiri, R., Svasti, J., and Ketudat Cairns, J.R. (2006). Purification, crystallization and preliminary X-ray

analysis of rice BGlu1 β -glucosidase with and without 2-deoxy-2-fluoro- β -D-glucoside. **Acta Cryst.** F62: 798-801.

Chuenchor, W., Pengthaisong, S., Robinson, R.C., Yuvaniyama, J., Oonanant, W., Bevan, D.R., Esen, A., Chen, C.-J., Opassiri, R., Svasti, J., and Ketudat Cairns, J.R. (2008). Structural insights into rice BGlu1 β -glucosidase oligosaccharide hydrolysis and transglycosylation. **J. Mol. Biol.** 377: 1200-1215.

Chuenchor, W., Pengthaisong, S., Robinson, R.C., Yuvaniyama, J., Svasti, J., and Ketudat Cairns, J.R. (2011). The structural basis of oligosaccharide binding by rice BGlu1 beta-glucosidase. **J. Struct. Biol.** 173: 169-179.

Davies, G.J., Ducros, V.M.-A., Varrot, A., and Zechel, D.L. (2003). Mapping the conformational itinerary of β -glycosidases by X-ray crystallography. **Biochem. Soc. Tran.** 31: 523-527.

Delano, W.L. (2002). **The Pymol Molecular Graphics System.** (Online). Available: <http://www.pymol.org.html>.

Ducros V.M., Zechel D.L., Murshudov G.N., Gilbert H.J., Szabo L., Stoll D., Withers S.G., and Davies G.J. (2002). Substrate distortion by a beta-mannanase: snapshots of the Michaelis and covalent-intermediate complexes suggest a B_(2,5) conformation for the transition state. **Angew. Chem. Int. Ed. Engl.** 41: 2824-2827.

Emsley, P. and Cowtan, K. (2004). Coot-model-building tools for molecular graphics. **Acta. Cryst.** D60: 2126-2132.

- Escamilla-Treviño, L.L., Chen, W., Card, M.L., Shih, M.C., Cheng, C.L., and Poulton, J.E. (2006). *Arabidopsis thaliana* beta-glucosidases BGLU45 and BGLU46 hydrolyse monolignol glucosides. **Phytochemistry**. 67: 1651-60.
- Henrissat, B. (1991). A classification of glycosyl hydrolase based on amino acid sequence similarities. **Biochem. J.** 280: 309-16.
- Hommelai, G., Chaiyen, P., and Svasti, J. (2005). Studies on the transglycosylation reactions of cassava and Thai rosewood β -glucosidases using 2-deoxy-2-fluoro-glycosyl-enzyme intermediates. **Arch. Biochem. Biophys.** 442: 11-20.
- Hommelai, G., Withers, S.G., Chuenchor, W., and Ketudat Cairns, J.R., Svasti, J. (2007). Enzymatic synthesis of cello-oligosaccharides by mutated rice β -glucosidases. **Glycobiology**. 17: 744-753.
- Hrmova, M. and Fincher, G.B. (2001). Structure-function relationships of beta-D-glucan endo- and exohydrolases from higher plants. **Plant Mol. Biol.** 47(1-2): 73-91.
- Hrmova, M., MacGregor, E.A., Biely, P., Stewart, R.J., and Fincher, G.B. (1998). Substrate binding and catalytic mechanism of a barley β -D-glucosidase (1,4)- β -D-glucan exohydrolase. **J. Biol. Chem.** 273: 11134-11143.
- Jahn, M., Marles, J., Warren, R.A.J., and Withers S.G. (2003). Thioglycoligases: mutant glycosidases for thioglycoside synthesis. **Angew. Chem. Int. Ed.** 42: 352-354.
- Jahn, M., Chen, H., Müllegger J., Marles, J., Warren R.A.J., and Withers S.G. (2004). Thioglycosynthases: double mutant glycosidases that serve as scaffolds for thioglycoside synthesis. **Chem. Commun.** 3: 274-275.

- Ketudat Cairns, J.R. and Esen, A. (2010). β -Glucosidases. **Cell Mol. Life Sci.** 67: 3389-3405.
- Koeller K.M. and Wong C. (2000). Synthesis of complex carbohydrates and glycoconjugates: enzyme-based and programmable one-pot strategies. **Chem. Rev.** 100: 4465-4493.
- Koshland, D.E., Jr. (1953). Stereochemistry and mechanism of enzymatic reaction. **Biol. Rev.** 28: 416-436.
- Kuntothom, T., Luang, S., Harvey, A. J., Fincher, G.B., Opassiri, R., Hrmova, M., and Ketudat Cairns, J.R. (2009). Rice family GH1 glycoside hydrolases with β -D-glucosidase and β -D-mannosidase activity. **Arch. Biochem. Biophys.** 491: 85-95.
- Laemmli, U.K. (1970). Cleavage of structural proteins during the assembly of the head of bacteriophage T4. **Nature.** 227: 680-685.
- Laskowski, R.A., MacArthur, M.W., Moss, D.S., and Thornton, J.M. (1993). PROCHECK: a program to check the stereochemical quality of protein structures. **J. Appl. Cryst.** 26: 283-291.
- Ly, H.D. and Withers, S.G. (1999). Mutagenesis of glycosidases. **Annu. Rev. Biochem.** 68: 487-522.
- Mackenzie, L.F., Wang, Q., Warren, R.A.J., and Withers, S.G. (1998). Glycosynthases: Mutant glycosidases for oligosaccharide synthesis. **J. Am. Chem. Soc.** 120: 5583-5584.
- Makropoulou, M., Christakopoulos, P., Tsitsimpikou, C., Kekos, D., Kolis, F.N., and Macris, B.J. (1998). Factors affecting the specificity of β -glucosidase from *Fusarium oxysporum* in enzymatic synthesis of alkyl- β -D-glucosides. **Int. J. Biol. Macromol.** 22: 97-101.

- McCarter, J. and Withers, S.G. (1994). Mechanisms of enzymatic glycoside hydrolysis. **Curr. Opin. Struc. Biol.** 4: 885-892.
- Mizutani, F.M., Nakanishi, H., Ema, J., Ma, S.J., Noguchi, N., Ochiai, M.I., Mizutani, M.F., Nakao, M., and Sakata, K. (2002). Cloning of β -primeverosidase from tea leaves, a key enzyme in tea aroma. **Plant Physiol.** 130: 2164-2176.
- Morant, A.V., Jørgensen, K., Jørgensen, C., Paquette, S.M., Sánchez-Pérez, R., Møller, B.L., and Bak, S. (2008). Beta-glucosidases as detonators of plant chemical defense. **Phytochemistry.** 69: 1795-813.
- Müllegger, J., Jahn, M., Chen, H.M., Warren, R.A.J., and Withers, S.G. (2005). Engineering of a thioglycoligase: randomized mutagenesis of the acid-base residue leads to the identification of improved catalysis. **Protein Eng. Des. Sel.** 18: 33-40.
- Notenboom, V., Birsan, C., Nitz, M., Rose, D.R., Warren, R.A.J., and Withers, S.G. (1998). Insights into transition state stabilization of the β -1,4-glycosidase Cex by covalent intermediate accumulation in active site mutants. **Nature Struct. Biol.** 5: 812-818.
- Opassiri, R., Ketudat Cairns, J.R., Akiyama, T., Wara-Aswapati, O., Svasti, J., and Esen, A. (2003) Characterization of a rice β -glucosidase genes highly expressed in flower and germinating shoot. **Plant Sci.** 165: 627-638.
- Opassiri, R., Hua, Y., Wara-Aswapati, O., Akiyama, T., Svasti, J., Esen, A., and Ketudat Cairns, J.R. (2004). β -Glucosidase, exo- β -glucanase and pyridoxine transglucosylase activities of rice BGlu1. **Biochem. J.** 379: 125-131.

- Opassiri R, Pomthong B, Onkoksoong T, Akiyama T, Esen A, and Ketudat Cairns J.R. (2006). Analysis of rice glycosyl hydrolase family 1 and expression of Os4BGlu12 beta-glucosidase. **BMC Plant Biol.** 6: 33.
- Otwinowski, Z. and Minor, W. (1997). Processing of X-ray diffraction data collected in oscillation mode. **Methods Enzymol.** 276: 307-326.
- Perugino, G., Trincone, A., Rossi, M., and Moracci, M. (2004). Oligosaccharide synthesis by glycosynthases. **Trends Biotechnol.** 22: 31-37.
- Raychaudhuri, A. and Tipton, P.A. (2002). Cloning and expression of the gene for soybean hydroxyisourate hydrolase. Localization and implications for function and mechanism. **Plant Physiol.** 130: 2061-2068.
- Reese, E.T. (1977). Degradation of polymeric carbohydrates by microbial enzymes. **Rec. Adv. Phytochemistry.** 11: 311- 364.
- Rempel, B.P. and Withers, S.G. (2008). Covalent inhibitors of glycosidases and their applications in biochemistry and biology. **Glycobiology.** 18: 570-586.
- Schroeder¹, J.I. and Nambara, E. (2006). A Quick Release Mechanism for Abscisic Acid. **Cell.** 126: 1023-1025.
- Shaikh, F.A. and Withers, S.G. (2008). Teaching old enzymes new tricks: engineering and evolution of glycosidases and glycosyl transferases for improved glycosides synthesis. **Biochem. Cell Biol.** 86: 169-177.
- Sinnott, M.L. (1990). Catalytic mechanism of enzymatic glycosyl transfer. **Chem. Rev.** 90: 1171-1202.
- Svasti, J., Phongsak, T., and Sarnthima, R. (2003). Transglycosylation of tertiary alcohols using cassava β -glucosidase. **Biochem. Biophys. Res. Commun.** 305: 470-475.

- Tailford, L.E., Offen, W.A., Smith, N.L., Dumon, C., Morland, C., Gratien, J., Heck, M.P., Stick, R.V., Blériot, Y., Vasella, A., Gilbert H.J., and Davies, G.J. (2008). Structural and biochemical evidence for a boat-like transition state in β -mannosidases. **Nature Chem. Biol.** 4: 306-312.
- Thiem, J. (1995). Application of enzymes in synthetic carbohydrate chemistry. **FEMS Microbiol. Rev.** 16: 193-211.
- Vagin, A. and Teplyakov, A. (1997). MOLREP: an automated program for molecular replacement. **J. Appl. Cryst.** 30: 1022-1025.
- Wang, Q. Graham, R.W., Trimbur, D., Warren, R.A.J., and Withers, S.G. (1994). Changing enzymatic reaction mechanisms by mutagenesis: conversion of a retaining glucosidase to an inverting enzyme. **J. Am. Chem. Soc.** 116: 11594-11595.
- Wang, Q., Trimbur, D., Graham, R., Warren, R.A.J., and Withers, S.G. (1995). Identification of the acid/base catalyst in *Agrobacterium faecalis* β -glucosidase by kinetic analysis of mutants. **Biochemistry.** 34: 14554-14562.
- Weber, P.C. (1997). **Methods Enzymol.** 276: 13-23.
- Withers, S.G., Warren R.A.J., Street, I.P., Rupitz, K., Kempton, J.B., and Aebersold, R. (1990). Unequivocal demonstration of the involvement of a glutamate residue as a nucleophile in the mechanism of retaining glycosidase. **J. Am. Chem. Soc.** 112: 5887-5889.
- Zechel, D.L. and Withers, S.G. (2000). Glycosidase mechanisms: anatomy of a finely tuned catalyst. **Acc. Chem. Res.** 33: 11-18.
- Zechel, D.L. and Withers, S.G. (2001). Dissection of nucleophilic and acid-base catalysis in glycosidases. **Curr. Opin. Chem. Biol.** 5: 643-649.

Zechel, D.L., Reid, S.P., Stoll, D., Nashiru, O., Warren, R.A.J., and Withers S.G. (2003). Mechanism, mutagenesis, and chemical rescue of a β -mannosidase from *Cellulomonas fimi*. **Biochemistry**. 42: 7195-7204.





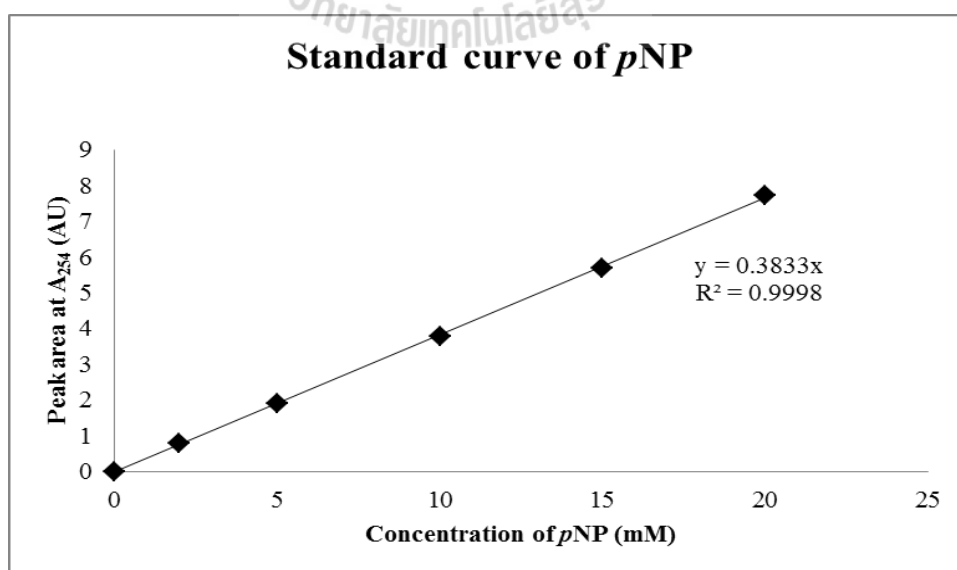
APPENDICES

APPENDIX A

STANDARD CURVE OF HPLC

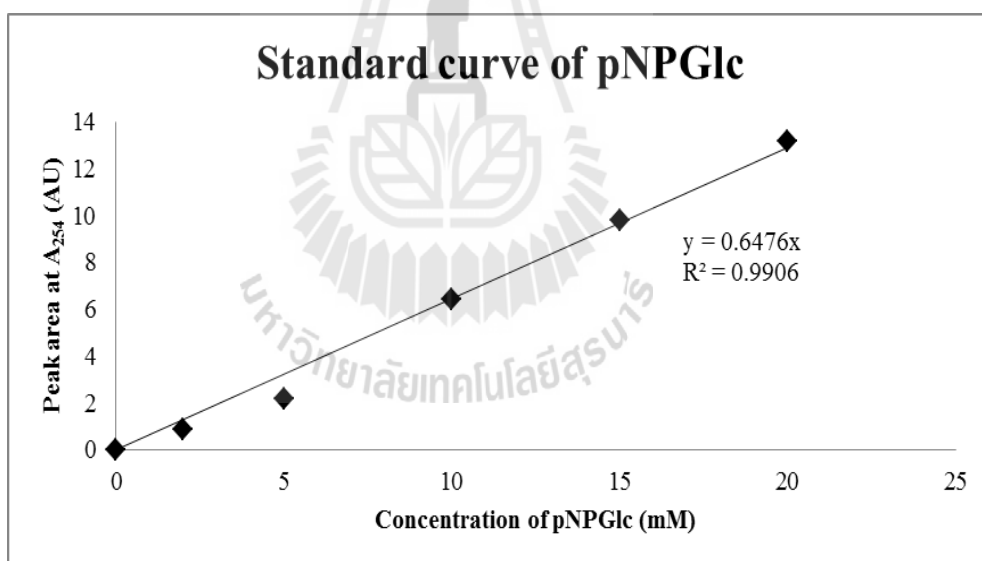
1.1 Standard curve of *p*NP from 254 nm absorbance peak area per concentration of *p*NP.

Concentration of <i>p</i> NP (mM)	Area (AU)
0	0.00
2	0.79
5	1.90
10	3.78
15	5.70
20	7.73



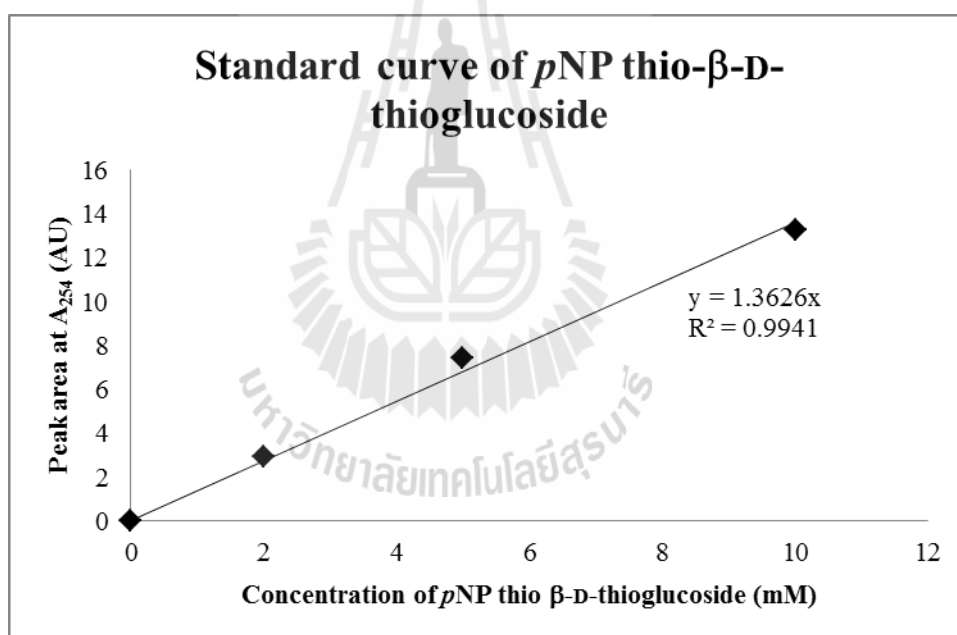
1.2 Standard curve for pNPGlc from 254 nm absorbance peak area per concentration of pNPGlc.

Concentration of pNPGlc (mM)	Area (AU)
0	0.00
2	0.91
5	2.18
10	6.47
15	9.82
20	13.18



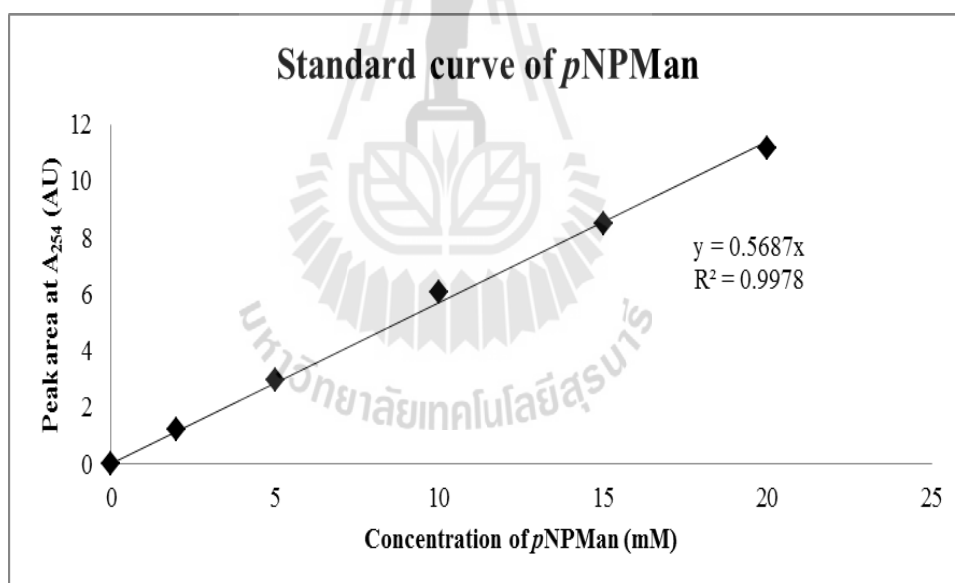
1.3 Standard curve of *p*NP β -D-thioglucoside from 254 nm absorbance peak area per concentration of *p*NP β -D-thioglucoside.

Concentration of <i>p</i> NP thio β -D-thioglucoside (mM)	Area (AU)
0	0.00
2	0.30
5	7.45
10	13.26



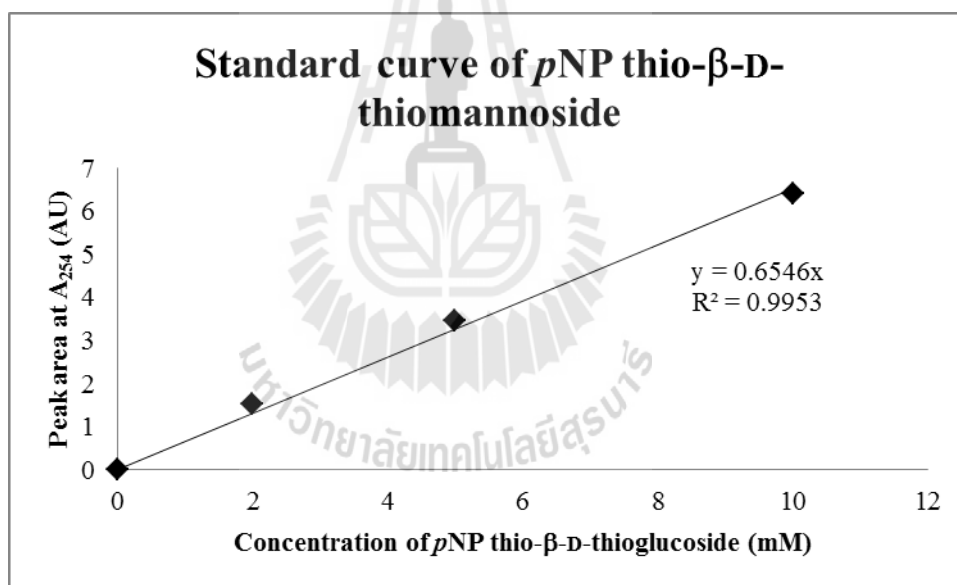
1.4 Standard curve for *p*NPMan from absorbance at 254 nm peak area per concentration of *p*NPMan.

Concentration of <i>p</i> NPMan (mM)	Area (AU)
0	0.00
2	1.23
5	2.97
10	6.06
15	8.50
20	11.17



1.5 Standard curve for *p*NP β -D-thiomannoside from absorbance at 254 nm peak area per concentration of *p*NP β -D-thiomannoside.

Concentration of <i>p</i> NP thio β -D-thiogluco- side (mM)	Area (AU)
0	0.00
2	1.52
5	3.48
10	6.40



APPENDIX B

LIST OF PROCEEDINGS AND ABSTRACTS

Proceedings

Prasert P., Ketudat Cairns J.R. The crystal structure of rice BGlu1 E176Q with 2,4-dinitrophenyl-2-deoxy-2-fluoro-mannoside or *p*-nitrophenyl β -D-mannoside. *The 19th National Graduate Research Conference*. 23-24 December 2010. Rajabhat Rajanagarindra University, Chachoengsao, Thailand.

Prasert P., Ketudat Cairns J.R. Crystals of BGlu1 E176Q with 4-nitrophenyl- β -D-mannoside and 2,4-dinitrophenyl-2-deoxy-2-fluoro-mannoside. *The 7th International Symposium of The Protein Society of Thailand*. 29-31 August 2012. Chulabhorn Research Institute Convention Center, Bangkok, Thailand.

Abstract

Prasert P., Ketudat-Cairns J.R. Preliminary structures of rice β -glucosidase BGlu1 E176Q covalent complexes with α -D-mannopyranoside and α -D-2-deoxy-2-fluoro-mannoside. *The 5th Annual Symposium of Protein Society of Thailand*. 23-25 July 2010. Chulabhorn Research Institute Convention Center, Bangkok, Thailand.

Other international publications

Negi, D.S., Kumar, A., Sharma, R.K., Shukla, N., Negi, N., Tamta, M.L., Bansal, Y., **Prasert, P.**, Ketudat Cairns, J.R. (2011). Structure conformation of rare conjugate glycosides from *Glycosmis arborea* (Roxb) with the action of β -glucosidases **Research Journal of Phytochemistry** 5: 32-40.



CURRICULUM VITAE

Name	Miss Por-ngam Prasert
Date of Birth	January 4, 1985
Place of Birth	Prachinburi
Education	
2007	Bachelor of Science (Chemistry), Valaya Alongkorn Rajabhat University, Under the Royal Patronage, Pathumthani, Thailand
2012	Master of Science (Biochemistry), Suranaree University of Technology, Thailand
Publication	Negi, D.S., Kumar, A., Sharma, R.K., Shukla, N., Negi, N., Tamta, M.L., Bansal, Y., Prasert, P. , Ketudat Cairns, J.R. (2011). Structure conformation of rare conjugate glycosides from <i>Glycosmis arborea</i> (Roxb) with the action of β -glucosidases Research Journal of Phytochemistry 5: 32-40.